

GENETIC HISTORY OF ANATOLIA DURING HOLOCENE

A THESIS SUBMITTED TO
THE GRADUATE SCHOOL OF INFORMATICS OF
THE MIDDLE EAST TECHNICAL UNIVERSITY
BY

DILEK KOPTEKIN

IN PARTIAL FULFILLMENT OF THE REQUIREMENTS FOR THE DEGREE OF
DOCTOR OF PHILOSOPHY
IN
MEDICAL INFORMATICS

SEPTEMBER 2022

GENETIC HISTORY OF ANATOLIA DURING HOLOCENE

submitted by **DILEK KOPTEKIN** in partial fulfillment of the requirements for the degree of **Doctor of Philosophy in Health Informatics Department, Middle East Technical University** by,

Prof. Dr. Deniz Zeyrek Bozşahin
Dean, **Graduate School of Informatics**

Assoc. Prof. Dr. Yeşim Aydın Son
Head of Department, **Health Informatics**

Prof. Dr. Mehmet Somel
Supervisor, **Biological Sciences, METU**

Examining Committee Members:

Assoc. Prof. Dr. Yeşim Aydın Son
Health Informatics, METU

Prof. Dr. Mehmet Somel
Biological Sciences, METU

Assist. Prof. Dr. Aybar Can Acar
Health Informatics, METU

Assoc. Prof. Dr. Can Alkan
Computer Engineering, Bilkent University

Prof. Dr. Anna-Sapho Malaspinas
Computational Biology, University of Lausanne

Date: 01.09.2022

I hereby declare that all information in this document has been obtained and presented in accordance with academic rules and ethical conduct. I also declare that, as required by these rules and conduct, I have fully cited and referenced all material and results that are not original to this work.

Name, Surname: Dilek Koptekin

Signature :

ABSTRACT

GENETIC HISTORY OF ANATOLIA DURING HOLOCENE

Koptekin, Dilek

Ph.D., Department of Health Informatics

Supervisor: Prof. Dr. Mehmet Somel

September 2022, 102 pages

Anatolia has been a key region in Eurasian history, acting as a bridge for cultural exchanges between Europe and Asia during the Holocene. However, the demographic transformation of Anatolian and neighbouring populations during these ten millennia is largely unknown. This work has two main research foci: 1) to investigate the role of gene flow in cultural interactions during the Neolithic period between Central Anatolian and Aegean communities and to evaluate the possibility of large-scale human movements during Neolithization of the Aegean, 2) to assess population continuity in Anatolia and its surrounding regions. For this aim, we produced 49 new ancient genomes and analysed this data in conjunction with published aDNA datasets.

We first investigated whether early Aegean Neolithic populations were established by farmer colonization from Central Anatolia or by local hunter-gatherers. Our results showed that the Aegean Neolithic populations may have been descendants of local hunter-gatherers who adapted farming.

We then tackled the question of how populations interacted in time and space from the Epipaleolithic period to the present-day. We found that genetic diversity within each region in Southwest Asia and East Mediterranean steadily increased through the Holocene. We further observed that the sources of gene flow shifted in time. In the first half of the Holocene, regional populations homogenised among themselves. Starting with the Bronze Age, however, they diverged from each other, driven most likely by gene flow from external sources. This expanding mobility in time was accompanied by growing male-bias in admixture events.

This work sheds new light on fine-scale population structure in Anatolian demographic history, filling a gap in our understanding of the nature of prehistoric and historic population interactions, not only among Anatolian populations but also with their neighbouring societies.

Keywords: ancient DNA, Anatolia, population genetics, human mobility, Neolithic

ÖZ

HOLOSEN BOYUNCA ANADOLU'NUN GENETİK TARİHİ

Koptekin, Dilek

Doktora, Sağlık Bilişimi Bölümü

Tez Yöneticisi: Prof. Dr. Mehmet Somel

Eylül 2022, 102 sayfa

Anadolu, Avrasya tarihinde önemli bir bölge olmuştur ve Holosen boyunca Avrupa ve Asya arasındaki kültürel alışverişler için bir köprü görevi görmüştür. Bununla birlikte, bu 10 bin yıl boyunca Anadolu ve komşu popülasyonlarının demografik değişimi büyük ölçüde bilinmemektedir. Bu çalışmanın iki ana araştırma odağı vardır: 1) Neolitik dönemde Orta Anadolu ve Ege toplulukları arasındaki kültürel etkileşimlerde gen akışının rolünü araştırmak ve Egenin Neolitikleşmesi sırasında büyük ölçekli insan hareketlerini araştırmak, 2) Anadolu ve çevresindeki bölgelerdeki popülasyon sürekliliğini değerlendirmek. Bu amaçla 49 yeni antik genom ürettik ve bu verileri yayınlanmış aDNA veri kümeleriyle birlikte analiz ettik.

İlk olarak, erken Ege Neolitik popülasyonlarının Orta Anadoludan çiftçi kolonizasyonu tarafından mı yoksa yerel avcı-toplayıcılar tarafından mı kurulduğunu araştırdık. Sonuçlarımız Ege Neolitik popülasyonlarının çiftçiliğe benimseyen yerel avcı-toplayıcıların torunları olabileceğini gösterdi.

Daha sonra, Epipaleolitik dönemden günümüze kadar popülasyonların zaman ve mekanda nasıl etkileşime girdiği sorusunu ele aldık. Güneybatı Asya ve Doğu Akdenizdeki her bölgede genetik çeşitliliğin Holosen boyunca sürekli bir şekilde arttığını bulduk. Ayrıca gen akışının kaynaklarının zamanla değiştiğini gözlemledik. Holosenin ilk yarısında bölgesel popülasyonlar kendi aralarında homojenleştirirken, Tunç Çağından başlayarak, büyük olasılıkla dış kaynaklardan gelen gen akışı nedeniyle birbirlerinden ayrıldılar. Zaman içindeki bu genişleyen hareketliliğe, karışım olaylarında artan erkek yanlılığı eşlik etti.

Bu alıřma, Anadolu demografik tarihindeki ince lekli poplasyon yapısına yeni bir ıřık tutarak ve yalnızca Anadolu poplasyonları arasında deęil, aynı zamanda komřu poplasyonlarda da tarih ncesi ve tarihi poplasyon etkileřimlerinin doęasına iliřkin anlayıřımızdaki bořluęu dolduracaktır.

Anahtar Kelimeler: antik DNA, Anadolu, poplasyon genetięi, insan hareketlilięi, Neolitik

From Halet Çambel to İnci Togan
To all La Loba's
who keep collecting bones and bringing them to life

ACKNOWLEDGMENTS

This study would not have been possible without the contribution of many people. I learned a lot and I'm grateful for them.

First and foremost, I would like to express my deepest gratitude and appreciation to my supervisor, *Mehmet Somel*, for his invaluable advice, continuous support, and patience during my PhD. His insight and scientific perspective steered me through my PhD and will guide me through life.

I would like to extend my deepest gratitude to *İnci Togan*, *Füsun Özer*, *Anders Götherström*, *Pavlos Pavlidis* and *Flora Jay* who have influenced and inspired me. Their immense knowledge and experience have encouraged me not just through this research but also in life. Their immense knowledge and experience have encouraged me not just through this research but also in life.

I would also like to show gratitude to my dissertation monitoring committee, *Yeşim Aydın Son* and *Can Alkan*, who generously provided knowledge and expertise to the improvement of this study over years.

I am deeply indebted to all current members and alumni of *Comparative & Evolutionary Biology (CompEvo)*, at METU Biology. I have been pleased to be a member of this great team. I would like to express my sincere gratitude to *Gülşah Merve Kılınç* for her invaluable assistance, supervision and support; to *Melike Dönertaş*, *Ayşin Ghalichi* and *Hamit İzgi* for being there to answer my never-ending questions from the very beginning; to *Ezgi Altınışık* for the sleepless nights while we were working together and for her effort to make my figures better; to *Eren Yüncü*, *Kıvılcım Başak Vural*, *Ayça Aydoğan* and *Kanat Gürün* for their contribution to analyses. I could not have undertaken this journey without you. This study is just as much yours as it is mine.

I would like to thank the wet-lab team of METU CompEvo, Hacettepe Human-G, Stockholm CPG and Greece FORTH-IMBB for their collaborative effort during data generation. I would like to recognise the effort of *Füsun Özer*, *Duygu Deniz Kazancı*, *Ricardo Rodríguez-Varela*, *Sevgi Yorulmaz*, *Damla Kaptan*, *Vendela K. Lagerholm*, *Robert George*, *Nikolaos Psonis*, *Despoina Vassou*, *Eugenia Tabakaki*, *Natalia Kashuba* and *Evangelia Daskalaki* in performing the experiments.

Thanks should also go to all archaeological and anthropological team members of the excavation sites, *Yılmaz Selim Erdal*, *Andreas Schachner*, *Handan Üstündağ*, *Mihriban Özbaşaran*, *Güneş Duru*, *Burçin Erdoğan*, *Taner Korkut*, *Özlem Çevik*, *Ömür Dilek Erdal*, *Ramaz Shengelia*, *Eleni Stravopodi*, *Argyro Nafplioti*, *Alexander Gavashelishvili*, *C. Brian Rose*, *Ali Metin Büyükkarakaya*, *Refik Duru* and *Gülsün Umurtak* for providing samples and their continued enthusiasm to discuss all questions and results we had. I would like to especially thank *Hasan*

Can Gemici, Cansu Karamurat, iğdem Atakuman, Yılmaz Selim Erdal and Jan Stora, for their momentous contribution to the archaeological/anthropological parts of the study.

I am deeply grateful to *Ecology and Evolutionary Biology Society (EkoEvo)*, Turkey for their willingness to impart their knowledge to young scientists like me and most importantly for their endless effort to improve the quality and quantity of scientific research in ecology and evolution in Turkey.

I also acknowledged support from Wenner-Gren Foundation (Dissertation Fieldwork Grant no. 9573 to Dilek Koptekin), EMBO Scientific Exchange Grant (no. 8883 to Dilek Koptekin), H2020 ERC Consolidator Grant (no. 772390 “NEOGENE” to Mehmet Somel), H2020 TWINNING Grant (no. 952317 “NEOMATRIX” to Mehmet Somel) and Scientific and Technical Research Council of Turkey (TÜBİTAK, no: 117Z229 to Mehmet Somel).

Words cannot express my gratitude to my dear "Lobsters", *Hazal Moğultay* and *Duha Aliođlu*, for their friendship. Knowing you are there in times of crisis was a privilege!

I owe special thanks to *Zeynep Yaşar, Kalender Arıkan, Seniha Ünay* and *Hazal Moğultay* for their generous support. Without their help, all this could not even begin!

Most importantly, none of this could have happened without my family. If I've accomplished anything in life, it's because you always believed in me and supported me. I love you all!

Last but not least, to my mother, *Sevim*, and all women who have been fighting for freedom. I will follow the path they opened!

TABLE OF CONTENTS

ABSTRACT.....	iv
ÖZ.....	vi
DEDICATION.....	viii
ACKNOWLEDGMENTS.....	ix
TABLE OF CONTENTS.....	xi
LIST OF TABLES.....	xv
LIST OF FIGURES.....	xvi
LIST OF ABBREVIATIONS.....	xvii
CHAPTERS	
1 INTRODUCTION.....	1
1.1 Summary of sociocultural developments in Anatolia and its neighboring regions	2
1.1.1 Neolithic transition in Southwest Asia and West Eurasia.....	2
1.1.2 Post-Neolithic populations in Anatolia.....	3
1.2 Ancient DNA.....	5
1.2.1 Ancient DNA studies.....	6
1.3 Research Questions.....	7
1.4 Organization of the Thesis.....	8

2	ARCHAEOGENOMIC ANALYSIS OF NEOLITHIZATION IN ANATOLIA AND THE AEGEAN	9
2.1	Introduction.....	9
2.2	Results and Discussion	13
2.2.1	Genetic Structure of the Aegean Neolithic Populations	14
2.2.2	Characterising the ancestry profile of Girmeler genome	15
2.2.3	Characterising the ancestry profile of the Aegean Neolithic populations	16
2.3	Conclusion	17
3	TRACKING POPULATION STRUCTURE OF SOUTHWEST ASIA AND THE EAST MEDITERRANEAN HUMAN POPULATIONS THROUGH TIME FROM ANCIENT AND MODERN DNA.....	19
3.1	Introduction.....	19
3.2	Results and Discussion	21
3.2.1	Genetic structure and continuity in Southwest Asia and the East Mediterranean	24
3.2.2	Regional mobility as reflected in ancestry components	26
3.2.2.1	Anatolia	26
3.2.2.2	The Aegean	28
3.2.2.3	Iran	29
3.2.2.4	South Caucasus	31
3.2.2.5	The Levant	33
3.2.3	The expanding nature of inter-regional mobility in Southwest Asia and the East Mediterranean	33
3.2.4	Regional diversity increases monotonously through the Holocene	36
3.2.5	Spatial heterogeneity in mobility levels	36

3.2.6	A possible temporal shift in sex-biased inter-regional mobility	37
3.2.7	Conclusion	39
4	MATERIALS AND METHODS	43
4.1	Sample preparation	43
4.2	Radiocarbon dating	44
4.3	Sequence data processing	45
4.4	Testing for authenticity and quality control	45
4.4.1	Post-mortem damage	45
4.4.2	Contamination estimation	45
4.5	Molecular sex determination	46
4.6	Estimating uniparental haplogroups	46
4.7	Ancient genome sample selection	46
4.8	Whole genome SNP datasets	47
4.9	Trimming and pseudo-haploid genotyping	48
4.10	Genetic kinship analyses	49
4.11	Principal component analysis (PCA)	49
4.12	Genetic differentiation among populations	49
4.13	Genomic similarity/distance among populations	49
4.14	Detecting gene flow among populations	50
4.15	Ancestry proportion estimation	50
4.16	Runs of homozygosity (ROH)	51
4.17	Coalescent simulations	51

4.18 Visualization	52
5 CONCLUSION	53
REFERENCES	57
APPENDICES	
A	75
CURRICULUM VITAE	99

LIST OF TABLES

Table 1	Summary of sociocultural developments in Southwest Asia and the East Mediterranean starting with the Neolithic Transition.....	4
Table 2	Anatolian and Aegean Neolithic settlements used in the analysis.....	12
Table 3	Archaeological and genetic information of the ancient individuals sequenced in this study	14
Table 4	Archaeological and genetic information of the ancient individuals sequenced in this study	22
Table 5	Information about all individuals used in the analyses.	76

LIST OF FIGURES

Figure 1	Summary of the data analyzed in this study.	13
Figure 2	Principal Component Analysis (PCA) and Multidimensional Scaling Analysis (MDS)	15
Figure 3	Genetic affinities of Girmeler and Pınarbaşı genomes.	16
Figure 4	Genetic affinities of Aegean Neolithic populations.	17
Figure 5	Geographical location of archaeological sites and dates of samples.	21
Figure 6	Principal Component Analysis (PCA).	25
Figure 7	Regional genomes converging in PC space over time.	26
Figure 8	Testing degree of geographic structure and regional continuity over time in Southwest Asia and the East Mediterranean.	27
Figure 9	Testing regional population continuity over time in Southwest Asia and the East Mediterranean.	28
Figure 10	qpAdm models for Neolithic and post-Neolithic populations of Southwest Asia and the East Mediterranean.	29
Figure 11	Genetic Affinity of Post-Neolithic Anatolian Populations.	30
Figure 12	Genetic Affinity of Post-Neolithic Aegean Populations.	30
Figure 13	Genetic Affinity of Post-Neolithic Iran Populations.	31
Figure 14	Genetic Affinity of Post-Neolithic South Caucasus Populations.	32
Figure 15	The impact of drift and admixture on three statistics of population differentiation evaluated by coalescent simulations.	34
Figure 16	Genetic differentiation over time in Southwest Asia and the East Mediterranean.	35
Figure 17	Genetic differentiation over time in Southwest Asia and the East Mediterranean.	37
Figure 18	Distribution of ancient individuals with sROH (4-8 cM)	38
Figure 19	Uniparental markers and sex-biased admixture.	40

LIST OF ABBREVIATIONS

aDNA	Ancient DNA
BA	Bronze Age
BCE	Before Common Era
BP	Before Present
CA	Chalcolithic
CE	Common Era
CHG	Caucasus Hunter Gatherers
cM	Centimorgan
EHG	Eastearn Hunter-Gatherer
EP	Epipaleolithic
HG	Hunter-gatherer
IA	Iron Age
LGM	Last Glacial Maximum
MDS	Multidimensional Scaling
MP	Medieval Period
N	Neolithic
NGS	Next Generation Sequencing
mtDNA	mitochondrial DNA
PCA	Principal Component Analysis
PCR	Polymerase Chain Reaction
PMD	Post-Mortem Damage
ROH	Runs of Homozygosity

sROH	Sum of ROH
UDG	Uracil-DNA-glycosylase
WSHG	West Siberian Hunter-Gatherers

CHAPTER 1

INTRODUCTION

The history of our species on Earth is relatively recent on an evolutionary time scale. Despite the ongoing and controversial debates, we now know that our species, *Homo sapiens*, originated in Africa about 400-200 thousand years ago [1]. The earliest known fossils from the *Homo sapiens* clade is located in Jebel Irhoud, Morocco and dating to ~315 thousand years ago [2]. Then, *Homo sapiens* spread all over the world from there. The emergence and spread out of Africa of *Homo sapiens* are one of the most studied topics in the history of science.

It is widely accepted that there were multiple out-of-Africa waves [3, 4]. Analysis of genetic variation among human populations indicates that the majority of non-African present-day human populations are descended from originally African populations who spread around the world approximately 100-60 thousand years ago. When *Homo sapiens* spread to continents outside of Africa, they met and mixed with other archaic humans there. Unfortunately, *Homo sapiens* became the only living Homo species 40-30 thousand years ago [5].

Humans first settled in Eurasia and later in Oceania and the Americas. Alongside the peopling of the continents, the mobility of human populations has been continuing across already populated regions [6].

After the Out-of-Africa migration, human populations quickly spread throughout Eurasia and the rest of the world, and hunting and gathering being dominant way of life for at least 95% of human history. Probably they lived as small groups during this time. As a consequence of the harsh effect of the Last Glacial Maximum (LGM) about 20,000 years ago, these groups remained highly isolated in different geographical regions [7].

As environmental conditions improved and the climate warmed about 12,000 years ago, human cultures shifted from hunting-gathering, which they had been doing for hundreds of years, to food production, independently in several locations such as Southwest Asia and East Asia [8].

The Neolithic transition refers to the adoption of sedentism and the shift in subsistence style from hunting-gathering to producing animals and crops. This new cultural innovation has become so successful that it has become the dominant way of life in the world today. According to earlier research, the mobility of European Holocene farmers was noticeably higher than European hunter-gatherers of both before and after the Last Glacial Maximum and continued to increase during the Holocene [9].

In this study, we investigate human mobility patterns in and around Anatolia and how these mobility patterns shaped the gene pool of Anatolian populations during the Holocene. Our aim is to understand how human mobility has changed over time and how the changing lifestyle during Neolithization and mobility patterns have changed the genetic diversity of Anatolian populations during the Holocene with a particular focus on the Neolithization of both Anatolia and the Aegean.

1.1 Summary of sociocultural developments in Anatolia and its neighboring regions

1.1.1 Neolithic transition in Southwest Asia and West Eurasia

When archaeologists found the first traces of the Neolithic lifestyle in Southwest Asia, they described this cultural shift as the "Neolithic Revolution" [10]. However, what is accepted by many researchers today is that the transition to settled life was not a rapid change. On the contrary, it was a process that spread over an extended time period. The Natufian Culture from the Southern Levant represents important first examples of pre-Neolithic settlement. The Natufian people (12,500 BCE –9,500 BCE) were semi-sedentary hunter-gatherers. They built round pit houses that were probably occupied just seasonally. They were intensively exploiting a diverse array of wild plants, including cereals and benefiting from wild herds of sheep, goats, and gazelle [11, 12]. The shift to a sedentary life centered around agriculture and eventual domestication of various plants and animals probably took place among similar groups of semi-sedentary hunter-gatherers some 12,000-10,000 years ago in different regions of Southwest Asia [13].

The primary zone of Neolithisation in Southwest Asia, also called the "Fertile Crescent", has been defined as the region spanning the Levant (present-day Syria, Lebanon, Jordan, Israel, Palestine), Iran (Zagros Mountains), and North Mesopotamia (North Iraq and Southeastern Anatolia) [14, 13]. Although the Neolithic Transition began to be recognized in Southwest Asia in the early 20th century, in the meantime, there was no known Neolithic settlement in Central Anatolia. However, many Neolithic settlements were discovered during the surveys carried out in both Southeastern and Central Anatolia in 1950-60. Since the late 1950s, our knowledge of the Neolithisation of Anatolia has increased considerably. Today, it is widely accepted that both Southeastern and Central Anatolia were a part of the primary zone [15, 16].

Archaeological records show that until 7,000 BCE, sedentary life and use of domesticates were mainly confined to this primary zone [17]. The Neolithic way of life induced several innovations even in early times. Besides domesticated animals and plants, some elements also frequently occurred in Neolithic villages, such as figurines, specific architectural features, or some prestige items [18]. However, the frequency of these traits in different regions was various. Each population that adopted the Neolithic lifestyle interpreted and changed it more or less in its own way. These patterns of differentiation and sharing have led to numerous predictions on how these populations may have interacted with each other and with neighboring regions as well as settlements that appeared post-7,000 BCE [19].

The Neolithic lifestyle spread to new territories in 7,000-5,500 BCE. The 8.2 KA event, known for the sudden decrease in temperature, is speculated to accelerate this spread [20]. Advances in agriculture probably made it possible to farm in different ecological niches. This dispersal also extended exchange between villages.

The Neolithic expansion of post-7,000 BCE is fascinating in this context. Neolithic villages appeared across the Aegean, including Western Anatolia, after 7,000 BCE and reached Central Europe and Iberia by the 6,000-5,000 BCE. These Neolithic villages contained elements like various domesticates, pottery, and figurines already familiar from earlier farming communities closer to the primary zone [21]. Given the lack of footprints of a gradual transition process, it has been proposed that the Neolithic way of life was driven into Europe as "waves of advances" [22]: the Aegean villages were colonists originating from Neolithic primary zones, either the Levant [23] or Central Anatolia [15] and Neolithic spread from there to rest of Europe step by step.

The first genetic research on Neolithic spread westward was conducted by Ammerman and Cavalli-Sforza (1984) [22]. They discovered a strong relationship between the emerging date of Neolithic sites and their distance from the Near East. When they displayed genetic distance (the output of PCA) and geographic distance on synthetic maps, they observed the pattern indicating the demic diffusion model together with acculturation for driving farming to Europe using present-day European gene frequencies. Ancient DNA studies later supported this model of European Neolithisation from a Near Eastern origin (see Chapter 2). However, some archaeologists have pointed out that heterogeneity in material culture among Aegean villages can be a sign of local cultural traditions, and that this suggests that these Aegean farmers may not have been colonists from the Near East [24, 25]. Neither archaeological nor genomic studies have yet fully resolved this question.

1.1.2 Post-Neolithic populations in Anatolia

Human populations have been changing the environment they live in. The Neolithic transition as a radical shift in lifestyle accelerated advancements and has been reshaping human populations worldwide since the early Holocene by constantly creating and spreading new cultural traits (see Table 1).

The Neolithic transition probably was the first step into the life we know today. The Neolithic way of life became the dominant way of life shortly after its emergence. The modest villages that were established settled down and larger settlements began to emerge. These changes probably formed the basis of the urbanization, and inequalities in social life in later periods.

After the Neolithic, populations and lifestyle during the Chalcolithic period (6,000-3,000 BCE) have remained somewhat obscure in Anatolia specially between 5,500-4,000 BCE. It was mainly characterized by advances in metallurgy. The Neolithic culture mostly continued in this period. It is estimated that the population size in the settlements has been growing since the Neolithic. Social networks and long-distance exchange have also improved during this period [26].

The Bronze Age (3,500-1,200 BCE) is one of the best studied pre-historical periods in Anatolia. While the metallurgy and long-distance networks arose in Chalcolithic, they expanded in the Bronze Age. The increase in population density and long-distance trade increased social complexity, and stratified societies, urbanization, and centralized governments emerged. The domestication of equids and the invention of the wheel allowed human populations to migrate long distances. Anatolia was also impacted by these expansions, such as the expansion of the Kura-Araxes culture, although the exact dynamics behind it are still a matter of debate [27].

Over time, the Anatolian plateau was dominated by several culturally and linguistically variable populations, including Assyrians, Kaskians, and Hattians, followed by the Hittites and Mycenaean [28, 29]. The first written remains in Anatolia also have been found in this period [30]. Moreover, the tablets found in Hittite settlements were written in the Indo-European language [31]. Anatolia continued to experience dramatic sociocultural and political changes that frequently involved interactions with immigration from populations outside the peninsula, such as the Greek colonization, Galatian migrations, the Achaemenid expansion, and the Hellenistic and Roman periods, and, more recently, Turkic expansions [32].

Table 1: Summary of sociocultural developments in Southwest Asia and the East Mediterranean starting with the Neolithic Transition. The table is not an exhaustive list of events but aims to provide an idea of major transformations that could have influenced human mobility. (-) indicates the persistence of pre-Neolithic lifeways. This table prepared by Hasan Can Gemici, Cansu Karamurat and Çiğdem Atakuman.

Anatolia	Historical developments
15,000 - 10,000 BP	Incipient farming, Semi-sedentism/sedentism
10,000 - 8,000 BP	Farming, Sedentism, Pottery
8,000 - 6,000 BP	Pyrometallurgy, Long-distance trade
6,000 - 4,000 BP	Wheel, Domestic equids, Centralisation/Urbanisation, Kura-Araxes expansion, Indo-European migrations?, Agricultural surplus
4,000 - 2,000 BP	Writing, Inter-regional empires, Greek/Hellenic expansion, Trade colonies, Iron production
2,000 BP- Present day	Roman Empire, Islamic expansion, Turkic migrations, Pilgrimage
Levant	Historical developments
15,000 - 10,000 BP	Incipient farming, Semi-sedentism/sedentism
10,000 - 8,000 BP	Farming, Sedentism, Pottery
8,000 - 6,000 BP	Pyrometallurgy, Long-distance trade
6,000 - 4,000 BP	Wheel, Domestic equids, Urbanisation, Writing, Agricultural surplus
4,000 - 2,000 BP	Inter-regional empires, Greek/Hellenic expansion, Iron production
2,000 BP- Present day	Roman Empire, Islamic expansion, Pilgrimage
Iran	Historical developments
15,000 - 10,000 BP	Incipient farming, Semi-sedentism/sedentism
10,000 - 8,000 BP	Farming, Sedentism, Pottery
8,000 - 6,000 BP	Pyrometallurgy
6,000 - 4,000 BP	Wheel, Domestic equids, Urbanisation, Writing, Long-distance trade, Indo-European migrations, Agricultural surplus
4,000 - 2,000 BP	Inter-regional empires, Greek/Hellenic expansion, Iron production
2,000 BP- Present day	Islamic expansion, Turkic migrations

Table 1 (continued)

South Caucasus	Historical developments
15,000 - 10,000 BP	-
10,000 - 8,000 BP	-
8,000 - 6,000 BP	Farming, Sedentism, Pottery, Pyrometallurgy
6,000 - 4,000 BP	Wheel, Domestic equids, Indo-European migrations
4,000 - 2,000 BP	Writing, Urbanisation, Inter-regional empires, Greek/Hellenic expansion, Iron production
2,000 BP- Present day	Roman Empire, Turkic migrations
the Aegean	Historical developments
15,000 - 10,000 BP	-
10,000 - 8,000 BP	Farming, Sedentism, Pottery
8,000 - 6,000 BP	Pyrometallurgy
6,000 - 4,000 BP	Wheel, Domestic equids, Centralisation/Urbanisation, Indo-European migrations, Agricultural surplus
4,000 - 2,000 BP	Writing, Inter-regional empires, Greek/Hellenic expansion, Iron production
2,000 BP- Present day	Roman Empire, Slavic migrations, Pilgrimage

Overall, human movement is essential to understand the history of our species, genetic diversity among present-day and past populations, human adaptation to different and changing environments, the transmission of diseases, relationships with other species, and especially for providing information about ourselves.

Until the last few decades, most of our knowledge about the evolutionary history of our species was based on fossils and archaeological findings, as well as limited molecular evidence based on present-day samples. Although present-day human genetic diversity contains information about past populations, aDNA studies provide an unprecedented opportunity to enhance our knowledge about our recent evolutionary past. Today, advances in DNA sequencing and experimental methods enabled the extraction and sequencing of ancient DNA and the investigation of many questions about recent human history and evolution.

1.2 Ancient DNA

The field of science that analyzes the DNA from organisms that lived in the past and investigates their histories is called ancient DNA (aDNA) research. aDNA is usually obtained from remains such as bones, teeth, and hair. It is also possible to get aDNA from coprolite, calculus, sediment, and soil samples, even from the remains of ancient chewed gum. In recent decades, aDNA studies together with population genetics studies, have brought a new perspective to many fields such as archaeology, anthropology, and linguistics. aDNA has made it possible to study past human movements, kinship levels, and lifestyles, which population genetic studies have been trying to understand over modern populations for many years, directly with genetic material from the past, in a sense, opening a direct window to the past.

DNA can be successfully preserved for hundreds of thousands of years. However, endogenous ancient DNA retrieval and analysis have several limitations. DNA preserved in ancient samples is highly fragmented due to decay after death and it continuously accumulates various types of damage, termed post-mortem damage (PMD) [33]. The most common PMD is cytosine deamination at the single-stranded ends of molecules that convert unmethylated cytosine to uracil and methylated cytosine to thymine.

Ancient samples (e.g. bone, teeth, etc.) also contain exogenous DNA. Exogenous contamination, the most common challenge in aDNA studies can originate from multiple sources: (i) microorganisms that colonized the bones ever since the death of the individual; (ii) humans working on the samples during excavation or experimental process in the laboratory; (iii) other ancient samples that have been in contact with the focal sample (cross-contamination). Because of decay and contamination, ancient samples mostly contain little and often no endogenous DNA. Therefore, extracting sufficient amounts of endogenous DNA can be expensive, time-consuming, and sometimes even impossible. Thus, the majority of ancient human individuals are only available at poor quality, often below a 1X read depth.

Ancient samples with relatively high coverage genomes (>10X) have generally been obtained from cold, sometimes permafrost environments where DNA preservation is better than in warmer or humid climates.

1.2.1 Ancient DNA studies

In the early 1980s, it was discovered that the DNA is preserved in tissues after death and can be extracted and sequenced. The first aDNA study extracted short mitochondrial DNA (mtDNA) sequence fragments from an extinct subspecies of the plains zebra named quagga [34]. With the development of the polymerase chain reaction (PCR) method, it became possible to create millions of copies of a targeted DNA fragment in test tubes. Thanks to PCR, the ability to reproduce and analyze very little DNA left in the tissues of ancient organisms created great excitement.

However, the widespread use of aDNA research methods is a much more recent development. It has been noticed that the studies, which started with great enthusiasm in the 1990s, often yielded unrepeatable results and the momentum of the studies decreased significantly in the following years. It was not easy to distinguish whether the DNA obtained from the archaeological remains belonged to that organism. Even if many measures were developed against contamination risks, the results were always viewed with suspicion due to the magnitude of the risk. Due to the highly degraded nature of ancient DNA and limitations of prior technologies, aDNA studies focused on mtDNA or Y chromosome rather than nuclear genome up to the 2010s. Although mtDNA or Y chromosome raises our knowledge of the human past movements, this information is limited to only one lineage of ancestries, either maternal or paternal lineage.

Thanks to the development of Next Generation Sequencing (NGS) techniques in the 2000s, aDNA studies gained tremendous momentum. NGS has made it possible to sequence hundreds of millions of short DNA fragments in parallel and obtain information about the organism's entire genome in a single experiment at much lower costs. Together with NGS, better

recognition of the structure of aDNA over the years and the development of new experimental and computational methods have also played an important role in this acceleration. These developments include the development of experimental protocols for efficient aDNA isolation and capture of fragmented short molecules, better recognition of post-mortem accumulated damages and their use in distinguishing authentic DNA from exogenous contaminated DNA, and recognition of the pars petrosa bone in the skeleton as the region where DNA is best preserved, as well as the development of effective bioinformatics tools and statistical methods for analyzing ancient genomes.

The first ancient whole human genome was sequenced from a ~4,000-year-old hair sample from extinct Palaeo-Eskimo [35]. In the same year, the draft genomes of Neanderthal have also been reconstructed, which allowed tracing the introgression between Neanderthal and the present-day human descendants of the out-of-Africa dated to around 120k years ago [36]. Moreover, the new archaic human was identified by using only aDNA called Denisovan [37]. Ancient DNA studies also found that Denisovan coexisted with *Homo sapiens* and mixed ancestors of East Asian and Oceanian [38] as well as several other populations whose ancestors are related to East Asians [39].

Since then, over 8,500 ancient genomes (though the majority only partial shotgun and SNP-capture-generated genomes) have been published. To date, the oldest published hominin DNA is 400,000 years old and belongs to Sima de los Huesos [40], whereas the oldest *Homo sapiens* DNA dates back more than 45,000 years [41, 42, 43]. The oldest DNA on record was obtained from a mammoth that lived 1.6 million years ago in Siberia [44]. With this study, the upper limit for the preservation time of DNA was pushed beyond million years, yet the vast majority of published ancient genomes date to much more recent times. For example, the majority of published ancient human genomes date from the Holocene, the last 11,500 years of Earth's history.

1.3 Research Questions

This thesis has two main research foci:

- I. To investigate the role of gene flow in cultural contacts among Anatolian Neolithic communities as well as large-scale movements of humans during Neolithization using ancient genome data. Here we tackle how populations interacted in time and space during Anatolian Neolithization and the westward Neolithic expansion, particularly in Aegean communities. The main question is whether early Aegean farmers were established by hunter-gatherer adoption or farmer colonization. Neither archaeological studies nor genomic studies have been able to reach a clear decision in this regard. This study involves a collection of genome data from various Neolithic sites across Anatolia, including newly generated genomes from Western Anatolia. These localities cover a large span of time within a defined geographical area and contain excellent contextual information for analyses of aDNA from Anatolia. This will improve our vision of the Neolithic.
- II. To evaluate continuity and change between ancient and modern populations in Southwest Asia and East Mediterranean, mainly in Anatolia. To what extent populations that

occupied the Anatolian plateau in the past 15,000 years passed on their alleles to present-day populations is unclear. Here we tested the possible intra-regional and inter-regional gene flow in each time period to infer population structure and human mobility across time and to describe the ancestral relationships between past and present populations. We investigated population structure resulting from interactions/gene flows in Anatolia as well as its neighboring regions, the Levant, Iran, South Caucasus, and the Aegean, starting with the Epipaleolithic/Mesolithic and proceeding into the present-day.

1.4 Organization of the Thesis

This thesis is organized into five chapters which are described as follows.

Chapter 2 presents our current understanding of how Neolithic lifestyle emerged in Anatolia and the Aegean mostly based on our four published articles [45, 46, 47, 48] together with published articles on this subject [49, 50]. It also provides new results about the Neolithization process of the Aegean basin (Western Anatolia and Northern Greece) with newly generated genomes from Western Anatolia (Koptekin et al, in preparation).

Chapter 3 presents how population structure and mobility changed populations over time in Anatolia as well as its neighbors such as the Aegean, Levant, South Caucasus, and Iran. This chapter is based on Koptekin et al, under review.

Chapter 4 presents details about materials and methods used both for Chapter 2 and Chapter 3.

Chapter 5 presents the conclusion of both studies to attempt to draw an overall picture of the genetic history of Anatolian populations during the Holocene.

CHAPTER 2

ARCHAEOGENOMIC ANALYSIS OF NEOLITHIZATION IN ANATOLIA AND THE AEGEAN

2.1 Introduction

Ancient genome analyses have shown that the earliest Neolithic populations in different regions of the Fertile Crescent, in the South Levant, in Zagros/Iran, and in Central Anatolia were genetically differentiated from each other. These Neolithic populations clustered with the local Epipaleolithic/Mesolithic hunter-gatherer populations from the same region in each region. Three major gene pools can be distinguished during the Epipaleolithic and early Neolithic periods between 13,500-7,000 BCE at these Neolithic sites across the Fertile Crescent: (i) *The Southern Levant gene pool*, which includes pre-Neolithic/Epipalaeolithic peoples of the Natufian culture represented by human remains from Raqefet Cave and early Neolithic human populations represented by Ain-Ghazal, Motza, Ba'ja and Kfar HaHoresh [51, 49]. (ii) *The Zagros/Iran gene pool*, which includes pre-Neolithic/Epipalaeolithic human remains excavated from Hotu and Belt Caves, and Neolithic people represented by Ganj Dareh, Tepe Abdul and Wezmeh Cave [51, 52, 53, 54]. (iii) *The Central Anatolia gene pool*, which includes pre-Neolithic/Epipalaeolithic human populations represented by a single genome dating to 13,500 BCE from Pınarbaşı and early Neolithic human populations represented by Boncuklu Höyük and Aşıklı Höyük [45, 49, 47].

Ancestral lineages of these three gene pools must have remained isolated from each other after out-of-Africa migration, possibly during the Last Glacial Maximum (LGM) about 20,000 years ago, and must have differentiated through genetic drift. These findings, together with archaeological evidence, suggest that Neolithic culture in the Fertile Crescent was a somewhat local development with limited interregional gene flow [45, 46, 49, 51, 52, 55]. Still, it probably also involved the exchange of technology and agriculture ideas, such as emulation or acculturation [46]. Interregional gene flow within the region is predicted to have become more common towards the late Neolithic [46, 49, 47].

Our recent study on the ancient genomes from an early Neolithic settlement in Southeast Anatolia represented by Çayönü Tepesi showed that the gene pool of this region could be modeled as a mixture of the three gene pool described above [48]. Archaeological evidence indicates that the Neolithization of Upper Mesopotamia (including Southeastern Anatolia) was part of primary zone in Southwest Asia. Therefore, this mixed gene pool of Southeastern Anatolia could be explained by the admixture of eastern and western populations of Southwest

Asia after the LGM. These semi-sedentary hunter-gatherers, known for the diversity of their cultural dynamics, built the monumental structures in the region the best-known example at Göbeklitepe [56] and they played an important role in the Neolithic transition of both Upper Mesopotamia (currently represented by only Çayönü in the archaeogenomic record) and Central Anatolia [48].

In contrast to the picture of limited gene flow in the Southwest Asia, archaeological and genetic data provide clear evidence for a substantial role of migration in the introduction of farming into Europe. Archaeogenetics studies have revealed significant genetic differences between European hunter-gatherers and early European farmers of the same regions [57, 58]. On the contrary, early European farmers were genetically close to Neolithic populations in Anatolia/the Aegean [59, 55, 51, 46]. The Neolithic spread to Europe was clearly driven by demic diffusion. Genetic results showed that interaction between the first migrant farmers and local hunter-gatherers was mostly limited in the early Neolithic and then increased over time [58, 59, 50]. Although it is estimated that the first farmers arrived from the Aegean basin, the source and exact date of these migrations are still uncertain.

Since Neolithic villages in the Aegean region were not seen before 7,000 BCE and emerged in a short period with already involving some Neolithic elements, it has been proposed that the Aegean villages were also colonists originating from Neolithic primary zones presumably from the Levant [23] or Central Anatolia [15]. The current mainstream narrative is that farmers from Central Anatolia (part of the primary zone of Neolithization) colonized the Aegean region post-7,000 BCE. However, it is an ongoing debate whether the earliest steps of westward Neolithic spread were driven by demic diffusion. This idea has yet to be comprehensively answered using genetic analyses.

In 2017, we undertook a reanalysis of 99 published ancient genomes from West Eurasia, including early Northern Aegean Neolithic communities (Barcın Höyük in Northwestern Anatolia and Revenia in Northern Greece) [46]. The study showed that the Northern Aegean communities were genetically closest to those from Central Anatolia and not the Levant, ruling out a Levant-derived colonist origin. Intriguingly, we also found that Neolithic Aegean genomes contained more diverse admixture signatures than those of Central Anatolian populations, such as higher levels of admixture with Levant, Iran, and the European Mesolithic populations. Moreover, Central Anatolian populations used in this study (Boncuklu Höyük and Tepecik-Çiftlik Höyük) had a higher affiliation to the Aegean Neolithic populations than to each other. These results raised doubt about the demic diffusion scenario within the Aegean - that the first Aegean farmers were colonists from Central Anatolia. We further assessed this demic diffusion model by studying several coalescent toy models and could not reproduce the observed patterns. We thus proposed an alternative acculturation scenario: during the early Holocene, the Aegean already hosted a local hunter-gatherer population, who adopted agriculture from neighboring farming populations after 7,000 BCE. This conclusion would be in line with archaeological observations, noting surprising variation in cultural elements among Aegean sites, including differences in domesticates, pottery, architectural traditions, figurine, and stamp seal use, even between neighboring sites [24, 60, 61]. Such variation appears inconsistent with colonist origins. The conclusion also resonates with a recent analysis of mitochondrial DNA variation suggesting that the Aegean was an Ice Age refugium and harbored a large human population [62] and mitochondrial haplogroups commonly seen in Southwest Asian Neolithic populations are also found in Mesolithic Balkan and Aegean pop-

ulations [55, 63]. However, the limited sample size (only two Northern Aegean sites and two Central Anatolian sites) precluded a final verdict. Overall, we suggested that Neolithization in Aegean may be more complex than assumed.

A recent study [50] inquired into the same question with demographic modeling using high-quality ancient genomes. This study had two important results concerning the history of Anatolia and the Aegean. First, they proposed that the Anatolian gene pool formed by the mixture of Balkan- and Levant-related groups after the LGM. This result is also compatible with the Epipaleolithic sample from Central Anatolia (Pınarbaşı, 13,642-13,073 cal BCE), which was predicted to be partly of European and partly of Levantine origin [49, 48]. Secondly, Marchi et al. (2022) tried to estimate the dynamics of the early Holocene Anatolia and the Aegean. According to their results, both the early Neolithic populations from Central Anatolia and the later Neolithic populations of the Aegean (Western Anatolia and Northern Greece) were the descendants of the same Anatolian gene pool. According to Marchi et al. (2022), the people of the Aegean did not recently migrate from Central Anatolia, as the two groups were estimated to have separated before Neolithization. Through cultural interactions, this model is also compatible with the Neolithisation model of local hunter-gatherers in the Aegean.

Our previous work using archaeogenomics [46] and the recently published study using demographic modeling [50] have supported the latter possibility, suggesting that local Aegean pre-Neolithic populations themselves adopted farming, although the evidence remains equivocal mainly. Since the published data consists of Northwest Anatolia and Northern Greece, and we do not know the Aegean Neolithic populations genetically well, nor pre-Neolithic genomes from Aegean basin have ever been published.

To fill this gap, we newly generated data from the following sites:

- Girmeler Cave (n=1) is located in Southwestern Anatolia (Fethiye, Turkey) and dates to 8,200–7,900 BCE. The Girmeler Cave is the only known sedentary site with a subsistence based mainly on intensive hunting and gathering in Southwest Anatolia in this period. [64]. It is interesting in presenting Neolithic-like buildings with plastered floors and subfloor burials, but without indication of animal management as in the contemporaneous Aşıklı Höyük in Central Anatolia.
- Ulucak Höyük (n=3) is a western Anatolian Neolithic settlement (İzmir, Turkey). The site exhibits a long stratigraphic sequence extending from 6,800 to 6,000 BCE. It is proposed that the earliest farmers appeared along with domesticated livestock and plants in the region between 7,000 – 6,600 BCE [65, 66, 67, 68].
- Bademağacı Höyüğü (n=10), also known as Kızılkaya, is located in the Lake District of Southwest Anatolia [69, 70] and dates to 7,100-6,100 BCE.

Table 2: Anatolian and Aegean Neolithic settlements used in the analysis

Settlement	Location	Region	Date	#N	Publication
Pınarbaşı	Karaman, Turkey	Central Anatolia	13642–13073 BCE	1	[49]
Çayönü Tepesi	Diyarbakır, Turkey	Southeast Anatolia	8500-7500 BCE	10	[48]
Boncuklu Höyük	Konya, Turkey	Central Anatolia	8,300–7,600 BCE	7	[45, 49]
Aşıklı Höyük	Aksaray, Turkey	Central Anatolia	8,350–7,300 BCE	4	[47]
Girmeler Cave	Fethiye, Turkey	the Aegean	7738-7597 BCE	1	This Study
Musular	Aksaray, Turkey	Central Anatolia	7400-7000 BCE	2	This Study
Çatalhöyük	Konya, Turkey	Central Anatolia	7,100–5,950 BCE	12	[47]
Ulucak Höyük	İzmir, Turkey	the Aegean	6800-6600 BCE	2	This Study
Tepecik-Çiftlik Höyük	Niğde, Turkey	Central Anatolia	6680-6590 calBCE	2	[45]
Aktopraklık Höyük	Bursa, Turkey	the Aegean	6600-6400 BCE	1	[50]
Barcın Höyük	Bursa, Turkey	the Aegean	6500-6200 BCE	22	[59, 55]
Revenia	Pieria, Greece	the Aegean	6438-6264 BCE	1	[55]
Bademağacı Höyük	Antalya, Turkey	the Aegean	6400-6100 BCE	10	This Study
Menteşe Höyük	Bursa, Turkey	the Aegean	6400-5600 BCE	5	[59]
Nea Nikomedeia	Veria, Greece	the Aegean	6,350–6,000 BCE	2	[50]

Our data analysis also contains published genomes from five Central Anatolian sites, three Western Anatolian sites, one Southeastern Anatolian site, as well as two Northern Greece sites that span in date from the Epipaleolithic (13,500 BCE) to the late Neolithic (5,600 BCE) (see Table 2). These localities cover a large span of time within a defined geographical area and contain contextual information for analyses of aDNA from Anatolia and the Aegean. We used these samples with published data from Southwest Asia and Eurasia to reconstruct the demographic connections among regional populations, especially those of the Aegean and Central Anatolia. Including an Aceramic individual from coastal Southwest Anatolia in this work could help fill a significant gap in the picture and significantly boost our knowledge of how the Aegean Neolithic developed. Both new genomes and the use of additional Anatolian sites allow us to test the demic vs. cultural diffusion model in explaining the Neolithic spread in the Aegean at its earliest stages.

2.2 Results and Discussion

We produced genome-wide sequence data with genome coverage between 0.1X and 6.32X (mean = 1.02X, median = 0.23X) per individual for 14 Neolithic individuals from Western Anatolia (Figure 1, Table 3). The samples includes genomes from Girmeler (n=1), from Ulucak (n=3) and from Bademağacı (n=10). We confirmed the authenticity of the ancient data using post-mortem damage profiles, mitochondrial contamination estimates, and the degree of X-chromosome contamination in males; we also confirmed that none of the individuals were close relatives using READ [71]. We further analyze them in the context of pre-Neolithic and Neolithic ancient genomes from a region extending from Southwest Asia and the East Mediterranean (Figure 1, see also Table 5).

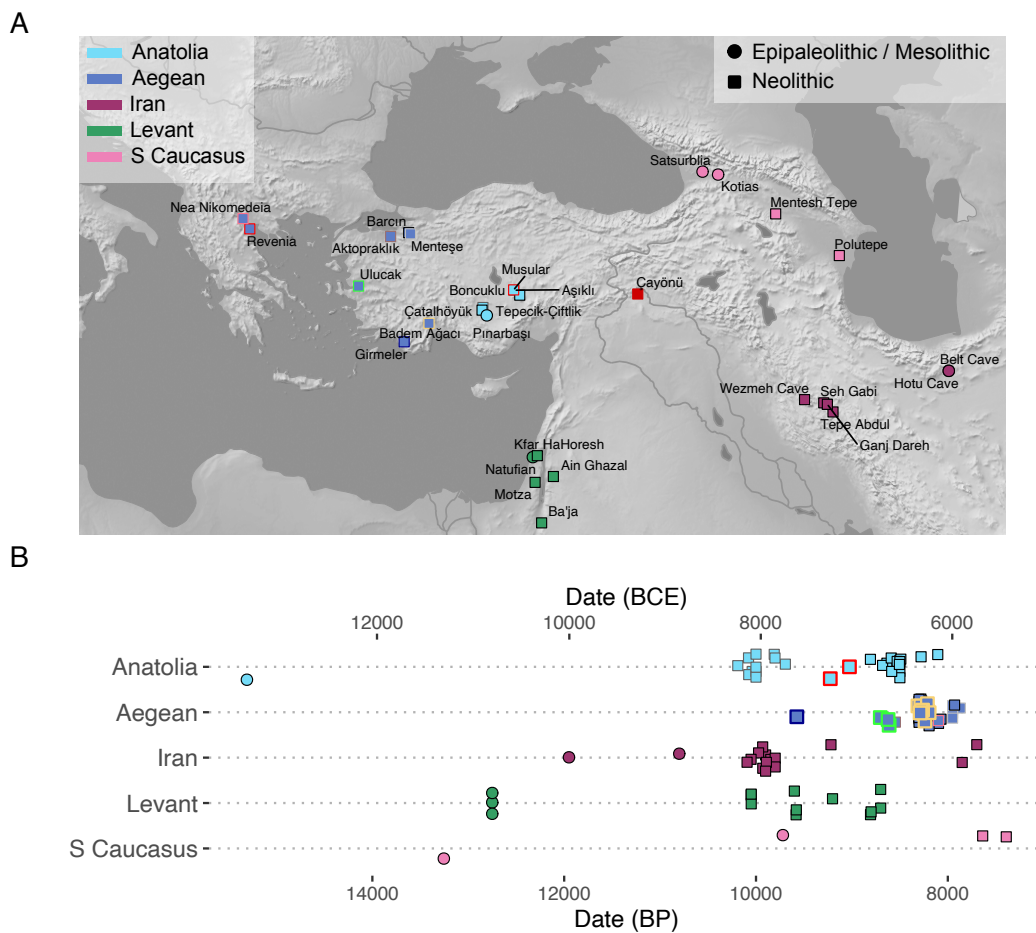


Figure 1: Summary of the data analyzed in this study. (A) Map showing the geographical locations and (b) timeline showing the date of ancient individuals investigated in the study. The colors and symbols for ancient samples are indicated in the figure. Larger symbols with colored outlines represent the new ancient individuals. To improve visualization, we used the “geom_jitter” function implemented in “ggplot”; therefore, the locations shown may slightly deviate from the exact coordinates.

Table 3: Archaeological and genetic information of the ancient individuals sequenced in this study

Settlement	Sample ID	Date (BCE/CE)	Genome Cov.	Sex	mtDNA haplogroup	Y chr haplogroup
Girmeler	gir001	7,738-7,597 BCE	0.109	XX	K1a	-
Ulucak	ulu007	6,800-6,600 BCE	0.139	XX	K1a	-
Ulucak	ulu008	6,800-6,600 BCE	0.476	XY	H	G2a2a1
Ulucak	ulu009	6,800-6,600 BCE	0.108	XY	K1a1	G2a2b2a1
Bademağacı	bad017	6,400-6,100 BCE	3.645	XX	H	-
Bademağacı	bad019	6,400-6,100 BCE	6.317	XY	T1a4	H2
Bademağacı	bad022	6,400-6,100 BCE	0.228	XY	T2b+16362	G2a2a1
Bademağacı	bad023	6,400-6,100 BCE	0.095	XY	K1a4	Unknown
Bademağacı	bad024	6,400-6,100 BCE	0.238	XX	T2c1+146	-
Bademağacı	bad025	6,400-6,100 BCE	1.443	XY	N1a1a1	J2a
Bademağacı	bad026	6,400-6,100 BCE	0.318	XY	H5	BT
Bademağacı	bad030	6,400-6,100 BCE	0.411	XY	HV+16311	T1a1
Bademağacı	bad033	6,400-6,100 BCE	0.087	XY	T2c	C1a1
Bademağacı	bad034	6,400-6,100 BCE	0.209	XX	J1c	-

2.2.1 Genetic Structure of the Aegean Neolithic Populations

We first summarised our data with PCA by calculating principal components using 49 west Eurasian populations from the Human Origins dataset. We projected 28 Central Anatolia and 54 Aegean Neolithic ancient genomes, including newly produced 14 genomes and 44 other ancient individuals from the Levant, Caucasus, Upper Mesopotamia, and Iran (Figure 2A) [72]. We further performed Multidimensional Scaling (MDS) analysis using only ancient genomes based on pairwise outgroup- f_3 -based distances (Figure 2B). Both PCA and MDS revealed results similar to those reported in prior studies, such that at least four distinct gene pools could be observed characterizing the ancestry of Southwest Anatolia in the early Holocene: (i) a Levant gene pool, (ii) a Caucasus/Iran gene pool, (iii) an Anatolian/Aegean gene pool and (iv) an Upper Mesopotamia gene pool positioned between on first three gene pools (Figure 2).

Our newly generated samples clustered within the Anatolian/Aegean gene pool. According to this clustering, the Girmeler genome, an ~9,617-year-old genome from Western Anatolia, was close to Epipaleolithic (13,642–13,073 cal BCE) and Early Neolithic Central Anatolia (8,300–7,700 cal BCE), whereas later Neolithic genomes appeared near the Neolithic Central and Aegean (7,300–5,600 cal BCE) (Figure 2).

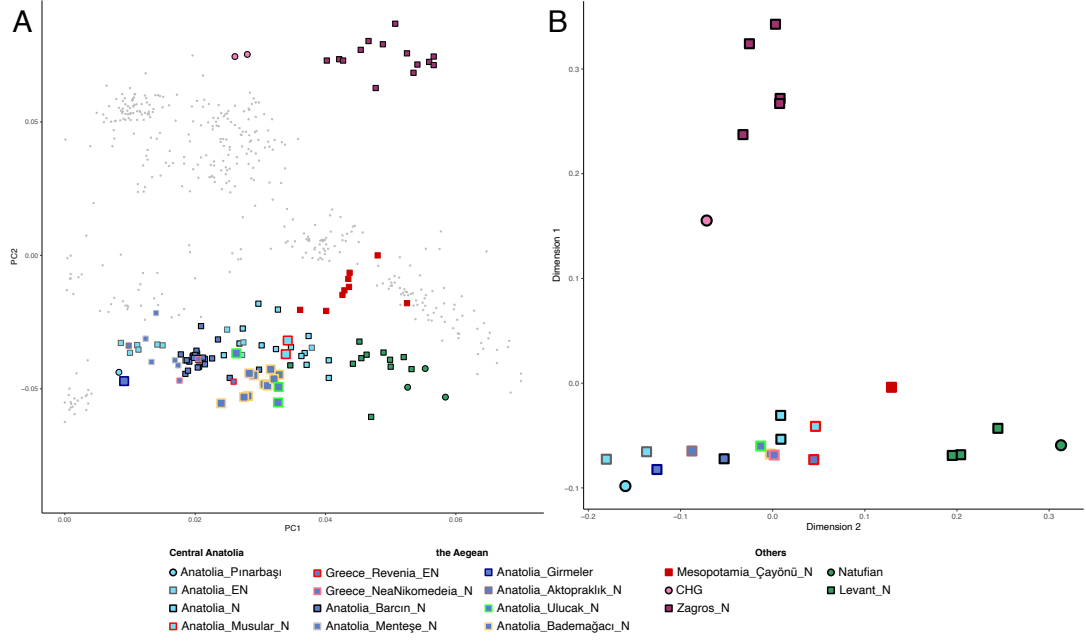


Figure 2: (A) Principal component analysis with modern and ancient genomes. The principal components were calculated using 49 modern west Eurasian populations and ancient individuals were projected onto these PCs. (B) Multidimensional scaling analysis based on pairwise f_3 -statistics among ancient populations from Southwest Asia. Larger, color-framed symbols highlight newly sequenced ancient individuals, published individuals are shown with small symbols, and present-day individuals are depicted as the smallest grey points. HG, Hunter-gatherers; N, Neolithic.

2.2.2 Characterising the ancestry profile of Girmeler genome

Girmeler (7,738 - 7,597 cal BCE), an Aceramic Neolithic population, was considered a semi-sedentary hunter-gatherer. We calculated f_4 -statistics [73] to examine whether Girmeler shared drift with early Holocene people from Central Anatolia as well as Southwest Asia.

We calculated f_4 -statistics of the form $f_4(\text{YRI}, \text{Girmeler}; \text{Pınarbaşı}, \text{PopX})$, where PopX refers to populations belonging to the different gene pool of Southwest Asia and pre-Neolithic European gene pool. In 79% of the comparisons, the Girmeler genome showed higher affinity to the Pınarbaşı genome than to other populations ($Z > -3$) (Figure 3A). We further computed f_4 -statistics of the form $f_4(\text{YRI}, \text{PopX}; \text{Girmeler}, \text{Pınarbaşı})$ and all comparisons were non-significant at $|Z| < 3$ (Figure 3C) which indicates there is no additional gene flow neither to Girmeler nor to Pınarbaşı from Southwest Asia early Holocene populations.

Using qpAdm modeling [74, 75], we could model both Pınarbaşı and Girmeler genomes as a mixture of Balkan Hunter Gatherer represented by Iron Gates populations (45-48%) and Levant Neolithic (55-52%) (Figure 3B).

Both f_4 -statistics and qpAdm results (Figure 3) showed that the earliest sample from Western Anatolia represented by Girmeler has a highly similar genetic profile to the Epipaleolithic sample from Central Anatolia (Pınarbaşı, 13,642–13,073 cal BCE) even though there is a 6,000-years gap between them.

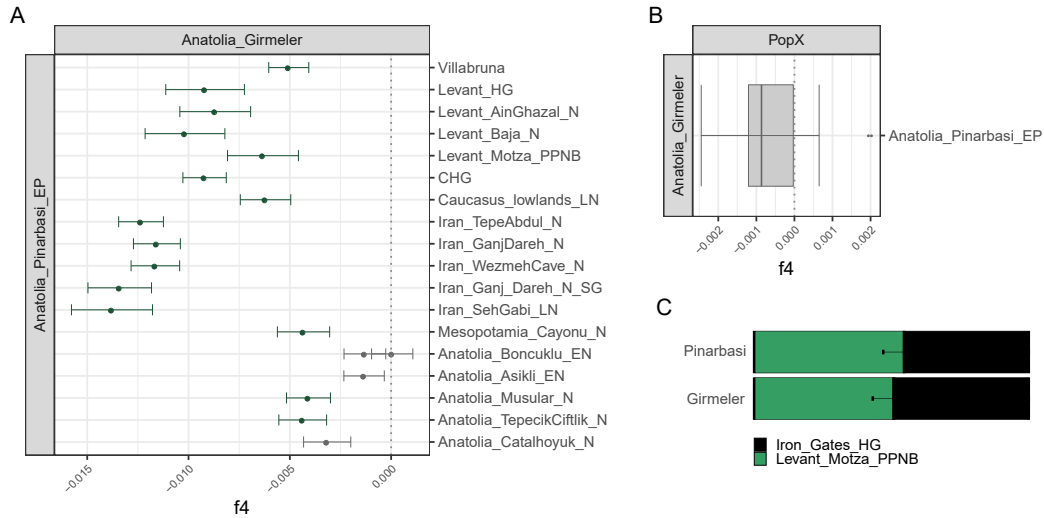


Figure 3: Genetic affinities of Girmeler and Pınarbaşı genomes. Results from (A) f_4 (YRI, Girmeler; Pınarbaşı, PopX) and (B) f_4 (YRI, PopX; Girmeler; Pınarbaşı). PopX refers to the European Hunter-Gatherers represented by Villabruna, Levant, Iran, South Caucasus pre-Neolithic/Neolithic populations and Mesopotamia Neolithic populations. All f_4 -statistics calculated by using at least 10K SNPs using all available populations in pattern, green-color show nominally significant f_4 -statistics with $|Z| > 3$, and gray color show non-significant f_4 -statistics with $|Z| < 3$. (C) qpAdm modelling for Girmeler and Pınarbaşı genomes.

2.2.3 Characterising the ancestry profile of the Aegean Neolithic populations

We then investigated the Aegean Neolithic gene pool, using Girmeler, the oldest Western Anatolian genome yet sequenced, to test whether the following Neolithic populations from the Aegean were more closely related to this lineage or to migrants from Central Anatolia as previously proposed. To test this, we calculated f_4 -statistics of the form f_4 (YRI, the Aegean Neolithic; Girmeler, Central Anatolia Neolithic). In 41 of the 48 comparisons revealed a tendency toward higher allele sharing with Girmeler ($Z < 0$), with 20% significant at $Z < -3$ (Figure 4). These findings suggest some degree of continuity between Girmeler and following early Neolithic populations from the Aegean (pre-6,000 BCE) represented by different regions of the Aegean: Aktopraklık, Barcın and Menteşe Höyük from Northwest Anatolia; Ulucak Höyük from Western Anatolia; Bademağacı Höyük from Southwest Anatolia; and Revenia and Nea Nikomedeia from Northern Greece.

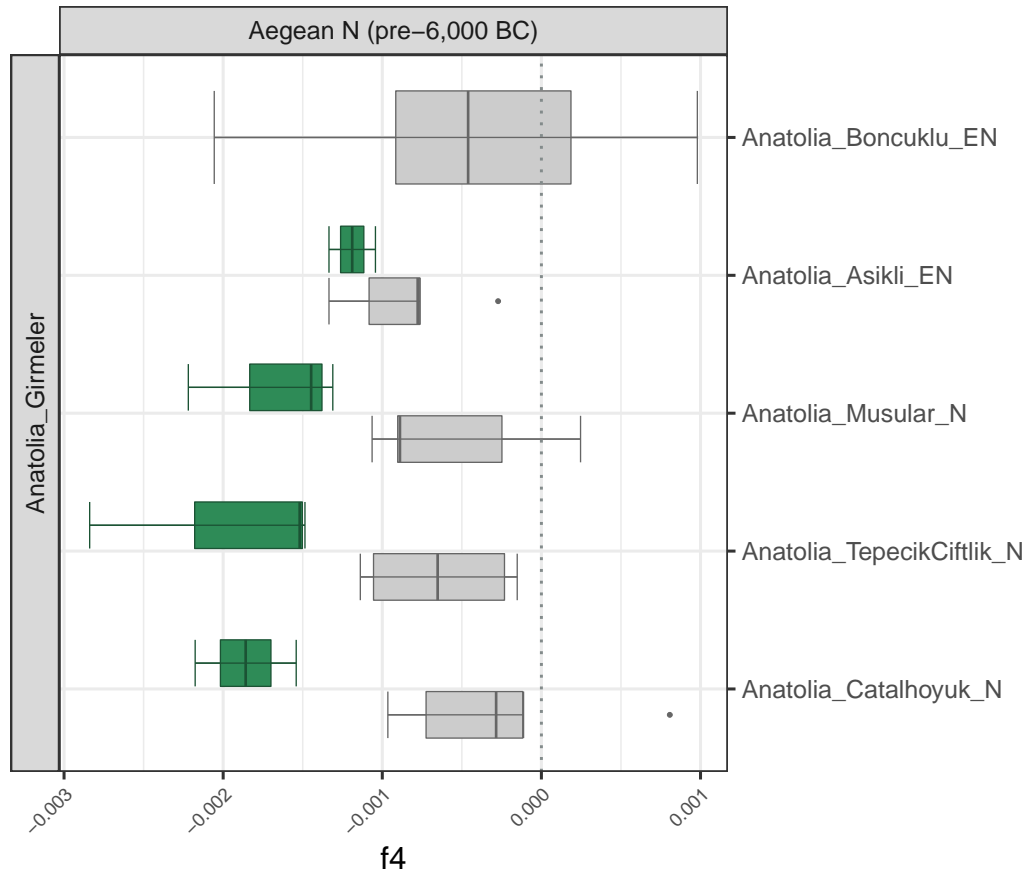


Figure 4: Genetic affinities of Aegean Neolithic populations. Results from f_4 (YRI, Aegean Neolithic (pre-6,000 BCE); Girmeler, Central Anatolia Neolithic). All f_4 -statistics calculated by using at least 10K SNPs using all available populations in pattern, green-color show nominally significant f_4 -statistics with $|Z| > 3$, and gray color show non-significant f_4 -statistics with $|Z| < 3$.

2.3 Conclusion

Anatolia was an important region that shaped the history of Eurasia during the Holocene and served as a bridge where technological and cultural innovations were produced, and cultural developments, domestic animals, and even microbes were exchanged between Europe and Asia. Although Anatolia was defined as just a bridge for many years, today it is known that Anatolia has been a heterogeneous peninsula. Each one of the regions of Anatolia has its rich and long-standing cultural history and played a vital role in an essential process in our recent history: the adoption and spread of the Neolithic lifestyle [16].

Broad-scale analyses of Neolithic genomes from the region during the last decade have led to the common narrative that "Anatolian farmers expanded into the Aegean and from there to Europe" [59, 55, 45]. However, the accuracy of this proposition is debatable [46, 50]. The exact origins of these migrations that spread farming in the Aegean and Europe are unknown.

Now, through newly generated data, we are closer to elucidating how the Neolithic emerged in the Aegean.

Previous studies have decisively shown that Aegean Neolithic populations differ from Levant or South Caucasus/Iran populations but have a very similar genetic profile to Central Anatolian Neolithic populations. However, the advent of Neolithic villages in the Aegean appeared 1,000 years later than in Central Anatolia and seemed to occur rapidly around 7,000-6,500 BCE. The rapid emergence of Neolithic villages in the Aegean region post-7,000 BCE has sometimes been interpreted as evidence of colonization [23, 15], while cultural heterogeneity among these villages has been interpreted as a sign of local population presence [26, 25]. Together with this archaeological debate, recent archeogenomic results also raise the possibility that the Neolithisation of the Aegean was carried out by the local hunter-gatherers who recently adapted farming [46, 50].

Here, we generated data from Girmeler Cave, one of the first early sedentary sites with a subsistence-based mainly on intensive hunting and gathering in Southwest Turkey. The Girmeler genome provides the first direct archaeological and genetic view of the early Neolithic (pre-7,000 BCE) in Western Anatolia. Our results revealed that the Girmeler genetic profile is highly similar to the Pınarbaşı Epipaleolithic genome from Central Anatolia. This genetic similarity between these two semi-sedentary hunter-gatherers suggests that these populations were descendants of the same populations whose ancestors expanded to Anatolia after the LGM. We also observed that post-Girmeler Neolithic Aegean populations share more alleles with Girmeler than Central Anatolia (Figure 4). Aegean Neolithic communities would show a higher genetic affinity to Central Anatolian Neolithic populations rather than Girmeler if the Neolithic transition of the Aegean was carried out by immigration from Central Anatolia. Our findings instead suggest that the first Aegean farmers may have been local hunter-gatherers who later adopted farming post-7,000 BCE by acculturation rather than colonists from Central Anatolia. This conclusion is in line with archaeological evidence that points to diverse cultural dynamics in the Aegean, such as the extensive use of obsidian from the Aegean island of Melos or the absence of Southeastern traditions for the manufacture of lithic tools, such as pressure flaking, in the area before the 7,500 BCE [26, 25, 61]. If so, acculturation could have had a more prominent role, at least during its early stages (pre-6,000 BCE), than currently accepted. Thus, this would have two major implications: (i) it would support acculturation as a mode of the Neolithic spread, at least during its early phases (pre-6,000 BCE), and (ii) it would suggest that the Neolithic expansion may have initiated from the Aegean, instead of the Anatolian mainland, as commonly assumed in the literature.

However, we currently know nothing about the genetic profile of pre-Neolithic Aegean populations. This problem can be entirely resolved after learning more about the Mesolithic Aegean and more data from Neolithic settlements.

CHAPTER 3

TRACKING POPULATION STRUCTURE OF SOUTHWEST ASIA AND THE EAST MEDITERRANEAN HUMAN POPULATIONS THROUGH TIME FROM ANCIENT AND MODERN DNA

3.1 Introduction

Human mobility can be a driver of sociocultural change, but also an outcome. Studying spatiotemporal patterns of mobility together with sociocultural transitions is of critical importance to understanding human history. Southwest Asia and the East Mediterranean present an attractive case here, with their exceptionally long history of food-producing societies. The region was the centre stage of key cultural and social transformations during the Holocene, from the earliest sedentary villages and agriculture, to the earliest metallurgy, the emergence of state-organized societies, the first writing systems, and more recently, inter-regional empires (see Chapter 1 and Table 1). This period also witnessed changes that directly affected human mobility, such as population growth, the establishment of long-distance trade networks supported by transport animals and road construction, the organization of invading armies, and mass deportations [76, 77, 28, 78, 79, 80].

Recently, archaeogenomic studies have revealed a number of interesting observations on inter-regional mobility in Southwest Asia and the East Mediterranean. One such finding is that within-population genetic diversity levels were low in the early Holocene, but increased following the Neolithic transition [50, 81, 82, 83, 45]. A parallel observation is that inter-population genetic differentiation, as measured by F_{ST} , was high among West Eurasian human groups before the Neolithic, but dropped sharply during the Neolithic and Chalcolithic periods [82, 83, 51]. Low genetic diversity and high F_{ST} observed by initial Holocene indicates population isolation in earlier periods. This changed with the Neolithic period, especially with the westward and eastward Neolithic expansions around 9,000 BP, leading to rapid admixture and consequent genetic homogenization across the region. However, the temporal decrease in inter-population differentiation (average F_{ST}) appears to reach a plateau out with the Chalcolithic and Bronze Ages [82, 83, 51].

Similar to F_{ST} , the results from ancestry component analyses reveal widespread inter-regional admixture from the Neolithic to the Bronze Ages, especially between eastern (Iran and South Caucasus) and western (Anatolia and Levant) Southwest Asia, and also extending into the

Aegean [84, 85, 49, 86, 87, 46, 51, 88, 54, 89, 90, 47]. For instance, by the Early Bronze Age, Anatolian groups carried approximately 50% ancestry of eastern origin (related to early Holocene South Caucasus/Iran populations), while Iran/Zagros populations carried approximately 50% ancestry of western origin (related to early Holocene Anatolian populations) [54, 89]. Steppe- or West Siberia-related gene flow is also observed in the region during the Bronze Age, albeit at lower levels and not ubiquitously [84, 85, 87, 51, 54, 89, 90]. Conversely, changes in admixture components appear to be more modest in the period between the Bronze Age and the present-day. Analyses on past and extant populations of present-day Iran [91], of the Levant [92, 86, 87], of the Caucasus [93, 90], and of present-day Greece have suggested limited or even no observable change in ancestry components over the last 3,000-4,000 years [88, 85]. While singular ancient genomes with non-local ancestry are occasionally discovered, these mobility events appear to not have left substantial traces in the local gene pools from the Bronze Age onwards [94, 87, 54, 89].

On the surface, these observations imply increasing genetic stability and possibly a decrease in mobility after the Bronze Age. However, this would be at odds with rich archaeological, historical and linguistic evidence for regional human movements in the same period, from the establishment of trade colonies to forced population transfers. A number of non-exclusive explanations could be conceived here. (1) Increase in genetic stability may be a real effect. For instance, large resident populations that emerged by the Bronze Age may have diluted the genetic impact of immigrants [82, 87]. (2) The signals of genetic stability increase or the plateau in homogenization may be technical artefacts: (2a) F_{ST} may not be the optimal statistic to gauge rates of inter-population migration, as it is influenced by within-population diversity and is sensitive to population size changes. (2b) The relative homogenization of regional gene pools by the Bronze Age may have rendered mobility events less visible to F_{ST} or qpAdm analyses. (2c) Low amounts of gene flow simultaneously occurring from diverse external sources may not be visible to F_{ST} or qpAdm analyses, especially using low coverage genomes. (2d) The sparsity of the post-Bronze Age samples from the region may not be sufficiently representative of demographic changes in this period. In fact, the latter two possibilities are supported by recent analyses of a relatively rich temporal sample from the Levant [87], which reported subtle admixture from the Iron Age to the Ottoman Period from external regions (the Steppe, Africa, South Asia, and Central Asia).

The tempo of inter-regional human mobility in Southwest Asia and the East Mediterranean during the Holocene thus remains an unsettled issue. Here, we systematically study this problem using published ancient and modern-day genomes complemented with 35 newly generated ancient genomes and 15 radiocarbon dates (see Table 4). We start by describing the overall genetic structure of the region and characterising the new genomes. We then explore temporal shifts in within-population diversity and inter-regional divergence and analyse inter-regional differences in mobility rates. Finally, we tackle the question of possible sex-bias in human mobility, given earlier suggestions of long-term matrilineal continuity in the region [95, 96, 97].

3.2 Results and Discussion

Our study focuses on human population dynamics on five geographically and culturally connected regions (Figure 5): (1) Anatolia, which we describe as the peninsula to the west of the Anatolian diagonal (the mountain range extending between the North Levant and the eastern Black Sea coast of present-day Turkey); (2) the Aegean, including sites from the present-day Greek mainland, Cyclades, and Crete; (3) present-day Iran (the Zagros area and South Caspian); (4) South Caucasus, comprising present-day Georgia, Southwest Russia, Armenia, Azerbaijan; (5) the Levant, comprising present-day West Syria, Lebanon, Palestine, Israel, and Jordan. These regions contain the highest intensity of published ancient genomes in Southwest Asia and the East Mediterranean (for which reason we did not include Mesopotamia or the Arabian Peninsula).

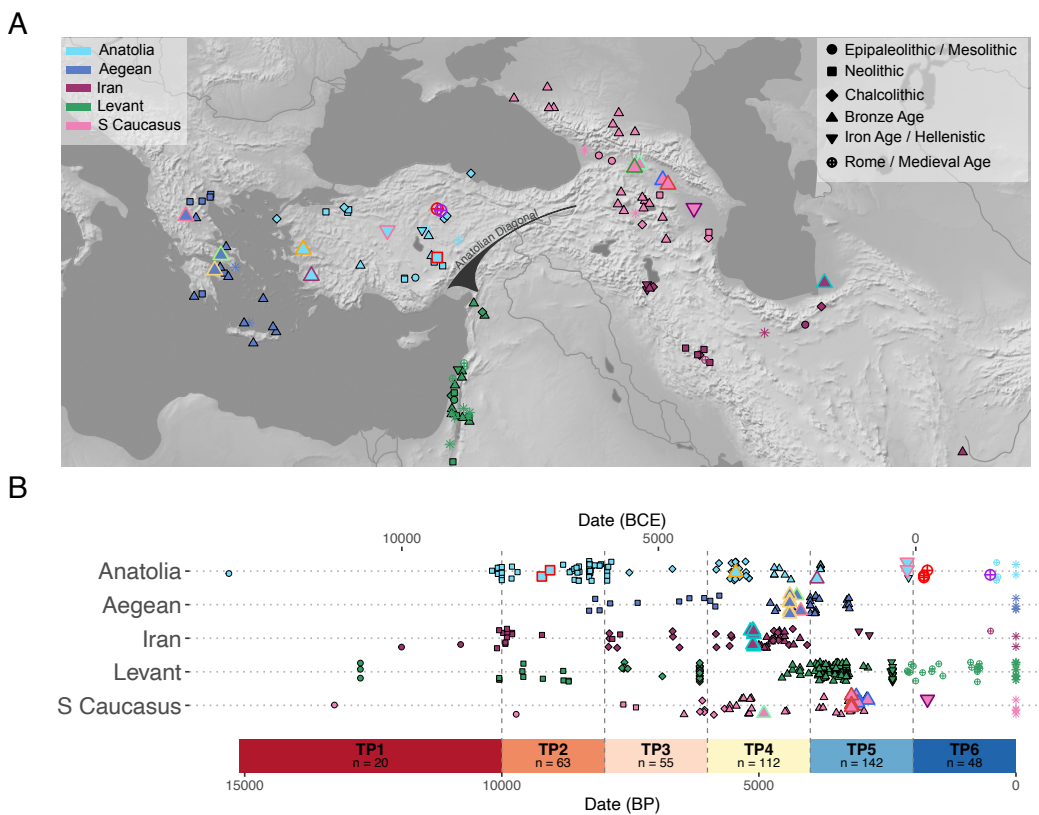


Figure 5: Geographical location of archaeological sites and dates of samples. (A) The locations and (B) dates of ancient individuals analysed in this study. TP denotes “Time Period”. Larger symbols with colored outlines represent the new ancient individuals; present-day samples are shown with an asterisk. To improve visualization, we used the “geom_jitter” function implemented in “ggplot”; therefore the locations shown may slightly deviate from the exact coordinates.

We produced 35 new ancient shotgun-sequenced genomes with coverages ranging between 0.02X and 7.5X per genome (mean = 1.11X, median = 0.33X) from Anatolia (n=10), the Aegean (n=3), Iran (n=9), and South Caucasus (n=6). The Anatolian samples included

genomes from Musular of Neolithic Central Anatolia (n=2), from Ulucak (n=1) and Çine-Tepecik (n=1) of Bronze Age Western Anatolia, from Gordion (n=2) of the Iron Age/Hellenistic Central Anatolia, and from Boğazköy in Central Anatolia dating to the Roman Period (n=3) and the Ottoman Period (n=1). The Aegean samples included Bronze Age genomes from Theopetra cave (n=1), Sarakinos cave (n=1) and Perachora cave (n=5) in mainland Greece. The Iran samples included Bronze Age genomes from the Shah Tepe site in North-east Iran near the Caspian Sea (n=9). The South Caucasus sample included Bronze Age genomes from Didnauri (n=3), Doghlauri (n=2) and Nazarlebi (n=3) in Georgia and an Iron Age genome from the Shamakhi in Azerbaijan (Table 4, Figure 5). We confirmed the authenticity of the ancient data using post-mortem damage profiles, mitochondrial contamination estimates, and the degree of X-chromosome contamination in males; we also confirmed that none of the individuals were close relatives by using READ [71]. We further collected 382 ancient published genomes, with dates ranging from 15,000 BP to 350 BP, as well as 23 published genomes from present-day individuals [38] from these five regions. By combining our new samples with published data we obtained a Holocene time transect with 440 genomes from Anatolia (n=106), the Aegean (n=43), the Levant (n=173), South Caucasus (n=52), and Iran (n=66) (Figure 5, Table 5). The new genomes extend the geographic and temporal coverage of the published sample, for instance by including South Caucasus Iron Age and Roman period in Anatolia. With the combined dataset we called SNPs using either 4.7 million SNPs ascertained in modern-day sub-Saharan African populations from the 1000 Genomes Project [98] or the 1240K SNP list [59] (see also Chapter 4).

Instead of grouping populations based on archaeological periodization, we decided to use temporal groups because of the difficulty in assigning matching cultural identities across regions. We thus divided the time range into six time periods (TP): TP1 ($\geq 10,000$ BP], TP2 (10,000 – 8,000 BP], TP3 (8,000 – 6,000 BP], TP4 (6,000 – 4,000 BP], TP5 (4,000 – 2,000 BP] and TP6 (2,000 BP - present] (Figure 5).

Table 4: Archaeological and genetic information of the ancient individuals sequenced in this study

Sample ID	Location	Av. Date (BP)	Date (BCE/CE)	Genome Cov.	Sex	mtDNA haplogroup	Y chr haplogroup
BOG019	Boğazköy, Turkey	1725	100-350 CE	0.326	XY	X2n	T1a1a
BOG020	Boğazköy, Turkey	1790	130-190 CE	2.202	XY	X2f	BT
BOG024	Boğazköy, Turkey	1790	130-190 CE	0.484	XY	H13c1a	J2a1
BOG028	Boğazköy, Turkey	500	1000 - 1900 CE	1.332	XX	HV1b3b	-
CTG025	Çine-Tepecik, Turkey	3869	1977-1772 calBCE	0.191	XX	W6b	-
GOR001	Gordion, Turkey	2116	333 BC -0	7.548	XY	H14a	J2a1

Table 4 (continued)

Sample ID	Location	Av. Date (BP)	Date (BCE/CE)	Genome Cov.	Sex	mtDNA haplogroup	Y chr haplogroup
GOR002	Gordion, Turkey	2116	333 BC -0	0.074	XX	K1a3	-
mus005	Musular, Turkey	9222	7377-7167 BCE	2.463	XX	K1a4	-
mus006	Musular, Turkey	9060	7180-7039 BCE	0.140	XY	N1a1a1b	F
ulu117	Ulucak, Turkey	5450	4000-3000 BCE	0.360	XX	J1c11	-
G23	Theopetra, Greece	4187	2335-2140 calBCE	0.426	XY	H5	I2a2a1b
G37	Sarakinos, Greece	4262	2325-2300 calBCE	0.228	XY	H11a2	J
G31	Perachora, Greece	4400	2700-2200 BCE	0.213	XY	J1c2	J
G62	Perachora, Greece	4400	2700-2200 BCE	0.628	XY	J1c	G2a2b2a
G65	Perachora, Greece	4400	2700-2200 BCE	0.271	XX	T2c1d+152	-
G66	Perachora, Greece	4400	2700-2200 BCE	0.112	XX	H2a	-
G76a	Perachora, Greece	4407	2565-2350 calBCE	0.739	XX	T2c1+146	-
geo005	Didnauri, Georgia	3104	1257-1051 calBCE	0.077	XY	U7b	NA
geo006	Didnauri, Georgia	2881	1017-846 calBCE	0.046	XY	X2	O1b1a2
geo015	Doghlauri, Georgia	4902	3015-2890 calBCE	0.189	XY	K1a	J2a1b1
geo017	Doghlauri, Georgia	3155	1291-1119 calBCE	0.033	XX	H4b	-
geo029	Didnauri, Georgia	3077	1219-1036 calBCE	0.092	XY	I5c	R1b1a2a2
gur016	Nazarlebi, Georgia	3250	1500-1000 BCE	0.021	XY	K2a2	H1b1
gur017	Nazarlebi, Georgia	3250	1500-1000 BCE	0.215	XY	N1a1a1a	I
gur019	Nazarlebi, Georgia	3251	1500-1000 BCE	0.030	XX	K1a4b	-
zrj003	Shamakhi, Azerbaijan	1722	133 - 324 calCE	0.273	XY	K1a19	J1
sha003	Shahtepe, Iran	5100	3200 - 3100 BCE	3.346	XX	H14	-
sha004	Shahtepe, Iran	5121	3240 - 3102 calBCE	3.877	XY	I1a	J1

Table 4 (continued)

Sample ID	Location	Av. Date (BP)	Date (BCE/CE)	Genome Cov.	Sex	mtDNA haplogroup	Y chr haplogroup
sha006	Shahtepe, Iran	5100	3200 - 3100 BCE	2.548	XX	J1b1b1	-
sha007	Shahtepe, Iran	5121	3242 - 3101 calBCE	3.945	XX	HV13b	-
sha008	Shahtepe, Iran	5100	3200 - 3100 BCE	1.805	XX	K1a12a	-
sha009	Shahtepe, Iran	5165	3344 - 3086 calBCE	0.250	XX	U5a2+16294	-
sha010	Shahtepe, Iran	5100	3200 - 3100 BCE	1.400	XX	HV2	-
sha012	Shahtepe, Iran	5100	3200 - 3100 BCE	1.075	XY	U1a	J1a3
sha014	Shahtepe, Iran	5100	3200 - 3100 BCE	1.996	XY	HV13b	T1a

3.2.1 Genetic structure and continuity in Southwest Asia and the East Mediterranean

We first performed principal components analysis (PCA) by projecting ancient genomes onto the first two PC spaces calculated using present-day West Eurasians. This recapitulated geographic differentiation patterns, with PC1 being correlated with the north-south, and PC2 with east-west differentiation across Southwest Asia and East Mediterranean. All 35 new ancient genomes clustered with previously published samples from broadly the same periods and regions (Figure 6). Beyond this general picture, we also investigated the PC locations of ancient genomes across time. We observed that, over time, genome pools of different regions converged in PC space, especially from TP1 to TP5 (Figure 7). This would be in line with the homogenization model [82, 83, 51]. However, regional clustering, or structure, was still visible in PC space for all periods, and we could also infer some degree of regional population continuity over time to a certain degree.

We next formally tested population structure and regional continuity using f_4 -statistics [73]. To test the former, we asked whether individuals from a specific region X from time period i (IndvXi) share more alleles with the sample (excluding that individual) from the same region and time period (PopXi) by calculating the f_4 -statistics between the region X and any other region Y as $f_4(\text{YRI}, \text{IndvXi}; \text{PopYi}, \text{PopXi})$, where PopXi and PopYi refer to the populations sampled from region X and Y, respectively. In 1,718 such tests, 85% revealed a tendency toward higher allele sharing with local genomes, with 46% significant at $p < 0.05$ after Benjamini-Hochberg correction for multiple testing. Only 4% of the tests were significant in the other direction, in support of widespread regional structure (Figure 8).

To test regional population continuity over time, as opposed to replacement, we compared each time period's samples per region, with the following two time periods, calculating

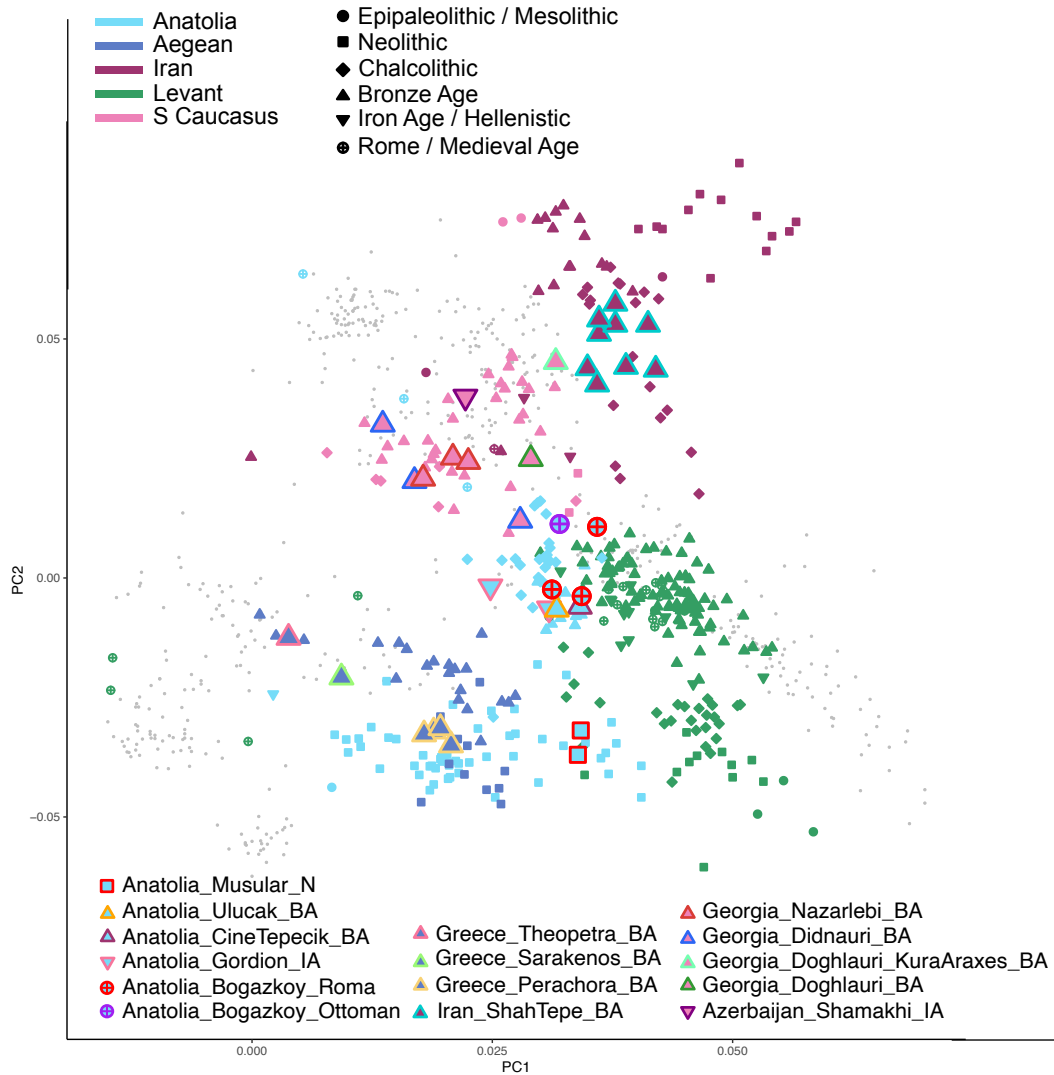


Figure 6: Principal Component Analysis (PCA). The plot shows the first two principal components calculated using genomes of 946 contemporary west Eurasian populations, onto which a total of 406 ancient individuals were projected. Newly sequenced ancient individuals are highlighted by larger, color-framed symbols, while published individuals are shown with small-symbols, and present-day individuals are depicted as smallest grey points. N, Neolithic; BA, Bronze Age; IA, Iron Age.

$f_4(\text{YRI}, \text{PopXi}; \text{PopXi}+1, \text{PopXi}+2)$, where PopXi, PopXi+1, PopXi+2 are populations from region X and from time periods i, i+1, and i+2. In 18 of the 19 comparisons we found higher allele sharing with the subsequent period (multiple testing-corrected $p < 0.05$) (Figure 9). These findings suggest continuity is the general pattern, although some cases do reveal strong shifts in the gene pool, as we describe in the following.

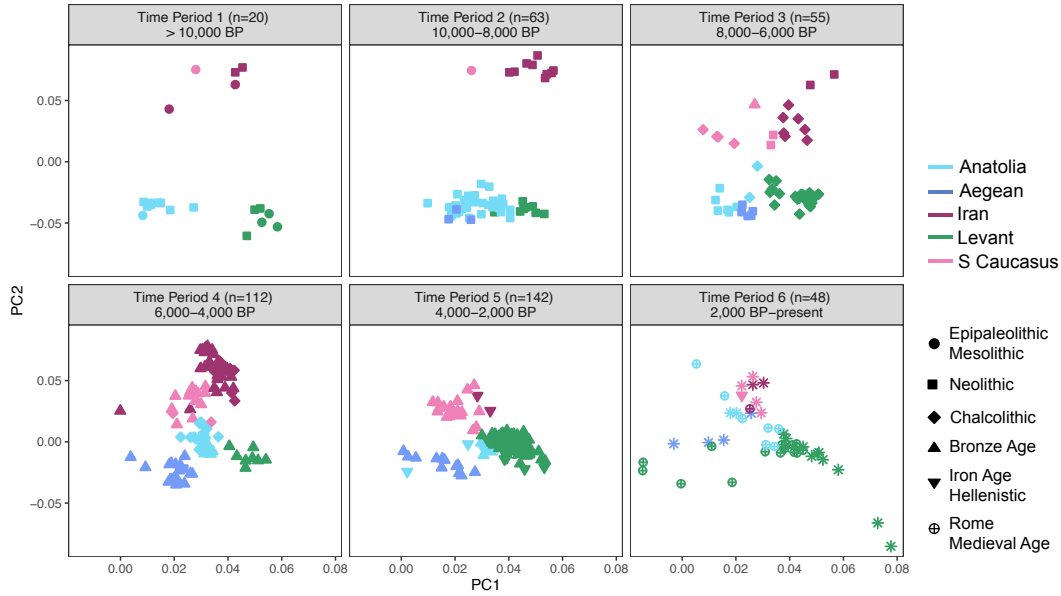


Figure 7: Regional genomes converging in PC space over time. The plots show ancient samples projected on the PC space constructed using 49 contemporary West Eurasian populations as in Figure 6. The colours and symbols for each individual are the same as in the main PCA in Figure 6.

3.2.2 Regional mobility as reflected in ancestry components

In the presence of regional genetic continuity, genomes from different time periods can be modelled as mixtures of early Holocene populations from Southwest Asia and the East Mediterranean as well as other regions. This would also uncover any homogenization signals and suggest plausible sources of gene flow. We thus performed qpAdm modelling [74, 75] on our newly generated genomes as well as previously published genomes from the five regions to describe changing sources of ancestry over time (Figure 10).

3.2.2.1 Anatolia

Earlier work had shown that Central Anatolia Ceramic (i.e., late) Neolithic groups, compared to those from the earlier Aceramic Neolithic period, carried additional southern (Levant-related) and eastern (Zagros/Caucasus-related) ancestry components [49, 46, 47]. Here, we report the earliest Anatolian Neolithic genomes that carry these admixture signals in Musular_N. Musular is an Aceramic site, but its genetic ancestry profile appears similar to mid-9th millennium BP Çatalhöyük of the Ceramic period. This suggests that putative eastern and southern gene flow events into Central Anatolia had occurred prior to the 10th millennium BP (Figure 10).

In the post-Neolithic period, our qpAdm results show that the Central Anatolia's gene pool can be described as a two-way admixture between Anatolian Neolithic ancestry and additional

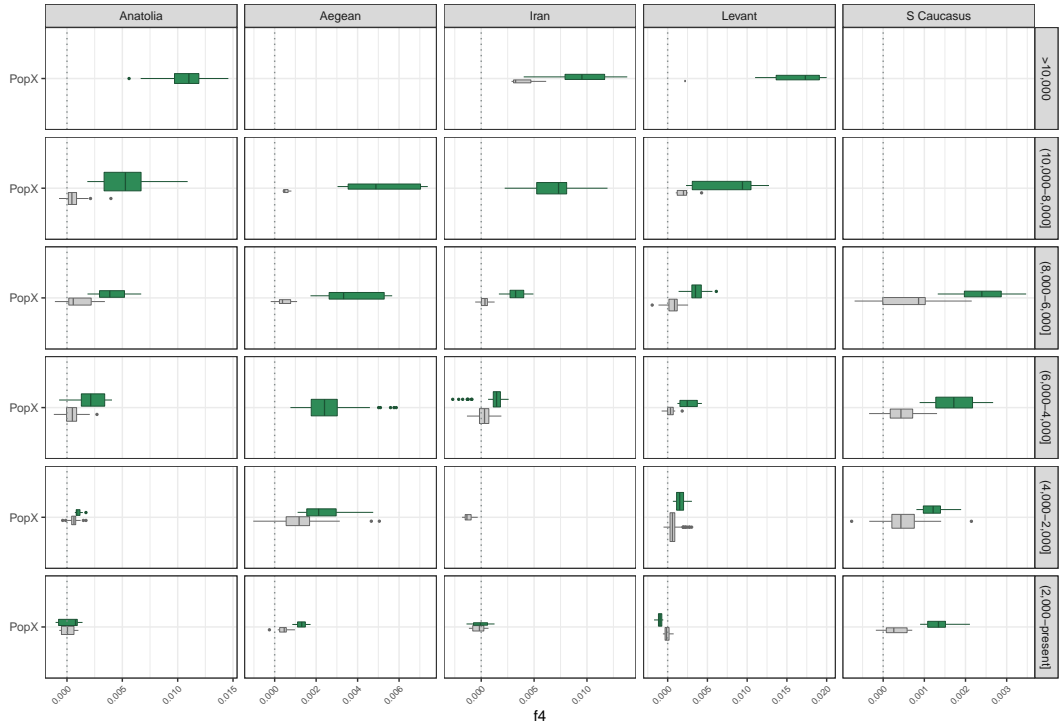


Figure 8: Testing degree of geographic structure and regional continuity over time in South-west Asia and the East Mediterranean. Results from $f_4(\text{YRI}, \text{IndvXi}; \text{PopYi}, \text{PopXi})$, where IndvXi is a individual genome of a specific region X from time period i , PopXi is samples of Region X (excluding that IndvXi) from time period i and PopYi is any other population. Boxplots show all f_4 -statistics calculated by using at least 10K SNPs using all available individuals/populations in pattern, green-color boxplots show significant f_4 -statistics with p -value < 0.05 and gray color show non-significant f_4 -statistics.

South Caucasus/Iran-related ancestry. Little to no Eastern Hunter-Gatherer (EHG)/Steppe-related ancestry is detected in Anatolia, as opposed to that in Europe, including neighboring mainland Greece [88, 85]. The only exception to this pattern was the Kaman Kalehöyük IA individual, that carried EHG-related ancestry, which could be related to historically known interactions between Central and West Anatolia and Southeast Europe that continued during the Iron Age [99, 100]. However, this individual does not appear to have left a legacy in the gene pool, at least given the lack of EHG ancestry in Boğazköy Roman individuals from Central Anatolia ($n=3$) (Figure 10, Figure 11).

Finally, the genomes of Ottoman individuals from Boğazköy and Kaman Kalehöyük carried variable levels of additional Baikal Neolithic-related alleles (0-50%), most likely representing heterogeneous levels of Turkic admixture in the 1st millennium BP, a signature detectable in the present-day Anatolian gene pool (Figure 10, 11, see also [101]).

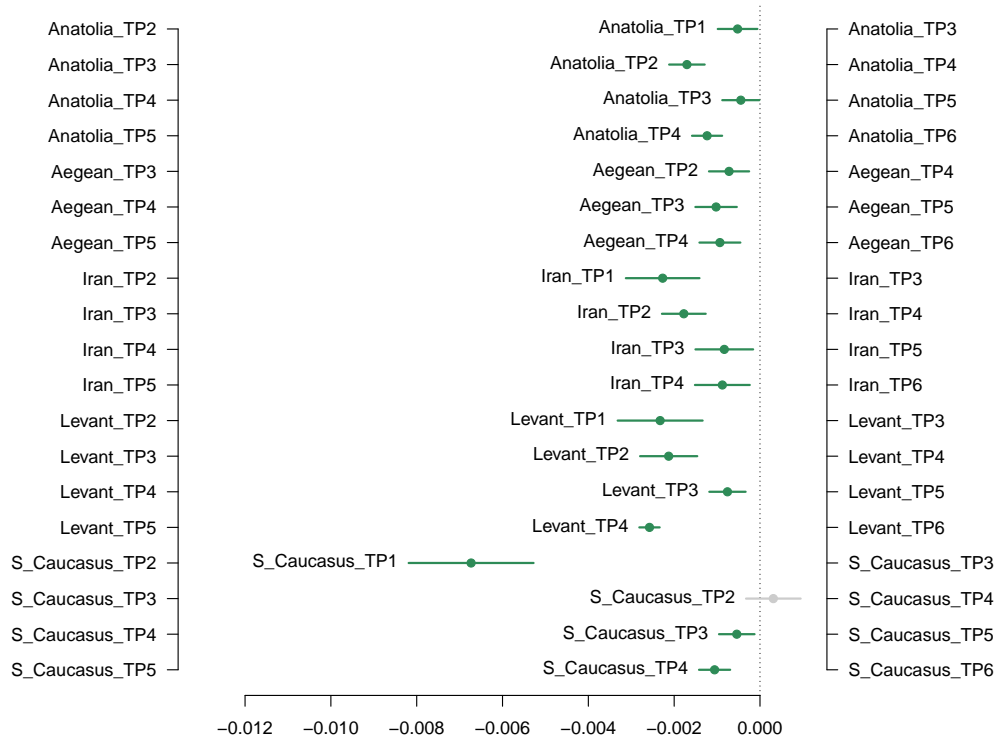


Figure 9: Testing regional population continuity over time in Southwest Asia and the East Mediterranean. Results from f_4 -statistics of the form $f_4(\text{YRI}, \text{PopXi}; \text{PopXi}+1, \text{PopXi}+2)$ calculated by using at least 10K SNPs, where PopXi, PopXi+1, PopXi+2 are populations from region X and from time periods i, i+1, and i+2, respectively. Green-color show significant f_4 -statistics with p-value < 0.05 and gray color show non-significant f_4 -statistics.

3.2.2.2 The Aegean

Recent studies showed the Neolithic Aegean populations were genetically highly similar to Anatolian Ceramic Neolithic populations, especially to the Western Anatolian Neolithic population represented by Barcın Höyük [55, 46, 88]. During the transition from the Neolithic to the Bronze Age (BA) the Aegean received eastern (South Caucasus/Iran-related) gene flow, in parallel with Anatolia, but further received a variable degree of EHG/Steppe-related ancestry [88, 85]. Accordingly, in our qpAdm analyses we could describe Bronze Age Aegeans via two- or three-way mixture models of Aegean Neolithic-related populations (60-83%), South Caucasus/Iran-related populations (12-20%), and EHG-related populations (0-25%). Notably, there was no evidence for EHG-related ancestry in Early BA individuals, including our earliest samples from Perachora (Figure 10, 12). Later BA individuals, however, including the new samples from Sarakinos and from Theopetra, as well as published Aegean MBA individuals, showed strong genetic affinity to EHG/Steppe populations and carried 17-25% EHG-related ancestry (Figure 10, 12). This confirms the earlier observation of a gradual and partial diffusion of EHG-related ancestry in present-day Greece [85] and further informs the current discussion about the timing of the first arrival(s) of people of Steppe-related ancestry in the Greek Mainland. Based on our new data, this appear to have started by c.4200 BP, thus

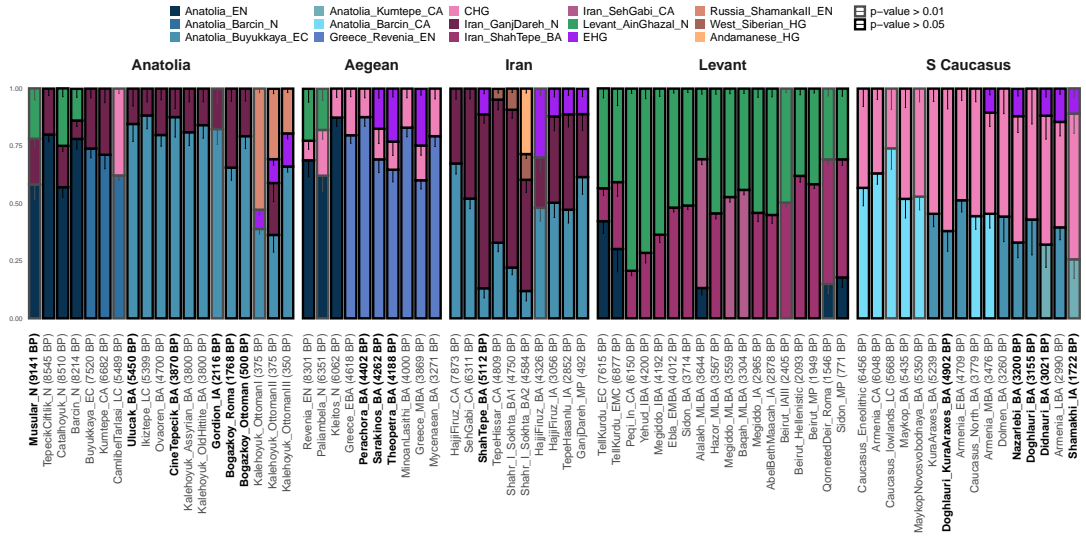


Figure 10: qpAdm models for Neolithic and post-Neolithic populations of Southwest Asia and the East Mediterranean. Each modelled genome or group of genomes is represented by columns in temporal order; the average dates are indicated in parentheses. All source populations are colour coded and shown above the figure. Vertical bars represent the coefficients of source populations. Error bars show one standard error. The border colours of the models that yielded p-values > 0.05 are shown in black, while those models that yielded p-value > 0.01 are shown in grey. Newly generated samples are highlighted in bold on the x-axis. Only those genomes that yielded reliable models were reported in the figure.

pushing these arrivals back into the late Early Bronze Age, i.e. before the beginning of the Middle Bronze Age as hitherto known.

3.2.2.3 Iran

Our qpAdm modelling consistent with f_4 -statistics showed that both during and after the Neolithic period, populations in Iran received gene flow from both western (Anatolia-related) and/or northern eastern (Central Asia-related) sources [51, 54]. However, these admixture events were not homogeneous across Iran. Northwest and Central Iran (Zagros) populations exhibit higher Anatolia-related ancestry (48-67%) than Northeast Iran (18-30%) (Figure 10, 13). Moreover, during the Chalcolithic and Bronze Age, individuals from Northeast Iran exhibit additional North Eurasian-related ancestry, represented by EHG or the West Siberian Hunter Gatherer sample (WSHG) (5-11%) (Figure 10, 13). This is notable as this occurs before the Yamnaya dispersal, as noted earlier [54]. This result is also consistent with material culture records from Northeast Iran in the Chalcolithic and Bronze Age, which show the influence of the Central Asian culture across various sites, including Shah Tepe [102, 103], from which we have produced genomes of 9 individuals.

During the Bronze Age and later periods, North Eurasian-related ancestry (11-30%) also appears in individuals from Northwest and Central Iran (Hajji Firuz BA, Hasanlu IA, Ganj Dareh

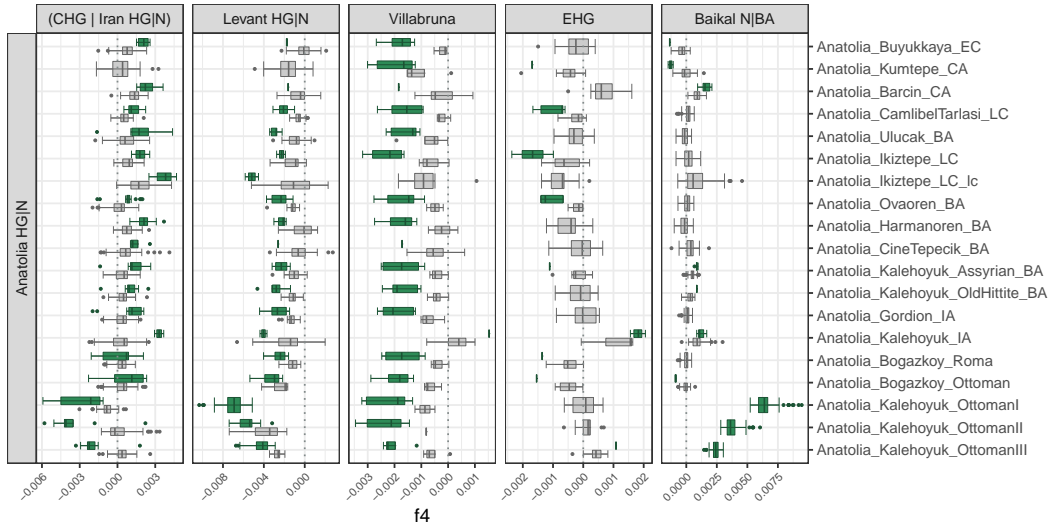


Figure 11: Genetic Affinity of Post-Neolithic Anatolian Populations. Results from f_4 (YRI, Test; Anatolia HG | N, Post Neolithic Anatolian). Test refers to the South Caucasus/Iran or Levant pre-Neolithic/Neolithic populations, Villabruna, EHG and Baikal populations. Boxplots show all f_4 -statistics calculated by using at least 10K SNPs using all available populations in pattern, green-color boxplots show nominally significant f_4 -statistics with $|Z| > 3$ and gray color boxplots show non-significant f_4 -statistics with $|Z| < 3$.

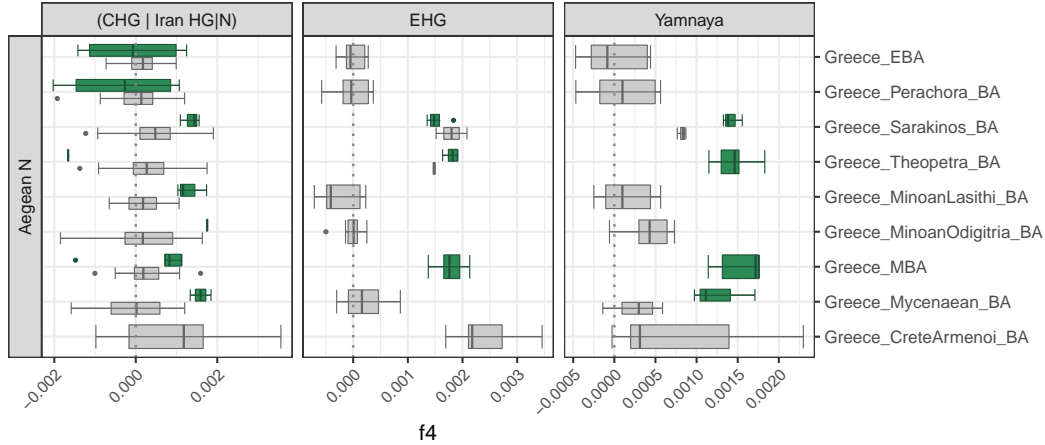


Figure 12: Genetic Affinity of Post-Neolithic Aegean Populations. Results from f_4 (YRI, Test; Aegean N, Post Neolithic Aegean). Test refers to the South Caucasus/Iran pre-Neolithic/Neolithic populations, EHG and Yamnaya populations (Table S3). Boxplots show all f_4 -statistics calculated by using at least 10K SNPs using all available populations in pattern, green-color boxplots show nominally significant f_4 -statistics with $|Z| > 3$ and gray color boxplots show non-significant f_4 -statistics with $|Z| < 3$.

MP). While the Hajji Firuz BA individual exhibited substantial EHG-related ancestry (30%), later individuals carried lower degrees of EHG-related ancestry (11-12%) (Figure 10, 13).

North Eurasian-related ancestry in these individuals could be also represented by WSHG or Botai Neolithic populations from Kazakhstan instead of EHG. Whether this North Eurasian-related ancestry spread through Iran from Northeast Iran or additional gene flow related to the Yamnaya expansion in Central Asia [54] was responsible, still remains unclear.

The history of Southeast Iran populations represented in Shahr-I Sokhta were more complex. Genetically there existed two distinct populations at this site. Shahr-I Sokhta-BA1 can be modelled similarly as Northeast Iran populations, while Shahr-I Sokhta-BA2 seem to exhibit additional Andamanese HG-related ancestry (Figure 10, 13), hypothesised to reflect human movement from South Asia and possibly related to the Indus Valley Civilisation [54]. In contrast to EHG-related ancestry, we do not observe this South Asian ancestry in later-coming individuals from Northwest and Central Iran.

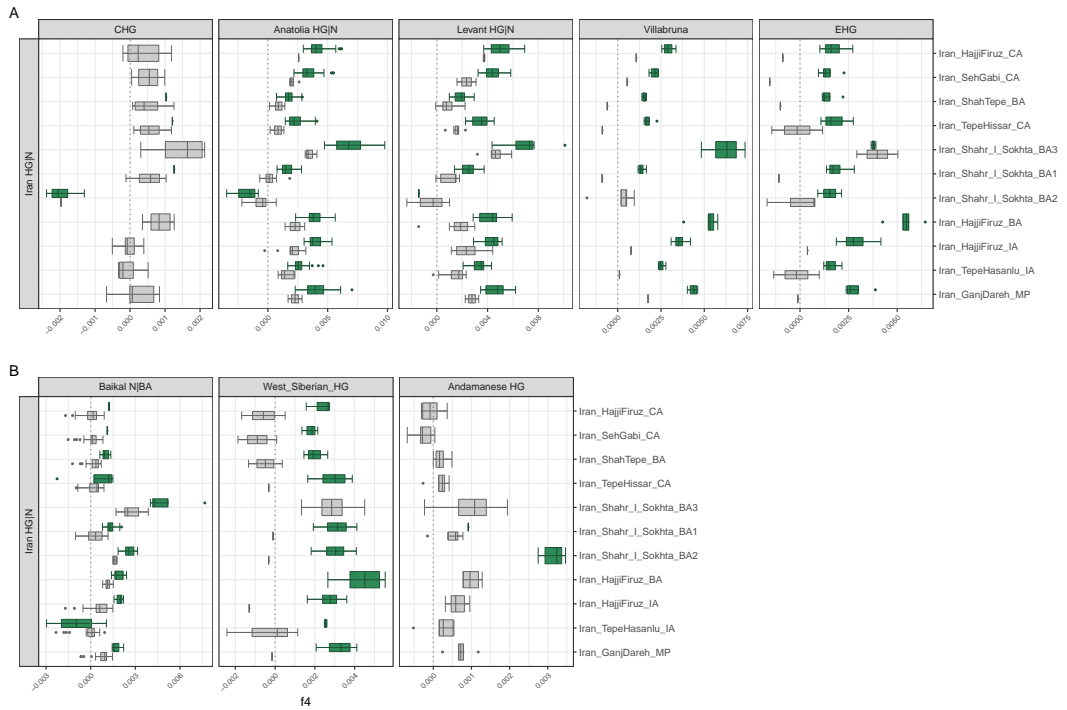


Figure 13: Genetic Affinity of Post-Neolithic Iran Populations. Results from f_4 (YRI, Test; Iran HG | N, Post Neolithic Iran). Test refers to (A) the Anatolian or Levant pre-Neolithic/Neolithic populations, CHG, EHG and Villabruna populations, and (B) Baikal, WSHG and Andamanese HG. Boxplots show all f_4 -statistics calculated by using at least 10K SNPs using all available populations in pattern, green-color boxplots show nominally significant f_4 -statistics with $|Z| > 3$ and gray color boxplots show non-significant f_4 -statistics with $|Z| < 3$.

3.2.2.4 South Caucasus

The gene pool of pre-Neolithic South Caucasus is represented by only two genomes (Caucasus Hunter-Gatherer, or CHG) [104]. After 8,000 BP, with the arrival of Neolithic culture in

the region, South Caucasus genomes exhibit a clear footprint of Anatolian Neolithic-related ancestry in contrast to pre-Neolithic genomes. Although this implies that Neolithic culture was established by substantial human movement and admixture in South Caucasus [51, 90], the lack of representation of genomes from early Holocene Caucasus and East Anatolia calls for a cautious interpretation. Here we could model the South Caucasus populations from 7,650 BP to 3,750 BP as two-way admixtures of local CHG (43-62%) and Anatolian Chalcolithic populations (38-57%). The new Doghlauri genome from the Early Bronze Age site in Georgia, associated with the Kura-Araxes culture [105], also closely follows this pattern (Figure 10, 14). However, by ca. 3750 BP Steppe/EHG-related ancestry appears in the Armenia MBA. This is also represented in the new Bronze Age genomes from Nazarlebi in Georgian, Late Bronze Age genomes from Didnauri in Georgia, and the new Iron Age genome from Azerbaijan (Figure 10, 14). Our findings imply that the Steppe-related gene flow permanently shaped the gene pool of the entire region, albeit potentially not to the extent as in the North Caucasus [90].

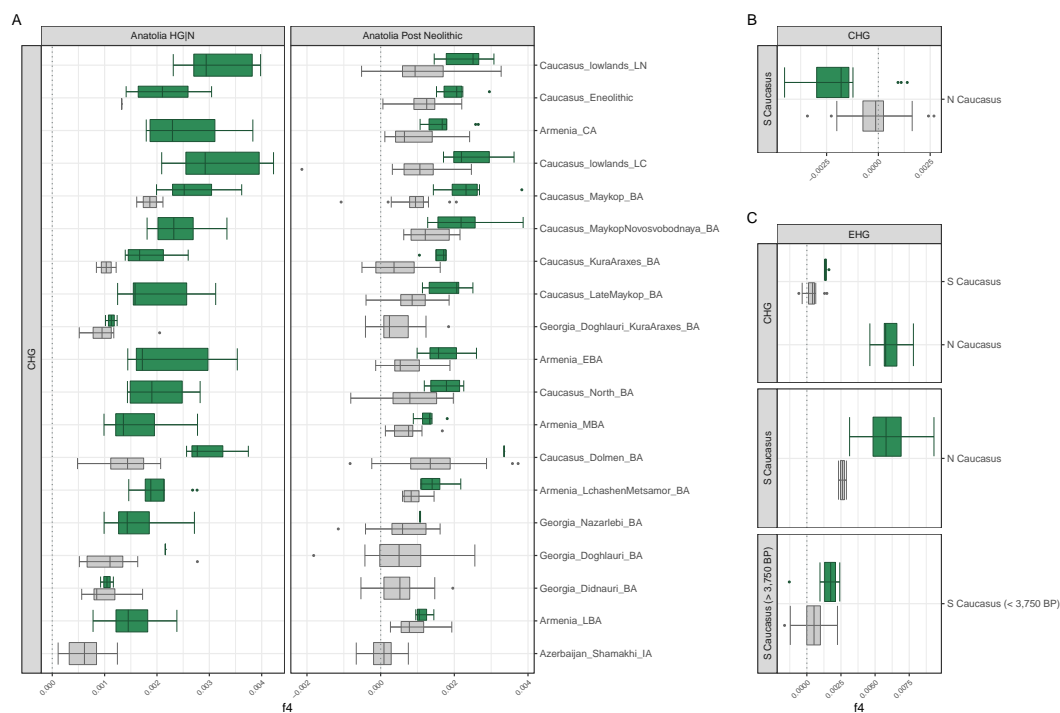


Figure 14: Genetic Affinity of Post-Neolithic South Caucasus Populations. Results from (A) f_4 (YRI, Anatolia HG | N; CHG, South Caucasus Post Neolithic), (B) f_4 (YRI, CHG; South Caucasus, North Caucasus) and (C) f_4 (YRI, EHG; Pop1, Pop2), where Pop1 or Pop2 refers CHG, South Caucasus or North Caucasus populations. Boxplots show all f_4 -statistics calculated by using at least 10K SNPs using all available populations in pattern, green-color boxplots show nominally significant f_4 -statistics with $|Z| > 3$ and gray color boxplots show non-significant f_4 -statistics with $|Z| < 3$.

3.2.2.5 The Levant

The genetic history of the Levant during the Holocene has been well-studied [51, 83, 92, 86, 106, 87, 89]. Levant Neolithic populations were mostly descendants of local foragers (Natufians), while Levant post-Neolithic populations could be modelled as two- or three-way admixtures of local Levant Neolithic populations (30-79%), and Iran post-Neolithic populations represented by Shah Tepe BA or Seh Gabi CA (14-62%) and/or Anatolian Early Neolithic populations (0-42%) (Figure 10). We note that alternative models using external sources such as EHG have also been proposed [106, 87]. We could not include here individuals from Bronze Age and Iron Age Ashkelon genomes [94] and Mediaeval Crusaders with West European ancestry [106]); both groups appear not to have left permanent signatures in the local gene pool.

3.2.3 The expanding nature of inter-regional mobility in Southwest Asia and the East Mediterranean

With these observations, we returned to the question of the rate of human mobility in Southwest Asia and the East Mediterranean over the Holocene. Our data and analyses have shown growing genetic similarity among populations over time, but at a slowing rate, in line with recent studies showing decreasing differentiation (F_{ST}) among West Eurasian [83, 51] or Southwest Asian populations [82]. Indeed, using our 440-individual dataset from the region, we found that average F_{ST} among regions drops dramatically over time in the early Holocene, and this continues in decelerating fashion in later periods (Spearman's rho= -1, p-value=0.002) (see Figure 16A).

However, interpreting the F_{ST} signal in the context of mobility is challenging. Instead, the outgroup- f_3 statistic is a more appropriate tool as it measures shared drift between two genomes relative to an outgroup and is robust to population size changes [107, 73]. Through coalescent simulations we confirmed the theoretical expectation that genetic distance between two groups measured as $(1 - f_3)$ is not affected by bottlenecks and directly reflects gene flow, while F_{ST} is sensitive to both types of demographic events (Figure 15). To do this, we used a four-population demographic model for simulations. n=100 simulations were run and the same set of statistics calculated in each run. We tested whether the distance between popA vs. popB was greater than the distance between popA vs. popC using the binomial test. The binomial test p-value and the success percentage are reported in each distribution plot on the top-left.

The differences among the models were as follows:

- *Model A*, PopC goes through a bottleneck size of 1,000 individuals before recovering to a size of 10,000 individuals 379 generations ago.
- *Model B*, Gene flow from PopA to PopC occurs at a rate of 10%, 517 generations ago.
- *Model C*, Gene flow from PopA to PopC occurs at a rate of 10%, 517 generations ago, and then PopC goes through a bottleneck with $N_e = 1,000$ individuals, before recovering to a size of $N_e = 10,000$ individuals 379 generations ago

- *Model D*, PopC goes through a bottleneck size of $N_e = 1,000$ individuals before recovering to a size of $N_e = 10,000$ individuals 482 generations ago, and later gene flow from PopA to PopC occurs at a rate of 10%, 344 generations ago.

We find that genetic distance ($1 - f_3$) and pairwise mismatch capture gene flow effectively and are not affected by drift, which is not true for F_{ST} (Figure 15).

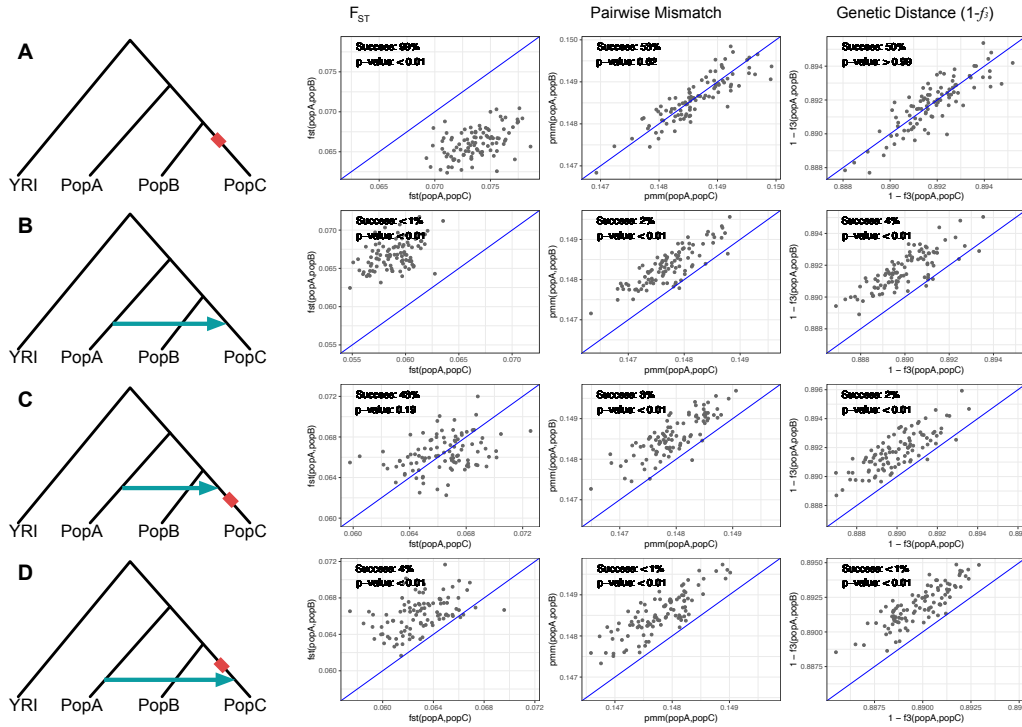


Figure 15: The impact of drift and admixture on three statistics of population differentiation evaluated by coalescent simulations. The red rectangle indicating a bottleneck, and the green arrow indicating gene flow. Each plot shows 3 differentiation-related statistics calculated from simulations from the model shown in the leftmost panel of that row. The 3 statistics were F_{ST} , pairwise mismatch (pmm), and $(1 - f_3)$, calculated between popA vs. popB (y-axis), and popA vs. popC (x-axis), from left to right, respectively. We tested whether the distance between popA vs. popC was greater than the distance between popA vs. popB using the one-sided binomial test. The binomial test p-value and the success percentage are reported in each distribution plot on the top-left.

We then used this distance ($1 - f_3$) to measure pairwise genetic differentiation among the five regional groups. This revealed an intriguing pattern: inter-regional genetic differentiation decreases until 6,000 BP and then increases again. The concave-up (down-up) shape of the average differentiation-time trajectory was significant over a linear model (F-test p-value=0.04) (Figure 16B). We repeated this analysis by calculating pairwise genetic distances between individuals (instead of grouping them as regional populations), which again revealed a concave-up pattern of differentiation (in 7 out of 10 comparisons: F-test p-value ≥ 0.10) (Figure 16C).

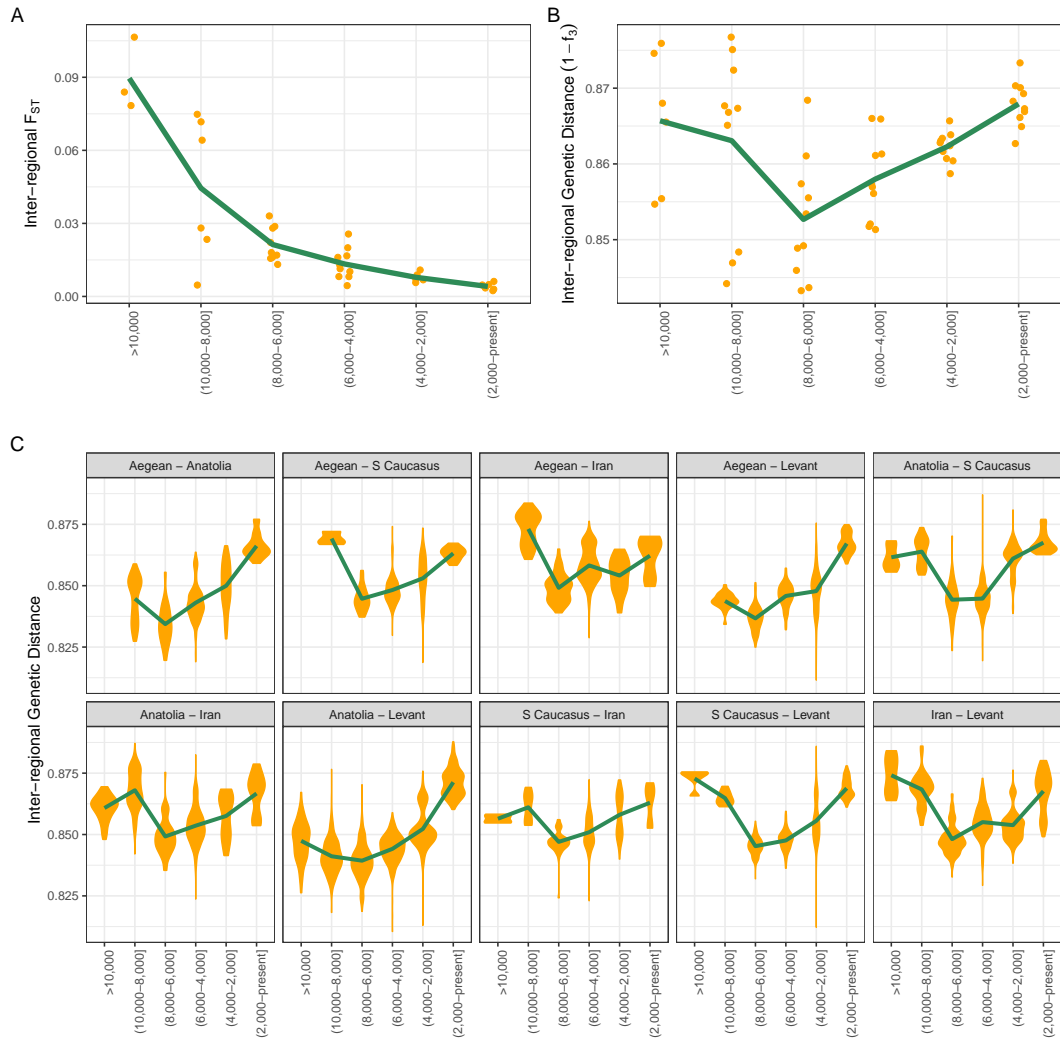


Figure 16: Genetic differentiation over time in Southwest Asia and the East Mediterranean. Panels A and B: the points show (A) pairwise F_{ST} and (B) pairwise $1-f_3$ values calculated among populations belonging to each time period and the green line indicates the mean. (C) The violin plots show pairwise genetic distance ($1-f_3$) between regions calculated by comparing all individuals between a pair of regions within each time period and the green lines show the mean. All analyses in the figure were performed using autosomal SNPs.

This suggests two sequential processes. The first involves intense mobility within Southwest Asia and the East Mediterranean after the Neolithic transition, in the early half of the Holocene. As evident in the qpAdm results: for instance, up to 6,000 - 4,000 BP Anatolian and Aegean populations received intense gene flow from South Caucasus/Iran-related populations, whereas groups from Caucasus and Iran received gene flow from Anatolian-related populations (Figure 10). These admixture events led to a reduction in genetic distance supported both by F_{ST} and $(1 - f_3)$ values (Figure 16A,B).

The second process involves external gene flow. After the 6,000 - 4,000 BP period, populations in all five regions likely received different degrees of gene flow from outside of Southwest Asia the East Mediterranean. Examples include EHG/Steppe-related ancestry in the Aegean, South Caucasus and Levant [87, 85], EHG- and Central Asian-related ancestry in Anatolia IA and later samples [84], WHG-, South Asia-, and Central Asia-related ancestries in Levant Mediaeval populations [106, 87], and West Siberian-related and South Asia-related ancestry in Iran [54] (see also Figure 10, 11, 12, 13, 14). As a consequence of these inferred long distance mobility events, genetic differentiation calculated as $(1 - f_3)$ within Southwest Asia rebounded over time (Figure 16B). We call this *the expanding-mobility model*.

3.2.4 Regional diversity increases monotonously through the Holocene

The expanding-mobility model predicts gene flow among Southwest Asian and the East Mediterranean populations and from external groups through the Holocene, both of which should elevate within-population genetic diversity. We thus estimated diversity per region and time period by calculating the pairwise genetic differences $(1 - f_3)$ among individuals within a group. We observed monotonous and significant trends of increasing diversity through the Holocene (Spearman correlation between diversity and time per region: $\rho > 0.94$, one-sided p -value < 0.04) except in the Aegean (Figure 17A).

De novo variants are not likely to be the main source of this signal, as we use SNPs ascertained in an outgroup populations (sub-Saharan African populations). Instead, the observed pattern is best attributed to effective migration into each region, i.e. migrants with non-local genetic ancestries breeding with locals and elevating diversity. This conclusion was also supported by an analysis of runs of homozygosity (ROH) estimated by hapROH [108]. In the three regions where we could reach sufficient sample sizes and excluding potentially consanguineous genomes in Anatolia, Iran and South Caucasus, we detected a consistent decrease in the average sum of relatively short (4-8 cM) ROH (Figure 18). This again suggests an increase in the within-region genetic diversity due to admixture [109, 108].

3.2.5 Spatial heterogeneity in mobility levels

An intriguing pattern in increasing diversity (Figure 17A) was the ostensible regional differences in time-dependent diversity changes, such as higher stronger magnitudes of change in Anatolia. We explored this further by calculating genetic distances $(1 - f_3)$ between all pairs of individuals from a region (irrespective of the time period), and then calculating the correlation between pairwise genetic distance versus time difference. This yields an estimate of overall (Holocene-wide) temporal differentiation in the gene pool of a region.

In all five regions we found positive correlations between genetic distance and separation time (each region: $\rho = [0.14-0.44]$, permutation test p -value < 0.06 ; Figure 17B). Anatolia exhibits the highest change, similar to the diversity analysis above. We repeated this analysis using X-chromosome SNPs, using subsets of individuals with similar numbers and/or temporal distributions across the five regions, or using only SNP capture- or shotgun-sequenced genomes. In all analyses except one we found that Anatolia shows the strongest magnitude of

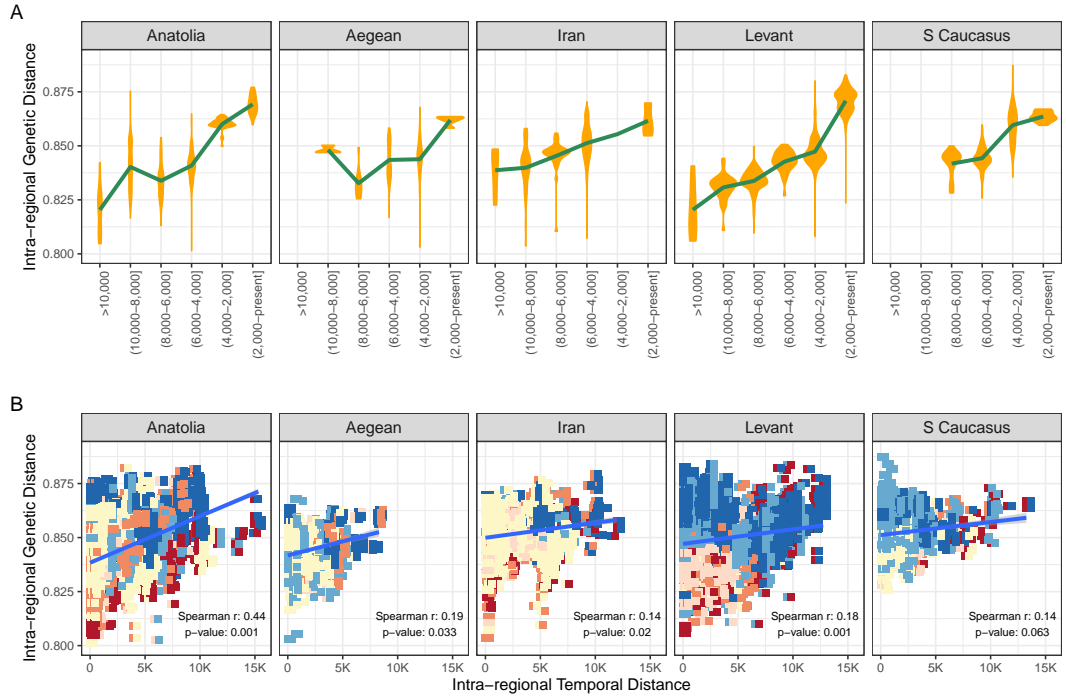


Figure 17: Genetic differentiation over time in Southwest Asia and the East Mediterranean. (A) The violin plots show genetic diversity calculated as pairwise genetic differences ($1 - f_3$) among individuals in a group. (B) Genetic distances ($1 - f_3$) (y-axis) versus time differences (x-axis) among all pairs of individuals within each region. Each point (a rectangle consisting of two squares) represents a pair of ancient individuals, with the squares are colored according to the respective time period (see Figure 1). The line represents linear regression. The Spearman correlation coefficient between time and distance, and the p-value calculated by random permutations of individuals across time ($n=1,000$) are indicated in the figure. All analyses in the figure were performed using autosomal SNPs.

change. Assuming that this result is reproducible, it would be tempting to investigate whether geographic factors, such as Anatolia being en route between Europe and Southwest Asia, or comprising large arable lands that could sustain sizeable populations, or idiosyncratic events, such as the strong East/Central Asia-related gene flow event into Anatolia over the last millennium, could also have contributed to this relatively high rate of change. However, the limited consistency among datasets indicates that our estimate of overall temporal differentiation may be sensitive to technical factors such as sequencing technology and SNP panels used.

3.2.6 A possible temporal shift in sex-biased inter-regional mobility

Finally, we addressed the question of sex-biased mobility in Southwest Asia and the East Mediterranean. We first analysed the distribution of mtDNA and Y-chromosomal haplogroups using F_{ST} and observed no significant difference in mtDNA haplogroup composition, but a number of significant shifts in Y-chromosomal haplogroup composition (Figure 19A). Al-

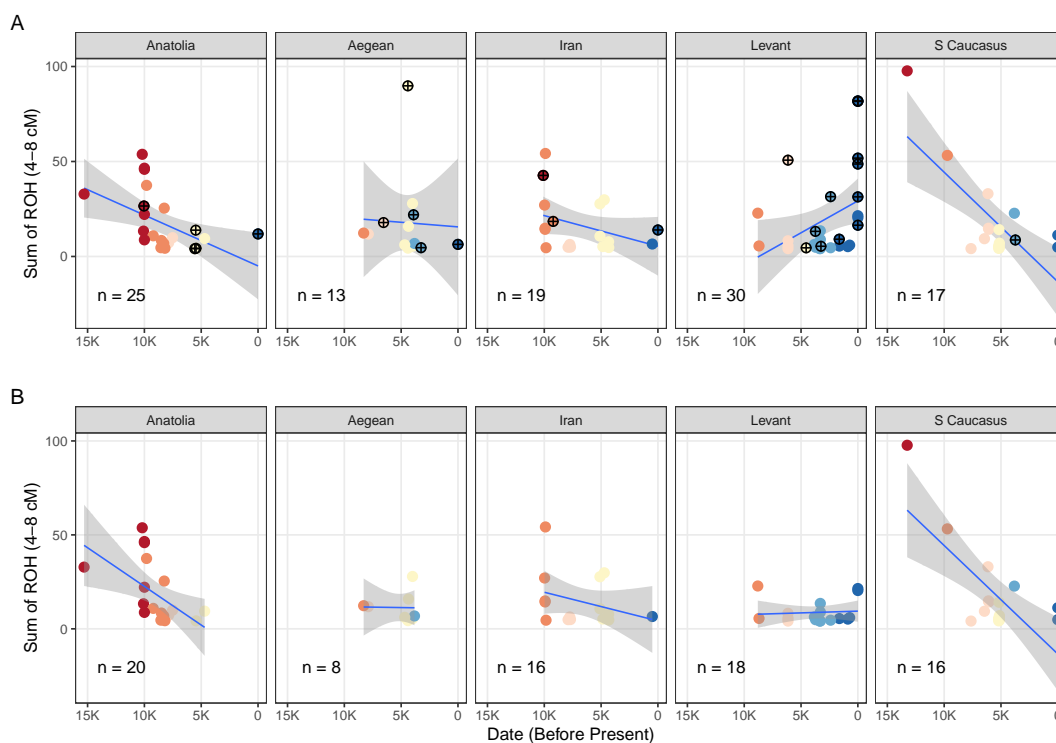


Figure 18: Distribution of ancient individuals with sROH (4-8 cM). Panel (A) shows all individuals for which ROH could be called (with minimum 400K SNPs), where individuals with ROH > 20cM, which represents consanguinity, are indicated with a plus symbol. Panel (B) is the same as panel A but without likely consanguineous individuals (with ROH > 20cM). In each panel the lines represent linear regression lines. Each point represents an ancient individual and is color coded based on its time period Figure 5. We note that we detect no decrease in the sROH values (4-8 cM) for the Aegean, but this is likely because we did not have Aegean genomic samples from the first half of the Holocene with sufficient SNPs to determine ROH. The increase of the sum of ROH in Levant we observed has been well-documented before and is due to an increase in consanguineous marriages in the region in the recent part of the Holocene

though this analysis is compromised by arbitrary assignment of data into haplogroups, it does suggest relative stability of the maternal gene pool, consistent with earlier work in various regions [95, 96, 97]. It also suggests either stronger genetic drift in the male gene pool, or higher rates of male mobility, with the most notable effect in the Levant.

We further compared the average genetic distance ($1 - f_3$) calculated from autosomes versus X chromosomes for each time period in all regions. These autosomal and X chromosomal distances were highly correlated, as expected (Spearman's $\rho=0.82$, $p\text{-value}<0.0001$) (Figure 19 B). However, when we calculated the change in genetic distance between consecutive time periods for autosomes and the X chromosome, we found a notable pattern: in early periods, genetic distances on the X chromosome increased more than on the autosomes, and vice versa in later periods. As we can rule out stronger drift in the male gene pool, for reasons discussed earlier (Figure 15), this result suggests that sex-bias in admixture events shifted over time,

with female mobility being relatively higher during early periods than later periods (Figure 19 B). This can be also caused by female mobility being relatively higher during early periods than later periods, or by higher reproductive success of migrant males in later periods (Figure 19 C).

This putative shift in sex-biased admixture patterns resembles observations in Europe, with low sex-bias in the Neolithic expansion, followed by highly male-biased Steppe expansion in the Bronze Age [85, 110, 111]. Time-dependent increase in sex-bias would also be consistent with the expanding mobility model, given observations that long-range migration tends to be more male-dominated than short-range migration [112]. Meanwhile, we cannot directly quantify sex-bias in this framework (i.e., we cannot distinguish whether early periods were devoid of sex-bias and male-bias emerged later, or early periods had female-bias that later disappeared). In addition, the haplogroup composition analysis described earlier provides only weak parallels to the observation of temporal shifts in male-bias. While we remain cautious about the generality of the observed sex-biased mobility patterns, we note that their study can provide vital insight into changing social dynamics and networks over time.

3.2.7 Conclusion

Our work reveals a number of novel observations. We show that rates of inter-regional genetic differentiation, as measured by $(1 - f_3)$ (Figure 16 A), did not decline over time in Southwest Asia and the East Mediterranean, in contrast to the implications of earlier F_{ST} analyses (Figure 16 B). On the contrary, while intra-regional diversity increases monotonously through the Holocene, inter-regional differentiation first declines and then rebounds with the Bronze Ages. This suggests that mobility continued unabated, and also with an expanding range, possibly both as a result and a consequence of increasing social and technological complexity (Table 1). We also observe a trend of increasing male-bias in mobility in the latter half of the Holocene (Figure 19), partly reminiscent of sex-biases observed in European history [110].

These changing patterns in mobility link well with archaeological and historical evidence regarding improvements in the means of transportation (e.g. horses and roads), the expanding scales of exchange networks (e.g. long-distance trade of raw material and produce, including the establishment of trade routes and trade colonies), and the trend towards more hierarchical and centralised polities able to exert an influence over larger territories and populations (e.g. organised invasions and forced displacements) that emerge in the second half of the Holocene in Southwest Asia and the East Mediterranean (Table 1). An attractive question for future studies would be whether this pattern of expanding mobility ranges may also be observed in other regions, such as South and East Asia, Africa, or the Americas.

We acknowledge that due to patchy distribution of our sample and the limited number of available genomes in several regions, the results of our trans-regional analyses must be treated cautiously. Denser and more homogeneous samples will allow possible confounding between population structure and temporal changes to be strictly ruled out. Nevertheless, the fact that we detect consistent trends across all five regions as well as in bootstrap analyses suggests the robustness of our main observations.

We note, however, that our statistics are only indirect measures of human mobility. This is because the amount of observed change in outgroup- f_3 (Figure 16B, 17) or ROH values (Fig-

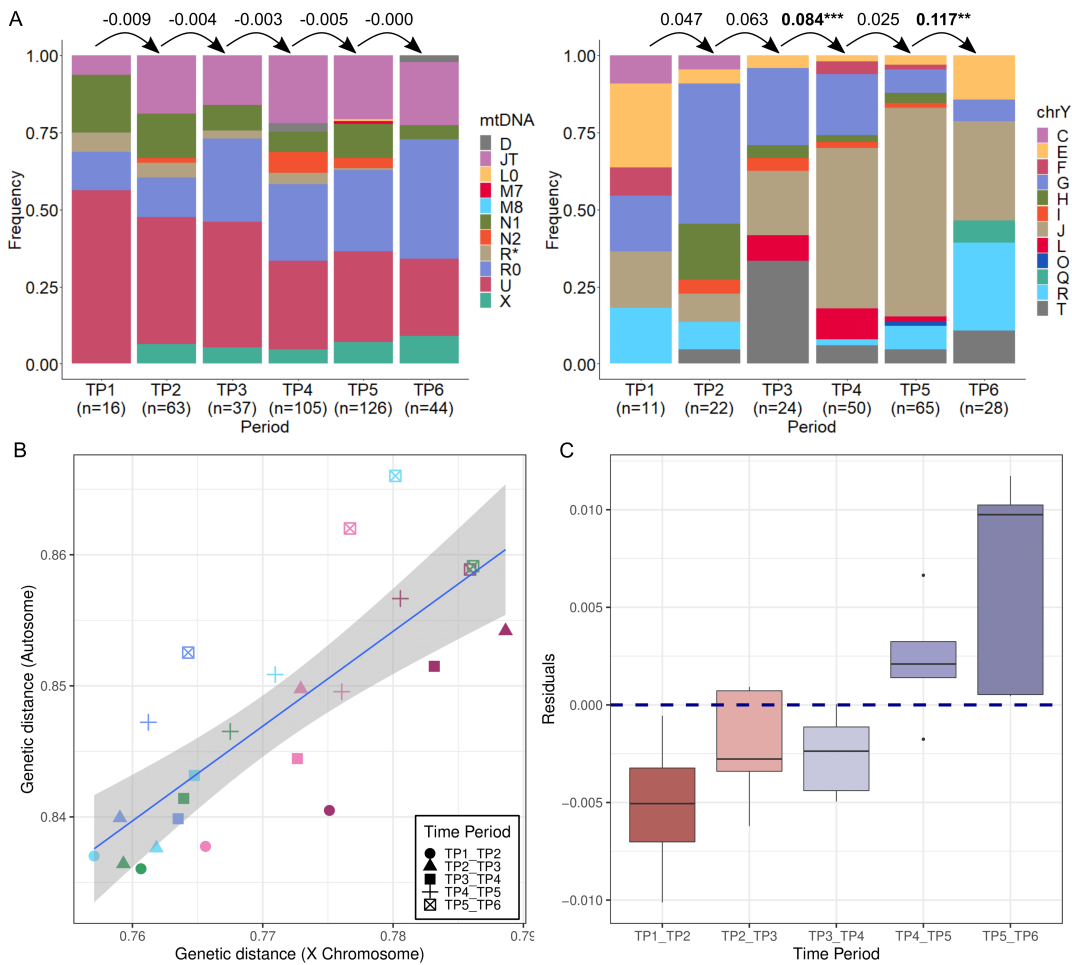


Figure 19: Uniparental markers and sex-biased admixture. (A) Distribution of mtDNA and Y-chromosome haplogroups in time in all regions of Southwest Asia and the East Mediterranean. The values between the bars are F_{ST} values, with negative values indicating practically no differentiation. Bold values indicate nominally significant differentiation between consecutive periods calculated using random permutations. (B) Comparison of average genetic distance ($1 - f_3$) calculated from autosomes versus X chromosomes. Each point represents the average genetic distance between genome samples from two consecutive time periods of the same region, i.e., a measure of genetic change. Comparisons involving the first half of the Holocene (TP1-TP2, TP2-TP3, TP3-TP4) are below the regression line, indicating relatively more change on the X chromosome than autosomes, while comparisons involving the latter half of the Holocene (TP4-TP5, TP5-TP6) tend to be above the line, indicating relatively more change on autosomes. (C) Distribution of residuals obtained from the linear regression model in Panel B. Residuals and time were highly correlated (Spearman's rho=0.70, p-value=0.0001).

ure 18) will depend not only on the migration rate (the proportion of incoming migrant alleles in the gene pool each generation), but also on the amount of genetic differentiation between incoming and local groups (e.g., see [9]). In addition, if one takes into account the fact that

human populations in Southwest Asia and the East Mediterranean grew significantly over the Holocene [113], the absolute amount of human movement (immigrant numbers) required to create a certain magnitude of change will also vary in time. Accordingly, our observation that diversity increased linearly in time cannot be interpreted as indicating constant migration rates through the Holocene. Quantifying the exact amount of mobility thus remains a future challenge.

CHAPTER 4

MATERIALS AND METHODS

4.1 Sample preparation

Samples were prepared at the aDNA laboratories of METU and Hacettepe (Ankara, Turkey), at the aDNA laboratory of the Centre for Palaeogenetics (CPG) (Stockholm, Sweden) as well as at the aDNA laboratory of FORTH (Crete, Greece).

(a) *Data produced in Ankara*

Samples were processed at the aDNA laboratories of METU and Hacettepe University (Ankara, Turkey). Both laboratories followed the same procedures to extract DNA and construct libraries. Prior to DNA extraction, the surface of bones and/or tooth samples was decontaminated with a 0.5% sodium hypochlorite solution and UV irradiated in a crosslinker (6 J/cm² at 254 nm). After decontaminating the bones, approximately 120mg of bone was cut out and ground to fine powder in the SPEX 6875 freezer mill. DNA was extracted and purified following the steps in [114]. Double-stranded, blunt-end, Illumina compatible sequencing libraries were prepared using 20ul of the DNA extracts as described in [115]. Negative controls at every step of DNA extraction and library preparation were also included to assess contamination. The number of PCR cycles for the enrichment of each library was determined using real-time PCR (qPCR). Next, the enriched libraries were purified using AMPure beads and then screened for DNA content using low-coverage shotgun sequencing on the Illumina HiSeq or Novaseq 6000 platform (at the Science for Life Laboratory in Stockholm). Finally, the samples that yielded roughly %1 authentic human DNA showing aDNA-related post-mortem damage (%15 C→T transitions at the first position of 5' end) [116, 33] were re-sequenced further for deeper coverage.

Experiments done by Füsün Özer, Duygu Deniz Kazancı, Sevgi Yorulmaz, Damla Kaptan and Dilek Koptekin.

(b) *Data produced in Stockholm*

Samples were prepared at the aDNA laboratory of the Centre for Palaeogenetics (CPG) (Stockholm, Sweden). The surface of bone and/or tooth samples was decontaminated with a 0.5% sodium hypochlorite solution and UV irradiated (6 J/cm² at 254 nm). Bone was drilled to powder, and the tip root of the teeth was cut with a multitool drill (Dremel) to obtain approximately 80 to 150 mg of bone powder/root tip. DNA was isolated and purified following [114, 117] protocols. Illumina sequencing libraries were prepared using

20ul of the DNA extracts as described in Meyer and Kircher (2010). All standard measures were taken to prevent exogenous DNA contamination, including the use of library negative controls (extraction blanks) and PCR blanks in every step of library preparation and amplification. Real-time PCR (qPCR) was used to determine the number of PCR cycles for each library during the amplification step. Double-stranded, blunt-end libraries were first screened using low-coverage shotgun sequencing on the Illumina HiSeq X or Novaseq 6000 platform (at the Science for Life Laboratory in Stockholm). Next, we chose the samples that yielded roughly 1% authentic human DNA showing aDNA-related post-mortem damage (15% C→T transitions at the first position of 5' end) [116, 33] and re-sequenced these for obtaining deeper coverage.

Experiments done by Ricardo Rodríguez-Varela, Vendela K. Lagerholm, Robert George, Evangelia Daskalaki and Natalia Kashuba.

(c) *Data produced in Crete*

Samples were prepared at the Ancient DNA Lab, Institute of Molecular Biology and Biotechnology (IMBB), Foundation for Research and Technology - Hellas (FORTH), Irakleio, Greece], following strict ancient DNA guidelines [118]. Negative extraction and library controls (water blanks) were included in all cases to monitor for contamination. All post-library preparation steps (i.e. qPCR, library amplification and indexing, indexed library purification and quantification) were performed (with the negative controls wherever applicable) in a standard molecular biology lab located in a different building. Sequencing was performed in the Genomics Facility of IMBB-FORTH. Sample processing and DNA extraction: For all petrous bones (490-1116 mg of powder) processing and DNA extraction were performed following established procedures [119] with a few modifications. Double-stranded library preparation and indexing for initial screening: For all samples, DNA extract was built into a blunt-end library according to procedures (library preparation, quantification, indexing) previously described [119] with a few modifications. Shallow shotgun sequencing (screening) was performed on an Illumina NextSeq 500 platform using 75+6 bp paired-end read chemistry (2 × 75 bp plus 6 bp index). Double-stranded library preparation for deeper sequencing. After initial examination of the screening results and confirmation that all samples a) are characterised by an ancient DNA-like post-mortem damage profile and b) have high human endogenous DNA content, new libraries were prepared, this time from DNA pre-treated with the USER enzyme [uracil-DNA-glycosylase (UDG) and Endonuclease VIII (EndoVIII)] as described in [120]. Library preparation, quantification and indexing were performed as described above. Deep sequencing was performed on an Illumina NextSeq 500 platform using 75+6 bp single-end read chemistry (75 bp plus 6 bp index). For more detail of the preparation of additional sequence data for the sample G31 see Psonis et al., 2021 [120].

Experiments done by Nikolaos Psonis, Despoina Vassou and Eugenia Tabakaki.

4.2 Radiocarbon dating

Sixteen individuals were C14 radiocarbon dated by the TÜBİTAK-MAM (gir001, mus005, mus006, CTG025), Beta Analytic Radiocarbon Dating Laboratory (G23, G37, G76a) and by

the Tandem Laboratory at Uppsala University (geo005, geo006, geo015, geo017, geo029, zrj003, sha004, sha007, sha009). All dates were calibrated using IntCal13 / IntCal20 [121].

4.3 Sequence data processing

Data was produced either in single-end or paired-end read mode. For all libraries we removed the residual adapter sequences from the raw FASTQ files by using the software “Adapter Removal” (version 2.3.1) with “-qualitybase 33 -qualitymax 60 -trimns” parameters. Paired-end reads from each library were merged by using also “-collapse” parameter, requiring at least 11 bp overlap between the pairs [122].

All libraries were mapped to the human reference genome (version hs37d5) using the program “BWA aln/samse” (version 0.7.15) [123] with parameters “-n 0.01, -o 2” and by disabling the seed with “-l 16500” [124].

Multiple libraries from the same individual were merged with the “samtools merge” (version 1.9) [125] and PCR duplicates with identical start and end coordinates were removed using “FilterUniqueSAMCons.py” [124]. Reads with >10% mismatches to the human reference genome, <35 base pairs and <30 mapping quality score were also removed.

We calculated average genome coverage by using the reads with mapping quality greater than 30 (see Table S1) by using “genomeCoverageBed” implemented in “bedtools2” [126]. We continued with the samples having genome coverage >0.01X.

To avoid biases, the previously published ancient genomic data were also remapped and filtered using the same procedure.

4.4 Testing for authenticity and quality control

4.4.1 Post-mortem damage

DNA continuously accumulates various types of damage after death, termed post-mortem damage (PMD). The most common PMD is cytosine deamination at the single stranded ends of molecules that convert unmethylated cytosine to uracil and methylated cytosine to thymine. We used “PMDtools” [33] to compute ancient DNA damage patterns to examine this ancient DNA specific damage.

4.4.2 Contamination estimation

- (a) mtDNA based contamination estimation in all samples by using “contamMix” (version 1.0-10) [127].
- (b) X-chromosome based contamination estimation in males by using “contamination.R” script in “ANGSD” (version 0.937) [128].

All libraries showed damage patterns ($\geq 15\%$ C \rightarrow T transitions for non-UDG samples, $\geq 5\%$ C \rightarrow T transitions for UDG samples at the first position of 5' end), containing $>93\%$ authentic DNA based on contamMix, and with $<5\%$ contamination based on X-chromosome contamination estimation in XY samples, and were used for downstream analyses.

4.5 Molecular sex determination

After extracting the reads of minimum base quality and mapping quality of 30, we used both the Ry [129] and Rx methods [130] to determine the molecular sex of all samples (Table 3 and Table 4).

4.6 Estimating uniparental haplogroups

Mitochondrial DNA and Y chromosome VCF files were generated from whole genome alignment data (BAM files) using “samtools mpileup” (version 1.9) and “bcftools call” (version 1.9) [131]. Nucleotides with quality score lower than 30 and depth lower than 2 are filtered by “bcftools filter” (version 1.9) [131]. mtDNA haplogroups were obtained using “Haplo-Grep” (version 2.4.0) [132] based on the build 17 of PhyloTree (<http://www.phylotree.org/>) and mtDNA quality score greater than 0.5 were used. Y chromosome haplogroups were determined for all male samples by using “Yhaplo” (version 1.1.2) based on Y-DNA Haplogroup Tree 2019-2020 of ISOGG (<https://isogg.org/>) (Table 3 and Table 4).

In Chapter 3 to analyse the distribution of mtDNA and Y-chromosomal haplogroups, we assigned major haplogroups for both mtDNA and Y-chromosome haplogroups. Major haplogroups that were inconsistent with previously published results and haplogroups that cannot be differentiated at high resolution (i.e. Y haplogroup CT) were removed from the analysis. In total 442 mtDNA and 226 Y-chromosome haplogroups were analyzed. mtDNA and Y-chromosome frequency haplogroup difference between periods was assessed using the F_{ST} statistic. F_{ST} values and possible significant deviations from “0” were calculated in “Arlequin” (version 3.5) with 10,000 permutations [133]. We applied the false discovery rate (FDR) correction [134] for multiple testing. This analysis was done by Eren Yüncü.

4.7 Ancient genome sample selection

1. *Ancient genomes used in Chapter 2* Our dataset included all published pre-Neolithic and Neolithic ancient genomes from Anatolia [45, 47, 50, 48], the Aegean [59, 55, 50], present-day Iran [52, 51, 53, 54], South Caucasus [104, 89], and the Levant [51, 49]. We did not include Ash002 and Ash040 from Yaka et al. (2021) due to their relatively high genetic similarity to each other as measured in their outgroup f_3 -scores ($f_3 > 0.30$). We also included genomes from European pre-Neolithic groups (“Hunter-Gatherers”) [58, 59, 135, 136, 63] (see Table 5).

2. *Ancient genomes used in Chapter 3* Our dataset included all published ancient genomes from Anatolia [59, 55, 137, 45, 51, 88, 84, 49, 97], the Aegean [88, 63, 55, 85], present-day Iran [52, 51, 53, 54], South Caucasus [119, 104, 51, 84, 90, 89], and the Levant [51, 86, 83, 106, 49, 87, 92, 89]. We also added 23 present-day genomes from the same five regions [38]. We did not include the Bronze Age and Iron Age samples from Ashkelon (n=10) from Feldman et al. (2019) due to low number of SNPs (< 2,000 SNPs) overlapping with the 1000 Genomes sub-Saharan African dataset and also Ash002 and Ash040 from Yaka et al. (2021) due to their relatively high genetic similarity to each other as measured in their outgroup f_3 -scores ($f_3 > 0.30$). In addition, we included genomes from European Hunter Gatherers [58, 59, 135, 136, 63], Baikal Neolithic and Bronze Age [84], West Siberian Hunter Gatherers [54] as well as Yamnaya [59, 119, 63, 136, 54] populations to analyse their relationships with Southwest Asian and East Mediterranean populations (see Table 5).

We also added two Aegean Mesolithic mtDNA genomes to mtDNA haplogroup analysis from Hofmanova et al. (2016).

In almost all population genetics analyses, sampling of individuals is assumed to be at random. Closely related individuals are more likely to be similar and share more of their genomes than a pair of people chosen at random from the population. As a result, including closely related individuals can drive prediction and cause bias. Thus, if there were either first- or second-degree related individuals from the same site, we retained the highest coverage genome and excluded the rest from the dataset (see Genetic Kinship analyses below).

On both studies we grouped ancient genomes following their original publications, except for MA2198 from Damgaard et al. (2018). The C14 date of MA2198 was reported earlier as Ottoman period [138], while the Iron Age date mentioned in the article appears to be mistake (Identification courtesy of Orhan Efe Yavuz). This sample was accordingly named *Anatolia_Kalehoyuk_OttomanIII*.

4.8 Whole genome SNP datasets

We prepared three different datasets to use in different population genetics analyses.

1. *the Human Origins SNP Array (HO) dataset* includes 2,583 present-day humans from 213 different populations genotyped on the Affymetrix Human Origins Array [58, 51], merged with newly generated and previously published ancient individuals and 300 present-day samples from Mallick et al., (2016) (downloaded from <https://reichdata.hms.harvard.edu/pub/datasets/sgdp/> as “PLINK format” on 30 Aug 2020) as well as 763 present-day samples from Jeong et al 2019 (downloaded from <https://edmond.mpdl.mpg.de/file.xhtml?fileId=101735version=1.0> as “EIGENSTRAT format” on 30 Aug 2020” on a total of 615,771 autosomal SNPs.
2. *the 1240K Capture Array dataset* includes 417 ancient and 23 present-day individuals from Southwest Asia and East Mediterranean on a total of 1,121,751 autosomal SNPs [59].

3. *the 1000 Genomes sub-Saharan African dataset*, which we created in this study as a high-quality and relatively unbiased SNP dataset to use in demographic inference in our sample. Our motivation was that SNP panels such as the Human Origins or 1240K panel created by using pre-ascertained SNPs in selected populations, often west Eurasians, and thus suffer from ascertainment bias [139, 140]. To avoid this as much as possible, while maintaining a large number of SNPs for statistical power, we also prepared this new SNP panel. Importantly, because these SNPs are ascertained in outgroup populations (sub-Saharan African populations) that are equally distant to all studied populations we can also directly interpret changes in diversity as admixture, instead of population size changes. The panel includes both autosomal and X-chromosome SNPs. We started with all bi-allelic SNPs in the 1000 Genomes Project phase 3 dataset [98]. We then masked the following sites, in the same fashion as [141]:

- within 5 bp of another SNPs, a short insertion or deletion,
- within structural variants that defined in in phase 3 of 1000 Genomes project,
- within segmental duplications (downloaded from: <http://hgdownload.cse.ucsc.edu/goldenPath/hg19database/genomicSuperDups.txt.gz>),
- within a CpG dinucleotide context,
- included in the 1000 Genomes accessibility mask (downloaded from ftp://ftp.1000genomes.ebi.ac.uk/vol1/ftp/release/20130502/supporting/accessible_genome_masks/20141020.pilot_mask.whole_genome.bed),
- not within “High_Mappability_island” (downloaded from <http://mitra.stanford.edu/kundaje/akundaje/release/blacklists/hg19-human/wgEncodeHg19ConsensusSignalArtifactRegions.bed.gz>),
- with minor allele frequency <5% in at least one of the 5 sub-Saharan African populations: Yoruba in Ibadan, Nigeria; Luhya in Webuye, Kenya; Gambian in Western Divisions in the Gambia; Mende in Nigeria; Esan in Nigeria (504 individuals) in phase 3 of the 1000 Genomes project,
- with Hardy-Weinberg equilibrium exact test p-value below the 0.001 in each of the 5 sub-Saharan African populations in phase 3 of the 1000 Genomes project,
- within pseudoautosomal regions in the X chromosome.

After filtering, 4,771,930 autosomal and 206,805 X chromosome SNPs remained.

We merged all ancient individuals and 300 present-day samples from Mallick et al., (2016) (downloaded from <https://reichdata.hms.harvard.edu/pub/datasets/sgdp/> as “PLINK format” on 30 Aug 2020) with these datasets.

We used the Human Origins SNP Array dataset for PCA and the 1240K Capture Array dataset to estimate Runs of Homozygosity (ROH), whereas the 1000 Genomes sub-Saharan African dataset was used for all other analyses.

4.9 Trimming and pseudo-haploid genotyping

To avoid possible confounding by deamination (C-to-T and G-to-A transitions) at the ends of the reads, we trimmed (a) 10 bases at the ends of each read in libraries obtained by shotgun

sequencing without Uracil-DNA-glycosylase (UDG) treatment, and (b) 2 bases at the ends of each read from libraries obtained with UDG treatment. Trimming (clipping) was performed using the “trimBam” command of “bamUtil” (version 1.0.14) [142]. To avoid genotype calling biases due to differential sequencing coverage among samples, we pseudo-haploidized the data by randomly selecting one allele for each of the targeted SNP positions using the genotype caller “pileupCaller” (version 1.2.2; <https://github.com/stschiff/sequenceTools>) on “samtools mpileup” output (base quality>30 and MAPQ>30) [125].

4.10 Genetic kinship analyses

We used “READ” [71] to determine genetic kinship between each pair of individuals from the same site using the 1000 Genomes sub-Saharan African SNP panel dataset and pseudo-haploidised genotypes. First, we ran READ to calculate pairwise mismatch rates (P0) for each 1 Mb window. For each population from different regions and time periods, we computed the P0 value separately by using all published and unpublished neighbouring contemporary samples except Shah Tepe and Bademağacı which have enough samples (n=9, n=10 respectively) for this analysis. To calculate a robust normalisation factor (median of P0 values for each population), we took into account only pairs that had more than 5,000 overlapping SNPs. We then calculated kinship coefficient (θ) for each window using (1 - Normalised P0) as a proxy utilising in-house script. Finally, we computed the mean value for each pair of individuals.

4.11 Principal component analysis (PCA)

We performed principal components analysis to obtain an overview of the possible relationships among populations and/or possible artefacts. We used the smartpca program (version: 18140) of “EIGENSOFT” (version 7.2.0) [72] with “lsqproject: YES, numoutlieriter: 0” parameters to construct the components of present-day West Eurasian populations from Human Origins SNP Array dataset. Ancient individuals were projected onto the first two principal components of the present-day variance.

4.12 Genetic differentiation among populations

We calculated inter-population differentiation using F_{ST} , separately for regional populations in each time period. We used the “smartpca” algorithm (version: 18140) of “EIGENSOFT” (version 7.2.0) [72], with parameters “inbreed: YES, fstonly: YES”. We used the $Z > 3$ cut-off for each comparison, representing nominally significant $p < 0.001$.

4.13 Genomic similarity/distance among populations

Genome-wide similarity was calculated using outgroup- f_3 statistics [73] implemented in the “qp3Pop” algorithm (version: 651) in “AdmixTools” (version 7.0.2). Outgroup- f_3 statistics

measure the amount of shared genetic drift between two populations from a common ancestor (outgroup). In a tree topology like {Outgroup, {PopA, PopB}}, outgroup- f_3 statistics measure the common branch length from the outgroup. We used genomes from all populations (i.e., all sites and periods), using the Yoruba population (n=108) as outgroup. We used $1-f_3$ as a measure of genetic distance. We used > 2,000 SNPs as cut-off for calculations for autosomal SNPs and > 1,000 SNPs for X chromosome SNPs.

4.14 Detecting gene flow among populations

To estimate gene flow between Population X and Population Y for autosomes, we used f_4 -statistics [73] implemented in the “qpDstat” algorithm (version: 980) in “AdmixTools” (version 7.0.2) with the “f4mode: YES” option. The f_4 -statistics for the tree-like topology of the form {Outgroup, {Test, {PopX, PopY}}} measures the shared genetic drift between Test population and PopX and PopY. Assuming no recent interactions between each of these four groups, tree topologies are balanced at zero, and deviation from zero implies a deviation from this proposed tree. Positive values indicate that Test population shares more alleles with PopY, and negative values indicate that Test population shares more alleles with PopX. We used the test of the form $f_4(\text{Outgroup, Test; PopX, PopY})$ using Yoruba population as outgroup and >10,000 overlapping SNPs cut-off for reporting calculations.

4.15 Ancestry proportion estimation

We estimated proportions of ancestry in Southwest Asia and East Mediterranean populations using the “qpAdm” (version: 1520) [74, 75], which is an f_4 -based admixture modelling implemented in “AdmixTools” (version 7.0.2). We ran the algorithm with “allsnps: YES, details: YES” parameters. This method does not require knowledge about the phylogeny of the populations of interest. To estimate mixture proportions for a studied population (‘Target’) as a combination of a variable number of ‘source’ populations, “qpAdm” exploits shared genetic drift with a set of ‘outgroup’ populations (also called ‘right’ populations). The target can thus be modelled as a combination of the source populations, and the admixture proportions can be estimated by solving a matrix of f_4 -statistics [74].

For all runs, we used a base set of “Right” populations (Base12) composed of Mbuti, Han, Papuan, Mixe, Ust_Ishim, Kostenki14, MA1, Villabruna, Levant_HG, Anatolia_HG, Iberomaurusian, AfontovaGora3, plus either CHG (Base12_CHG) or Iran_GanjDareh_N (Base12_Iran) (13 in total [41, 135, 58, 38, 143, 49]). To model Anatolia Ottoman individuals, we also added Botai_EN [84] to the right populations (Base12_Iran_Botai, Base12_CHG_Botai) (14 in total). In choosing “Right” populations we followed [49, 89, 48] with some modifications to improve resolution. We checked whether the populations of interest were well distinguished by their relationship with the right populations. We then modelled populations as mixtures of two or more sources. When alternative combinations of ancient populations provided similarly fitting models, we selected one of them randomly to be presented in Figure 3C and Figure 10.

4.16 Runs of homozygosity (ROH)

We estimated ROH using “hapROH” (version 0.3a4) [108] with default parameters that were optimised for the 1240K SNPs. The default genetic map of hapROH and 5,008 global haplotypes from the 1000 Genomes Project were used [108, 98]. hapROH can detect ROH longer than 4 centimorgan (cM) in individuals with 400,000 SNPs in 1240K dataset and can work with pseudo-haploid genotypes. sROH values between 4-8 cM indicate population background relatedness (genetic diversity), such that high sROH values per genome indicate low diversity caused by small population size. Meanwhile, sROH > 20 cM represent consanguinity and/or recent inbreeding. We screened Southwest Asia and East Mediterranean individuals for ROH, in which at least 400,000 SNPs of the 1240K Capture Array dataset were covered. We plotted the values of the sROH (4-8 cM) in time transects for Anatolia, Aegean, modern-day Iran, Levant and South Caucasus (Figure 18).

4.17 Coalescent simulations

We performed coalescent simulations using the software “msprime” (version 0.7.4) [144] under four various demographic models involving four populations. We assumed a mutation rate of 1.25×10^{-8} bp yr⁻¹, and a recombination rate of 1.0×10^{-8} bp yr⁻¹ and 29 years per generation [145]. For all models, we sampled 100 Mbp DNA sequences for 100 representatives of present-day Yoruba individuals ($N_e = 100,000$) and 10 individuals of PopC, PopB and PopA ($N_e = 10,000$). The tree topology used was in the form of { YRI { PopA { PopB, PopC } } }, and the respective divergence times were 160,000 BP, 40,000 BP and 20,000 BP.

In all simulations we sampled 100 present-day YRI individuals, which had $N_e = 100,000$, and we sampled 10 individuals from PopA, PopB and PopB, each of which had $N_e = 10,000$, except for bottlenecks. The differences among the models were as follows:

- **Model A:** PopC goes through a bottleneck size of 1,000 individuals before recovering to a size of 10,000 individuals 379 generations ago.
- **Model B:** Gene flow from PopA to PopC occurs at a rate of 10%, 517 generations ago.
- **Model C:** Gene flow from PopA to PopC occurs at a rate of 10%, 517 generations ago, and then PopC goes through a bottleneck with $N_e = 1,000$ individuals, before recovering to a size of $N_e = 10,000$ individuals 379 generations ago
- **Model D:** PopC goes through a bottleneck size of $N_e = 1,000$ individuals before recovering to a size of $N_e = 10,000$ individuals 482 generations ago, and later gene flow from PopA to PopC occurs at a rate of 10%, 344 generations ago.

We computed F_{ST} , outgroup- f_3 and pairwise mismatch using “weir_cockerham_fst”, “patterson_f3”, “mean_pairwise_difference_between” functions respectively from the “scikit-allel” Python package (version 1.3.2; <https://scikit-allel.readthedocs.io/>) (see Figure 15).

4.18 Visualization

We produced all graphs in R (<https://www.r-project.org/>) after reading and manipulating data using “tidyverse” [146], “plyr” [147], “reshape2” [148], and “gsheet” [149] packages. All figures produced by using “ggplot” [150] and its extension packages such as “ggtext” [151], “ggforce” [152], “ggpubr” [153], “ggrepel” [154]. In Figure 1 and 5, we used freely available Natural Earth data (<https://www.naturalearthdata.com>) to create the maps by using “maps” [155], “raster” [156] and “rgdal” [157] packages. The multiple panel figures combined by using “patchwork” package [158].

CHAPTER 5

CONCLUSION

Past demographic changes and migrations can be traced using modern genomes, as well as ancient genome data. In recent years, ancient DNA studies have shown that changes in ancestry composition as a result of migration and admixture from different geographic sources over time generated the population structure of present-day human populations. Recent paleogenomic studies have provided new insights into large-scale human population movements during the Holocene.

Ancient DNA together with population genetics quickly evolved into instruments for identifying genetic relationships in time (specific time period and/or consecutive times) and space (within and among regions). The significance and long-term viability of these new archaeogenomics studies shed insight into our recent evolutionary history.

This study attempted to describe broad-scale population dynamics of Anatolia over the last 15,000 years. Humans and ideas have long travelled across Anatolia. All wide-ranging movements in West Eurasia are likely to either occur or pass through Anatolia, and the region played a key role in the most essential processes in our prehistory. The goal of my research is to significantly advance our understanding of how the lifestyle and mobility of Anatolian populations have changed over time, with particular attention to the transition from hunter-gathering to farming.

The first process focused on here is the dynamics within and around Anatolia linked to the transition from hunter-gatherer to farming. Anatolia had two major roles in the development and spread of Neolithic lifestyle in West Eurasia. First, it was part of the primary zone of Neolithisation where the first sedentary village cultures and the cultivation of animal and plant domesticates emerged [51, 45, 46, 49, 48]. Second, it was one of the main hypothesized sources of the westward expansion of Neolithic cultures.

The first steps of this expansion were the rapid emergence of Neolithic villages around the Aegean Sea (Western Anatolia and Greece) post-7,000 cal BCE. The aim of the study was to investigate Neolithisation of the Aegean and try to distinguish between two proposed models: The Aegean Neolithic villagers were (i) colonists from Central Anatolia or (ii) descendants of Aegean Mesolithic groups who adopted farming? Neither archaeological nor genomic studies have yet been able to fully resolve this question. Our findings showed that despite a 6,000-year age difference, the earliest sample from Girmeler, Western Anatolia, shares a significant genetic similarity with the Epipaleolithic sample from Pınarbaşı, Central Anatolia (13,642-13,073 cal BCE) (Figure 3). The population represented by Girmeler may be ancestors in

later Neolithic populations from the Aegean (Western Anatolia and Northern Greece) (Figure 4). Our findings support the hypothesis that Aegean local hunter-gatherers were the ancestors of Aegean Neolithic groups. Prior to the Neolithic, genetically linked populations lived in Asia Minor (encompassing both Central and Western Anatolia). Mitochondrial haplogroup-based investigations [62] and the discovery of Anatolian-like mitochondrial haplogroups in Mesolithic Balkan and Aegean populations [55, 63] support the existence of an Aegean human population dating to the LGM. These pre-Neolithic populations rehearsed agriculture and sedentism without engaging in extensive human mobility. However, we still do not have genomes from either the Aegean Mesolithic populations or South Aegean early Neolithic populations. We specifically needed to know the genetic profile of the local hunter-gatherers from the region in order to come to a conclusion about this matter. We also note that given the earliest samples from Central Anatolia and Western Anatolia were represented by one genome, creates limitations to interpreting and discussing results and we consider our results under the assumption of limited population structure within Asia Minor.

The second question focused on here was how populations interacted in time and space from the Epipaleolithic period to the present-day in Southwest Asia. We found that the Anatolian gene pool could be largely traced back to Anatolian Epipalaeolithic population, which itself was a mixture of Balkan HG-related and Levant Neolithic-related populations after LGM. Early Neolithic populations were descendants of these local hunter-gatherers with limited gene flow from their east and south. Starting with Late Neolithic/Chalcolithic, strong mixing from South Caucasus-/Iran-related populations continuously occurred in this gene pool.

In this work we showed that the genetic diversity of Anatolia as well as its neighbouring population in Southwest Asia increased over time. Moreover, we demonstrate that the interaction among populations from Southwest Asia and East Mediterranean changed over time. While intra-regional diversity increases monotonously through the Holocene, inter-regional differentiation first declines and then rebounds with the Bronze Ages. These results suggest that human mobility continued with an expanding range, possibly both as a result and a consequence of increasing social and technological complexity. We also observe a trend of increasing male-bias in mobility in the latter half of the Holocene, partly reminiscent of sex-biased mobility observed in European history [110].

Long-distance trade, the advancement of transportation technology, and the emergence of more centralized social organization systems beginning with the Bronze Age are consistent with the shifting patterns of human mobility. In the future, understanding this pattern of mobility and investigating how it affected social interaction among populations together with archaeological and anthropological data and studying other regions such as South and East Asia will enable us to understand the relationships among the human populations and their social networks.

Meanwhile, the statistics used here are only indirect measures of human mobility, and the absolute magnitudes of these movements remain uncertain. This is because the amount of observed change in outgroup- f_3 or ROH values will depend not only on the migration rate (the proportion of incoming migrant alleles in the gene pool each generation), but also on the amount of genetic differentiation between incoming and local groups (e.g., see Loog et al., 2017). In addition, if one takes into account the fact that human populations in Southwest Asia and the East Mediterranean grew significantly over the Holocene (Palmisano et al., 2021), the

absolute amount of human movement (immigrant numbers) required to create a certain magnitude of change will also vary in time. Accordingly, our observation that diversity increased linearly in time cannot be interpreted as an indication of constant migration rates through the Holocene. Quantifying the exact amount of mobility thus remains a future challenge.

Many aspects of this project are new, and will therefore have a notable impact. However, to obtain a full-scale map of population dynamics in the last 10,000-15,000 years, it is critical to examine and document the connection of cultures and traditions with demography, together with material culture data. Therefore, we will need comprehensive, dense and systematic sampling and genomic analyses and further co-analysis of this data with archaeological and bioarchaeological data will provide a better understanding of our species' history in the future. To improve these studies we can also do the following. First, we can expand our data. The new data will allow for the formulation of new questions as well as a more thorough examination of existing ones. Yet, when it comes to ancient DNA, it is plausible that the essential samples (e.g. Aegean Mesolithic) may have very low coverage that current methods applicable to low-coverage ancient genomes could not directly quantify. Or they may even not be available at all. In such cases, we could try to gain more information from the available data by using genotype imputation to infer missing genotypes from known haplotypes such as those from the 1000 Genomes Project [159]. Regardless, simulation-based approaches and artificial intelligence methodology have been increasingly employed in population genetics, offering an alternative approach to investigating demographic history of human populations. These kinds of approaches have great potential to assess some observed patterns. Using Approximate Bayesian Computation framework and/or machine learning we can identify the best model of the Neolithic transition in the Aegean, and also we can test our observation of possible sex-bias in human mobility in Southwest Asia and the East Mediterranean.

REFERENCES

- [1] C. Stringer, “The origin and evolution of *Homo sapiens*,” *Philosophical Transactions of the Royal Society B: Biological Sciences*, vol. 371, p. 20150237, July 2016. Publisher: Royal Society.
- [2] J.-J. Hublin, A. Ben-Ncer, S. E. Bailey, S. E. Freidline, S. Neubauer, M. M. Skinner, I. Bergmann, A. Le Cabec, S. Benazzi, K. Harvati, and P. Gunz, “New fossils from Jebel Irhoud, Morocco and the pan-African origin of *Homo sapiens*,” *Nature*, vol. 546, pp. 289–292, June 2017. Number: 7657 Publisher: Nature Publishing Group.
- [3] I. Hershkovitz, G. W. Weber, R. Quam, M. Duval, R. Grün, L. Kinsley, A. Ayalon, M. Bar-Matthews, H. Valladas, N. Mercier, J. L. Arsuaga, M. Martínón-Torres, J. M. Bermúdez de Castro, C. Fornai, L. Martín-Francés, R. Sarig, H. May, V. A. Krenn, V. Slon, L. Rodríguez, R. García, C. Lorenzo, J. M. Carretero, A. Frumkin, R. Shahack-Gross, D. E. Bar-Yosef Mayer, Y. Cui, X. Wu, N. Peled, I. Groman-Yaroslavski, L. Weissbrod, R. Yeshurun, A. Tsatskin, Y. Zaidner, and M. Weinstein-Evron, “The earliest modern humans outside Africa,” *Science*, vol. 359, pp. 456–459, Jan. 2018. Publisher: American Association for the Advancement of Science.
- [4] C. Stringer and J. Galway-Witham, “When did modern humans leave Africa?,” *Science*, vol. 359, pp. 389–390, Jan. 2018. Publisher: American Association for the Advancement of Science.
- [5] T. Higham, K. Douka, R. Wood, C. B. Ramsey, F. Brock, L. Basell, M. Camps, A. Arizabalaga, J. Baena, C. Barroso-Ruíz, C. Bergman, C. Boitard, P. Boscatto, M. Capparrós, N. J. Conard, C. Draily, A. Froment, B. Galván, P. Gambassini, A. Garcia-Moreno, S. Grimaldi, P. Haesaerts, B. Holt, M.-J. Iriarte-Chiapusso, A. Jelinek, J. F. Jordá Pardo, J.-M. Maíllo-Fernández, A. Marom, J. Maroto, M. Menéndez, L. Metz, E. Morin, A. Moroni, F. Negrino, E. Panagopoulou, M. Peresani, S. Pirson, M. de la Rasilla, J. Riel-Salvatore, A. Ronchitelli, D. Santamaria, P. Semal, L. Slimak, J. Soler, N. Soler, A. Villaluenga, R. Pinhasi, and R. Jacobi, “The timing and spatiotemporal patterning of Neanderthal disappearance,” *Nature*, vol. 512, pp. 306–309, Aug. 2014. Number: 7514 Publisher: Nature Publishing Group.
- [6] P. Manning and T. Trimmer, *Migration in World History*. London: Routledge, 3 ed., May 2020.
- [7] “Intensification: Mid-to-Late Upper Palaeolithic Population Dynamics (~35,000–15,000 years ago),” in *Palaeolithic Europe: A Demographic and Social Prehistory* (J. C. French, ed.), Cambridge World Archaeology, pp. 214–258, Cambridge: Cambridge University Press, 2021.

- [8] O. Bar-Yosef, “Chapter 19 - Multiple Origins of Agriculture in Eurasia and Africa,” in *On Human Nature* (M. Tibayrenc and F. J. Ayala, eds.), pp. 297–331, San Diego: Academic Press, Jan. 2017.
- [9] L. Loog, M. Mirazón Lahr, M. Kovacevic, A. Manica, A. Eriksson, and M. G. Thomas, “Estimating mobility using sparse data: Application to human genetic variation,” *PNAS*, vol. 114, no. 46, pp. 12213–12218, 2017.
- [10] M. N. Brami, “The Invention of Prehistory and the Rediscovery of Europe: Exploring the Intellectual Roots of Gordon Childe’s ‘Neolithic Revolution’ (1936),” *Journal of World Prehistory*, vol. 32, pp. 311–351, Dec. 2019.
- [11] E. Asouti and D. Q. Fuller, “A contextual approach to the emergence of agriculture in Southwest Asia: Reconstructing early Neolithic plant-food production,” *Current Anthropology*, vol. 54, no. 3, pp. 299–345, 2013.
- [12] O. Bar-Yosef, “The Natufian culture in the Levant, threshold to the origins of agriculture,” *Evolutionary Anthropology: Issues, News, and Reviews*, vol. 6, no. 5, pp. 159–177, 1998. [_eprint: https://onlinelibrary.wiley.com/doi/pdf/10.1002/%28SICI%291520-6505%281998%296%3A5%3C159%3A%3AAID-EVAN4%3E3.0.CO%3B2-7](https://onlinelibrary.wiley.com/doi/pdf/10.1002/%28SICI%291520-6505%281998%296%3A5%3C159%3A%3AAID-EVAN4%3E3.0.CO%3B2-7).
- [13] J. J. Ibáñez, J. González-Urquijo, L. C. Teira-Mayolini, and T. Lazuén, “The emergence of the Neolithic in the Near East: A protracted and multi-regional model,” *Quaternary International*, vol. 470, pp. 226–252, Mar. 2018.
- [14] D. Q. Fuller, G. Willcox, and R. G. Allaby, “Early agricultural pathways: moving outside the ‘core area’ hypothesis in Southwest Asia,” *Journal of Experimental Botany*, vol. 63, pp. 617–633, Jan. 2012.
- [15] M. Özdoğan, “Archaeological evidence on the westward expansion of farming communities from Eastern Anatolia to the Aegean and the Balkans,” *Current Anthropology*, vol. 52, no. S4, pp. S415–S430, 2011.
- [16] M. Özdoğan, “Reconsidering the Early Neolithic of Anatolia. Recent recoveries, some excerpts and generalities,” *L’Anthropologie*, p. 103033, June 2022.
- [17] M. N. Brami, “A graphical simulation of the 2,000-year lag in Neolithic occupation between Central Anatolia and the Aegean basin,” *Archaeological and Anthropological Sciences*, vol. 7, pp. 319–327, Sept. 2015.
- [18] I. Kuijt, *Life in Neolithic Farming Communities: Social Organization, Identity, and Differentiation*. Springer Science & Business Media, Apr. 2006. Google-Books-ID: 2D8OBwAAQBAJ.
- [19] S. K. Kozłowski and O. Aurenche, *Territories, Boundaries and Cultures in the Neolithic Near East*. Archaeopress, 2005. Google-Books-ID: 0ChmAAAAMAAJ.
- [20] B. Weninger, L. Clare, E. Rohling, O. Bar-Yosef, U. Böhner, M. Budja, M. Bundschuh, A. Feurdean, H. G. Gebe, O. Jöris, J. Linstädter, P. Mayewski, T. Mühlenbruch, A. Reingruber, G. Rollefson, D. Schyle, L. Thissen, H. Todorova, and C. Zielhofer, “The

Impact of Rapid Climate Change on Prehistoric Societies during the Holocene in the Eastern Mediterranean,” *Documenta Praehistorica*, vol. 36, pp. 7–59, Dec. 2009.

- [21] S. Shennan, *The First Farmers of Europe: An Evolutionary Perspective*. Cambridge World Archaeology, Cambridge: Cambridge University Press, 2018.
- [22] A. J. Ammerman and L. L. Cavalli-Sforza, *The Neolithic Transition and the Genetics of Populations in Europe*. Princeton University Press, 1984.
- [23] B. Horejs, B. Milić, F. Ostmann, U. Thanheiser, B. Weninger, and A. Galik, “The Aegean in the Early 7th Millennium BC: Maritime Networks and Colonization,” *Journal of World Prehistory*, vol. 28, pp. 289–330, Dec. 2015.
- [24] B. S. Düring, “Breaking the Bond: Investigating The Neolithic Expansion in Asia Minor in the Seventh Millennium BC,” *Journal of World Prehistory*, vol. 26, pp. 75–100, June 2013.
- [25] A. Reingruber, “Early Neolithic settlement patterns and exchange networks in the Aegean,” *Documenta Praehistorica*, vol. 38, pp. 291–306, Dec. 2011.
- [26] B. S. Düring, *The Prehistory of Asia Minor: From Complex Hunter-Gatherers to Early Urban Societies*. Cambridge: Cambridge University Press, 2010.
- [27] G. Palumbi and C. Chataigner, “The Kura-Araxes Culture from the Caucasus to Iran, Anatolia and the Levant: Between unity and diversity. A synthesis,” *Paléorient*, vol. 40, no. 2, pp. 247–260, 2014. Publisher: Persée - Portail des revues scientifiques en SHS.
- [28] M. Van De Mierop, *A History of the Ancient Near East, ca. 3000-323 BC*. John Wiley & Sons, Aug. 2015.
- [29] A. Palmisano, *The Geography of Trade: Landscapes of competition and long-distance contacts in Mesopotamia and Anatolia in the Old Assyrian Colony Period*. Archaeopress Publishing Ltd, Oct. 2018. Google-Books-ID: mLETEAAAQBAJ.
- [30] C. Michel, “The Kārum Period on the Plateau,” Sept. 2011.
- [31] D. W. Anthony, *The horse, the wheel, and language: how bronze-age riders from the Eurasian steppes shaped the modern world / David W. Anthony*. Princeton, N.J: Princeton University Press, 2007.
- [32] C. Marek and P. Frei, *In the Land of a Thousand Gods: A History of Asia Minor in the Ancient World*. Princeton University Press, June 2016. Google-Books-ID: yOo9DwAAQBAJ.
- [33] P. Skoglund, B. H. Northoff, M. V. Shunkov, A. P. Derevianko, S. Pääbo, J. Krause, and M. Jakobsson, “Separating endogenous ancient DNA from modern day contamination in a Siberian Neandertal,” *PNAS*, vol. 111, no. 6, pp. 2229–2234, 2014.
- [34] R. Higuchi, B. Bowman, M. Freiburger, O. A. Ryder, and A. C. Wilson, “DNA sequences from the quagga, an extinct member of the horse family,” *Nature*, vol. 312, pp. 282–284, Nov. 1984. Number: 5991 Publisher: Nature Publishing Group.

- [35] M. Rasmussen, Y. Li, S. Lindgreen, J. S. Pedersen, A. Albrechtsen, I. Moltke, M. Metspalu, E. Metspalu, T. Kivisild, R. Gupta, M. Bertalan, K. Nielsen, M. T. P. Gilbert, Y. Wang, M. Raghavan, P. F. Campos, H. M. Kamp, A. S. Wilson, A. Gledhill, S. Tridico, M. Bunce, E. D. Lorenzen, J. Binladen, X. Guo, J. Zhao, X. Zhang, H. Zhang, Z. Li, M. Chen, L. Orlando, K. Kristiansen, M. Bak, N. Tommerup, C. Bendixen, T. L. Pierre, B. Grønnow, M. Meldgaard, C. Andreasen, S. A. Fedorova, L. P. Osipova, T. F. G. Higham, C. B. Ramsey, T. v. O. Hansen, F. C. Nielsen, M. H. Crawford, S. Brunak, T. Sicheritz-Pontén, R. Villems, R. Nielsen, A. Krogh, J. Wang, and E. Willerslev, “Ancient human genome sequence of an extinct Palaeo-Eskimo,” *Nature*, vol. 463, pp. 757–762, Feb. 2010. Number: 7282 Publisher: Nature Publishing Group.
- [36] R. E. Green, J. Krause, A. W. Briggs, T. Maricic, U. Stenzel, M. Kircher, N. Patterson, H. Li, W. Zhai, M. H.-Y. Fritz, N. F. Hansen, E. Y. Durand, A.-S. Malaspinas, J. D. Jensen, T. Marques-Bonet, C. Alkan, K. Prüfer, M. Meyer, H. A. Burbano, J. M. Good, R. Schultz, A. Aximu-Petri, A. Butthof, B. Höber, B. Höffner, M. Siegemund, A. Weihmann, C. Nusbaum, E. S. Lander, C. Russ, N. Novod, J. Affourtit, M. Egholm, C. Verna, P. Rudan, D. Brajkovic, Kucan, I. Gušić, V. B. Doronichev, L. V. Golovanova, C. Lalueza-Fox, M. de la Rasilla, J. Fortea, A. Rosas, R. W. Schmitz, P. L. Johnson, E. E. Eichler, D. Falush, E. Birney, J. C. Mullikin, M. Slatkin, R. Nielsen, J. Kelso, M. Lachmann, D. Reich, and S. Pääbo, “A draft sequence of the Neandertal genome,” *Science*, vol. 328, pp. 710–722, 2010.
- [37] D. Reich, R. E. Green, M. Kircher, J. Krause, N. Patterson, E. Y. Durand, B. Viola, A. W. Briggs, U. Stenzel, P. L. F. Johnson, T. Maricic, J. M. Good, T. Marques-Bonet, C. Alkan, Q. Fu, S. Mallick, H. Li, M. Meyer, E. E. Eichler, M. Stoneking, M. Richards, S. Talamo, M. V. Shunkov, A. P. Derevianko, J.-J. Hublin, J. Kelso, M. Slatkin, and S. Pääbo, “Genetic history of an archaic hominin group from Denisova Cave in Siberia,” *Nature*, vol. 468, pp. 1053–1060, Dec. 2010. Number: 7327 Publisher: Nature Publishing Group.
- [38] S. Mallick, H. Li, M. Lipson, I. Mathieson, M. Gymrek, F. Racimo, M. Zhao, N. Chennagiri, S. Nordenfelt, A. Tandon, P. Skoglund, I. Lazaridis, S. Sankararaman, Q. Fu, N. Rohland, G. Renaud, Y. Erlich, T. Willems, C. Gallo, J. P. Spence, Y. S. Song, G. Poletti, F. Balloux, G. Van Driem, P. De Knijff, I. G. Romero, A. R. Jha, D. M. Behar, C. M. Bravi, C. Capelli, T. Hervig, A. Moreno-Estrada, O. L. Posukh, E. Balanovska, O. Balanovsky, S. Karachanak-Yankova, H. Sahakyan, D. Toncheva, L. Yepiskoposyan, C. Tyler-Smith, Y. Xue, M. S. Abdullah, A. Ruiz-Linares, C. M. Beall, A. Di Rienzo, C. Jeong, E. B. Starikovskaya, E. Metspalu, J. Parik, R. Villems, B. M. Henn, U. Hodoglugil, R. Mahley, A. Sajantila, G. Stamatoyannopoulos, J. T. Wee, R. Khusainova, E. Khusnutdinova, S. Litvinov, G. Ayodo, D. Comas, M. F. Hammer, T. Kivisild, W. Klitz, C. A. Winkler, D. Labuda, M. Bamshad, L. B. Jorde, S. A. Tishkoff, W. S. Watkins, M. Metspalu, S. Dryomov, R. Sukernik, L. Singh, K. Thangaraj, S. Pääbo, J. Kelso, N. Patterson, and D. Reich, “The Simons Genome Diversity Project: 300 genomes from 142 diverse populations,” *Nature*, vol. 538, pp. 201–206, 2016.

- [39] S. R. Browning, B. L. Browning, Y. Zhou, S. Tucci, and J. M. Akey, “Analysis of Human Sequence Data Reveals Two Pulses of Archaic Denisovan Admixture,” *Cell*, vol. 173, pp. 53–61.e9, Mar. 2018.
- [40] M. Meyer, J.-L. Arsuaga, C. de Filippo, S. Nagel, A. Aximu-Petri, B. Nickel, I. Martínez, A. Gracia, J. M. B. de Castro, E. Carbonell, B. Viola, J. Kelso, K. Prüfer, and S. Pääbo, “Nuclear DNA sequences from the Middle Pleistocene Sima de los Huecos hominins,” *Nature*, vol. 531, pp. 504–507, Mar. 2016. Number: 7595 Publisher: Nature Publishing Group.
- [41] Q. Fu, H. Li, P. Moorjani, F. Jay, S. M. Slepchenko, A. A. Bondarev, P. L. Johnson, A. A. Petri, K. Prüfer, C. de Filippo, M. Meyer, N. Zwyns, D. C. Salazar-Garcia, Y. V. Kuzmin, S. G. Keates, P. A. Kosintsev, D. I. Razhev, M. P. Richards, N. V. Peristov, M. Lachmann, K. Douka, T. F. Higham, M. Slatkin, J.-J. Hublin, D. Reich, J. Kelso, T. B. Viola, and S. Pääbo, “The genome sequence of a 45,000-year-old modern human from western Siberia,” *Nature*, vol. 514, pp. 445–449, Oct. 2014.
- [42] K. Prüfer, C. Posth, H. Yu, A. Stoessel, M. A. Spyrou, T. Deviese, M. Mattonai, E. Ribechini, T. Higham, P. Velemínský, J. Brůžek, and J. Krause, “A genome sequence from a modern human skull over 45,000 years old from Zlatý kůň in Czechia,” *Nature Ecology & Evolution*, vol. 5, pp. 820–825, June 2021. Number: 6 Publisher: Nature Publishing Group.
- [43] M. Hajdinjak, F. Mafessoni, L. Skov, B. Vernot, A. Hübner, Q. Fu, E. Essel, S. Nagel, B. Nickel, J. Richter, O. T. Moldovan, S. Constantin, E. Endarova, N. Zahariev, R. Spasov, F. Welker, G. M. Smith, V. Sinet-Mathiot, L. Paskulin, H. Fewlass, S. Talamo, Z. Rezek, S. Sirakova, N. Sirakov, S. P. McPherron, T. Tsanova, J.-J. Hublin, B. M. Peter, M. Meyer, P. Skoglund, J. Kelso, and S. Pääbo, “Initial Upper Palaeolithic humans in Europe had recent Neanderthal ancestry,” *Nature*, vol. 592, pp. 253–257, Apr. 2021. Number: 7853 Publisher: Nature Publishing Group.
- [44] T. van der Valk, P. Pečnerová, D. Díez-del Molino, A. Bergström, J. Oppenheimer, S. Hartmann, G. Xenikoudakis, J. A. Thomas, M. Dehasque, E. Sağlıcan, F. R. Fidan, I. Barnes, S. Liu, M. Somel, P. D. Heintzman, P. Nikolskiy, B. Shapiro, P. Skoglund, M. Hofreiter, A. M. Lister, A. Götherström, and L. Dalén, “Million-year-old DNA sheds light on the genomic history of mammoths,” *Nature*, vol. 591, pp. 265–269, Mar. 2021. Number: 7849 Publisher: Nature Publishing Group.
- [45] G. M. Kılınç, A. Omrak, F. Özer, T. Günther, A. M. Büyükkarakaya, E. Bıçakçı, D. Baird, H. M. Dönertaş, A. Ghalichi, R. Yaka, D. Koptekin, S. C. Açıkan, P. Parvizi, M. Krzewińska, E. A. Daskalaki, E. Yüncü, N. D. Dağtaş, A. Fairbairn, J. Pearson, G. Mustafaoğlu, Y. S. Erdal, Y. G. Çakan, Togan, M. Somel, J. Stora, M. Jakobsson, and A. Götherström, “The demographic development of the first farmers in Anatolia,” *Current Biology*, vol. 26, no. 19, pp. 2659–2666, 2016.
- [46] G. M. Kılınç, D. Koptekin, Atakuman, A. P. Sümer, H. M. Dönertaş, R. Yaka, C. C. Bilgin, A. M. Büyükkarakaya, D. Baird, E. Altınışik, P. Flegontov, A. Götherström, Togan, and M. Somel, “Archaeogenomic analysis of the first steps of Neolithization in Anatolia and the Aegean,” *Proceedings of the Royal Society B*, vol. 284, p. 20172064, 2017.

- [47] R. Yaka, I. Mapelli, D. Kaptan, A. Doğu, M. Chyleński, D. Erdal, D. Koptekin, K. B. Vural, A. Bayliss, C. Mazzucato, E. Fer, S. S. Çokoğlu, V. K. Lagerholm, M. Krzewińska, C. Karamurat, H. C. Gemici, A. Sevkar, N. D. Dağtaş, G. M. Kılınç, D. Adams, A. R. Munters, E. Sağlıcan, M. Milella, E. M. Schotsmans, E. Yurtman, M. Çetin, S. Yorulmaz, N. E. Altınışık, A. Ghalichi, A. Juras, C. C. Bilgin, T. Günther, J. Storå, M. Jakobsson, M. de Kleijn, G. Mustafaoğlu, A. Fairbairn, J. Pearson, Togan, N. Kayacan, A. Marciniak, C. S. Larsen, I. Hodder, Atakuman, M. Pilloud, E. Sürer, F. Gerritsen, R. Özbal, D. Baird, Y. S. Erdal, G. Duru, M. Özbaşaran, S. D. Haddow, C. J. Knüsel, A. Götherström, F. Özer, and M. Somel, “Variable kinship patterns in Neolithic Anatolia revealed by ancient genomes,” *Current Biology*, vol. 31, pp. 2455–2468, 2021.
- [48] N. E. Altınışık, D. D. Kazancı, A. Aydoğan, H. C. Gemici, D. Erdal, S. Sarıaltun, K. B. Vural, D. Koptekin, K. Gürün, E. Sağlıcan, G. Çakan, M. M. Koruyucu, V. K. Lagerholm, C. Karamurat, M. Özkan, G. M. Kılınç, A. Sevkar, E. Sürer, A. Götherström, Atakuman, Y. S. Erdal, F. Özer, A. E. Özdoğan, and M. Somel, “A genomic snapshot of demographic and cultural dynamism in Upper Mesopotamia during the Neolithic Transition,” tech. rep., bioRxiv, Feb. 2022.
- [49] M. Feldman, E. Fernández-Domínguez, L. Reynolds, D. Baird, J. Pearson, I. Herškowitz, H. May, N. Goring-Morris, M. Benz, J. Gresky, R. A. Bianco, A. Fairbairn, G. Mustafaoğlu, P. W. Stockhammer, C. Posth, W. Haak, C. Jeong, and J. Krause, “Late Pleistocene human genome suggests a local origin for the first farmers of central Anatolia,” *Nature Communications*, vol. 10, p. 1218, 2019.
- [50] N. Marchi, L. Winkelbach, I. Schulz, M. Bami, Z. Hofmanová, J. Blöcher, C. S. Reyna-Blanco, Y. Diekmann, A. Thiéry, A. Kapopoulou, V. Link, V. Piuz, S. Kreutzer, S. M. Figarska, E. Ganiatsou, A. Pukaj, T. J. Struck, R. N. Gutenkunst, N. Karul, F. Gerritsen, J. Pechtl, J. Peters, A. Zeeb-Lanz, E. Lenneis, M. Teschler-Nicola, S. Triantaphyllou, S. Stefanović, C. Papageorgopoulou, D. Wegmann, J. Burger, and L. Excoffier, “The genomic origins of the world’s first farmers,” *Cell*, vol. 185, pp. 1842–1859.e18, May 2022.
- [51] I. Lazaridis, D. Nadel, G. Rollefson, D. C. Merrett, N. Rohland, S. Mallick, D. Fernandes, M. Novak, B. Gamarra, K. Sirak, S. Connell, K. Stewardson, E. Harney, Q. Fu, G. Gonzalez-Fortes, E. R. Jones, S. Alpaslan Roodenberg, G. Lengyel, F. Bocquentin, B. Gasparian, J. M. Monge, M. Gregg, V. Eshed, A. S. Mizrahi, C. Meiklejohn, F. Gerritsen, L. Bejenaru, M. Blüher, A. Campbell, G. Cavalleri, D. Comas, P. Froguel, E. Gilbert, S. M. Kerr, P. Kovacs, J. Krause, D. McGettigan, M. Merrigan, D. A. Merriwether, S. O’Reilly, M. B. Richards, O. Semino, M. Shamoony-Pour, G. Stefanescu, M. Stumvoll, A. Tönjes, A. Torroni, J. F. Wilson, L. Yengo, N. A. Hovhannisyanyan, N. Patterson, R. Pinhasi, and D. Reich, “Genomic insights into the origin of farming in the ancient Near East,” *Nature*, vol. 536, pp. 419–424, 2016.
- [52] F. Broushaki, M. G. Thomas, V. Link, S. López, L. van Dorp, K. Kirsanow, Z. Hofmanová, Y. Diekmann, L. M. Cassidy, D. Díez-del Molino, A. Kousathanas, C. Sell, H. K. Robson, R. Martiniano, J. Blöcher, A. Scheu, S. Kreutzer, R. Bollongino, D. Bobo, H. Davoudi, O. Munoz, M. Currat, K. Abdi, F. Biglari, O. E. Craig, D. G. Bradley, S. Shennan, K. R. Veeramah, M. Mashkour, D. Wegmann, G. Hellenthal,

and J. Burger, “Early Neolithic genomes from the eastern Fertile Crescent,” *Science*, vol. 353, pp. 499–503, July 2016. Publisher: American Association for the Advancement of Science.

- [53] M. Gallego-Llorente, S. Connell, E. R. Jones, D. C. Merrett, Y. Jeon, A. Eriksson, V. Siska, C. Gamba, C. Meiklejohn, R. Beyer, S. Jeon, Y. S. Cho, M. Hofreiter, J. Bhak, A. Manica, and R. Pinhasi, “The genetics of an early Neolithic pastoralist from the Zagros, Iran,” *Scientific Reports*, vol. 6, p. 31326, Aug. 2016. Number: 1 Publisher: Nature Publishing Group.
- [54] V. M. Narasimhan, N. Patterson, P. Moorjani, N. Rohland, R. Bernardos, S. Mallick, I. Lazaridis, N. Nakatsuka, I. Olalde, M. Lipson, A. M. Kim, L. M. Olivieri, A. Coppa, M. Vidale, J. Mallory, V. Moiseyev, E. Kitov, J. Monge, N. Adamski, N. Alex, N. Broomandkoshbacht, F. Candilio, K. Callan, O. Cheronet, B. J. Culleton, M. Ferry, D. Fernandes, S. Freilich, B. Gamarra, D. Gaudio, M. Hajdinjak, Harney, T. K. Harper, D. Keating, A. M. Lawson, M. Mah, K. Mandl, M. Michel, M. Novak, J. Oppenheimer, N. Rai, K. Sirak, V. Slon, K. Stewardson, F. Zalzal, Z. Zhang, G. Akhatov, A. N. Bagashev, A. Bagnera, B. Baitanayev, J. Bendezu-Sarmiento, A. A. Bissembaev, G. L. Bonora, T. T. Charynov, T. Chikisheva, P. K. Dashkovskiy, A. Derevianko, M. Dobeš, K. Douka, N. Dubova, M. N. Duisengali, D. Enshin, A. Epimakhov, A. V. Fribus, D. Fuller, A. Goryachev, A. Gromov, S. P. Grushin, B. Hanks, M. Judd, E. Kazizov, A. Khokhlov, A. P. Krygin, E. Kupriyanova, P. Kuznetsov, D. Luiselli, F. Maksudov, A. M. Mamedov, T. B. Mamirov, C. Meiklejohn, D. C. Merrett, R. Micheli, O. Mochalov, S. Mustafokulov, A. Nayak, D. Pettener, R. Potts, D. Razhev, M. Rykun, S. Sarno, T. M. Savenkova, K. Sikhymbaeva, S. M. Slepchenko, O. A. Soltobaev, N. Stepanova, S. Svyatko, K. Tabaldiev, M. Teschler-Nicola, A. A. Tishkin, V. V. Tkachev, S. Vasilyev, P. Velemínský, D. Voyakin, A. Yermolayeva, M. Zahir, V. S. Zubkov, A. Zubova, V. S. Shinde, C. Lalueza-Fox, M. Meyer, D. Anthony, N. Boivin, K. Thangaraj, D. J. Kennett, M. Frachetti, R. Pinhasi, and D. Reich, “The formation of human populations in South and Central Asia,” *Science*, vol. 365, p. eaat7487, 2019.
- [55] Z. Hofmanová, S. Kreutzer, G. Hellenthal, C. Sell, Y. Diekmann, D. Díez-Del-Molino, L. Van Dorp, S. López, A. Kousathanas, V. Link, K. Kirsanow, L. M. Cassidy, R. Martiniano, M. Strobel, A. Scheu, K. Kotsakis, P. Halstead, S. Triantaphyllou, N. Kyparissi-Apostolika, D. Urem-Kotsou, C. Ziota, F. Adaktylou, S. Gopalan, D. M. Bobo, L. Winkelbach, J. Blöcher, M. Unterländer, C. Leuenberger, Çilingiroğlu, B. Horejs, F. Gerritsen, S. J. Shennan, D. G. Bradley, M. Currat, K. R. Veeramah, D. Wegmann, M. G. Thomas, C. Papageorgopoulou, and J. Burger, “Early farmers from across Europe directly descended from Neolithic Aegeans,” *PNAS*, vol. 113, no. 25, pp. 6886–6891, 2016.
- [56] J. Notroff, Dietrich, and K. Schmidt, “Building Monuments, Creating Communities: Early Monumental Architecture at Pre-Pottery Neolithic Göbekli Tepe,” in *Approaching Monumentality in Archaeology*, pp. 83–106, SUNY Press, Oct. 2014. Google-Books-ID: nvAQBQAAQBAJ.
- [57] B. Bramanti, M. G. Thomas, W. Haak, M. Unterlaender, P. Jores, K. Tambets, I. Antanaitis-Jacobs, M. N. Haidle, R. Jankauskas, C.-J. Kind, F. Lueth, T. Terberger,

- J. Hiller, S. Matsumura, P. Forster, and J. Burger, "Genetic Discontinuity Between Local Hunter-Gatherers and Central Europe's First Farmers," *Science*, vol. 326, pp. 137–140, Oct. 2009. Publisher: American Association for the Advancement of Science.
- [58] I. Lazaridis, N. Patterson, A. Mittnik, G. Renaud, S. Mallick, K. Kirsanow, P. H. Sudmant, J. G. Schraiber, S. Castellano, M. Lipson, B. Berger, C. Economou, R. Bollongino, Q. Fu, K. I. Bos, S. Nordenfelt, H. Li, C. de Filippo, K. Prüfer, S. Sawyer, C. Posth, W. Haak, F. Hallgren, E. Fornander, N. Rohland, D. Delsate, M. Francken, J.-M. Guinet, J. Wahl, G. Ayodo, H. A. Babiker, G. Bailliet, E. Balanovska, O. Balanovsky, R. Barrantes, G. Bedoya, H. Ben-Ami, J. Bene, F. Berrada, C. M. Bravi, F. Brisighelli, G. B. Busby, F. Cali, M. Churnosov, D. E. Cole, D. Corach, L. Damba, G. van Driem, S. Dryomov, J.-M. Dugoujon, S. A. Fedorova, I. Gallego Romero, M. Gubina, M. Hammer, B. M. Henn, T. Hervig, U. Hodoglugil, A. R. Jha, S. Karachanak-Yankova, R. Khusainova, E. Khusnutdinova, R. Kittles, T. Kivisild, W. Klitz, V. Kučinskas, A. Kushniarevich, L. Laredj, S. Litvinov, T. Loukidis, R. W. Mahley, B. Melegh, E. Metspalu, J. Molina, J. Mountain, K. Näkkäläjärvi, D. Nesheva, T. Nyambo, L. Osipova, J. Parik, F. Platonov, O. Posukh, V. Romano, F. Rothhammer, I. Rudan, R. Ruizbakiev, H. Sahakyan, A. Sajantila, A. Salas, E. B. Starikovskaya, A. Tarekegn, D. Toncheva, S. Turdikulova, I. Uktveryte, O. Utevska, R. Vasquez, M. Villena, M. Voevoda, C. A. Winkler, L. Yepiskoposyan, P. Zalloua, T. Zemunik, A. Cooper, C. Capelli, M. G. Thomas, A. Ruiz-Linares, S. A. Tishkoff, L. Singh, K. Thangaraj, R. Villems, D. Comas, R. Sukernik, M. Metspalu, M. Meyer, E. E. Eichler, J. Burger, M. Slatkin, S. Pääbo, J. Kelso, D. Reich, and J. Krause, "Ancient human genomes suggest three ancestral populations for present-day Europeans," *Nature*, vol. 513, pp. 409–413, 2014.
- [59] I. Mathieson, I. Lazaridis, N. Rohland, S. Mallick, N. Patterson, S. A. Roodenberg, E. Harney, K. Stewardson, D. Fernandes, M. Novak, K. Sirak, C. Gamba, E. R. Jones, B. Llamas, S. Dryomov, J. Pickrell, J. L. Arsuaga, J. M. B. de Castro, E. Carbonell, F. Gerritsen, A. Khokhlov, P. Kuznetsov, M. Lozano, H. Meller, O. Mochalov, V. Moiseyev, M. A. R. Guerra, J. Roodenberg, J. M. Vergès, J. Krause, A. Cooper, K. W. Alt, D. Brown, D. Anthony, C. Lalueza-Fox, W. Haak, R. Pinhasi, and D. Reich, "Genome-wide patterns of selection in 230 ancient Eurasians," *Nature*, vol. 528, pp. 499–503, Dec. 2015.
- [60] L. Thissen, H. Özbal, A. Türkekul-Bıyık, F. Gerritsen, and R. Özbal, "The land of milk? Approaching dietary preferences of Late Neolithic communities in NW Anatolia," *The Leiden Journal of Pottery Studies*, vol. 26, pp. 157–172, 2010.
- [61] J. Yakar, *The nature and extent of Neolithic Anatolia's contribution to the emergence of farming communities in the Balkans: an overview*. Habelt, R (22 Dec. 2016), in south east europe and anatolia in prehistory band 263: essays in honor of vassil nikolov on his 65th anniversary (eds bacvarov k, gleser r), pp. 25–68. bonn, germany: verlag dr. rudolf habelt gmbh. ed., 2016.
- [62] J. B. Pereira, M. D. Costa, D. Vieira, M. Pala, L. Bamford, N. Harich, L. Cherni, F. Alshamali, J. Hatina, S. Rychkov, G. Stefanescu, T. King, A. Torroni, P. Soares, L. Pereira, and M. B. Richards, "Reconciling evidence from ancient and contemporary genomes: a major source for the European Neolithic within Mediterranean Europe,"

Proceedings of the Royal Society B: Biological Sciences, vol. 284, p. 20161976, Mar. 2017. Publisher: Royal Society.

- [63] I. Mathieson, S. Alpaslan-Roodenberg, C. Posth, A. Szécsényi-Nagy, N. Rohland, S. Mallick, I. Olalde, N. Broomandkoshbacht, F. Candilio, O. Cheronet, D. Fernandes, M. Ferry, B. Gamarra, G. G. Fortes, W. Haak, E. Harney, E. Jones, D. Keating, B. Krause-Kyora, I. Kucukkalıpcı, M. Michel, A. Mittnik, K. Nägele, M. Novak, J. Oppenheimer, N. Patterson, S. Pfrenge, K. Sirak, K. Stewardson, S. Vai, S. Alexandrov, K. W. Alt, R. Andreescu, D. Antonović, A. Ash, N. Atanassova, K. Bacvarov, M. B. Gusztáv, H. Bocherens, M. Bolus, A. Boroneanț, Y. Boyadzhiev, A. Budnik, J. Burmaz, S. Chohadzhiev, N. J. Conard, R. Cottiaux, M. Čuka, C. Cupillard, D. G. Drucker, N. Elenski, M. Francken, B. Galabova, G. Ganetsovski, B. Gély, T. Hajdu, V. Handzhyiska, K. Harvati, T. Higham, S. Iliev, I. Janković, I. Karavanić, D. J. Kennett, D. Komšo, A. Kozak, D. Labuda, M. Lari, C. Lazar, M. Leppik, K. Leshtakov, D. Lo Vetro, D. Los, I. Lozanov, M. Malina, F. Martini, K. McSweeney, H. Meller, M. Mentušić, P. Mirea, V. Moiseyev, V. Petrova, T. D. Price, A. Simalcsik, L. Sineo, M. Šlaus, V. Slavchev, P. Stanev, A. Starović, T. Szeniczey, S. Talamo, M. Teschler-Nicola, C. Thevenet, I. Valchev, F. Valentin, S. Vasilyev, F. Veljanovska, S. Venelinova, E. Veselovskaya, B. Viola, C. Virag, J. Zaninović, S. Zäuner, P. W. Stockhammer, G. Catalano, R. Krauß, D. Caramelli, G. Zarin, B. Gaydarska, M. Lillie, A. G. Nikitin, I. Potekhina, A. Papatthasiou, D. Borić, C. Bonsall, J. Krause, R. Pinhasi, and D. Reich, “The genomic history of southeastern Europe,” *Nature*, vol. 555, pp. 197–203, 2018.
- [64] T. Takaoğlu, T. Korkut, B. Erdoğan, and G. Işın, “Archaeological evidence for 9th and 8th millennia BC at Girmeler Cave near Tlos in SW Turkey,” *Documenta Praehistorica*, vol. 41, pp. 111–118, Dec. 2014.
- [65] A. Çilingiroğlu, Z. Derin, E. Abay, I. Kayan, and H. Sağlamtimur, *Ulucak Höyük: Excavations Conducted Between 1995 and 2002*. Peeters Publishers, 2004. Google-Books-ID: SOasYQdH6NoC.
- [66] C. Çakırlar, “The evolution of animal husbandry in Neolithic central-west Anatolia: the zooarchaeological record from Ulucak Höyük (c. 7040–5660 cal. BC, Izmir, Turkey),” *Anatolian Studies*, vol. 62, pp. 1–33, 2012.
- [67] Çevik and E. Abay, “Neolithisation in Aegean Turkey: Towards a more realistic reading,” in *Anatolian Metal VII: Anatolien und Seine Nachbarn vor 10.000 Jahren/Anatolia and Neighbours 10,000 Years Ago* (Yalçın, ed.), pp. 199–209, Bochum: Dt. Bergbau Museum, 2016.
- [68] Çevik and B. Erdoğan, “Absolute chronology of cultural continuity, change and break in Western Anatolia, between 6850-5480 calBC: The Ulucak Höyük case,” *Mediterranean Archaeology and Archaeometry*, vol. 20, no. 1, pp. 77–92, 2020.
- [69] R. Duru, “Bademağacı Höyüğü (Kızılkaya) Kazıları 1993 Yılı Çalışma Raporu,” *BELLETTEN*, vol. 60, pp. 783–800, Dec. 1996. Number: 229.
- [70] R. Duru and G. Umurtak, “Bademağacı Kazıları 2004, 2005 ve 2006 Yılları Çalışma Raporu,” *BELLETTEN*, vol. 72, pp. 193–250, Apr. 2008. Number: 263.

- [71] J. M. M. Kuhn, M. Jakobsson, and T. Günther, “Estimating genetic kin relationships in prehistoric populations,” *PLOS ONE*, vol. 13, p. e0195491, Apr. 2018.
- [72] N. Patterson, A. L. Price, and D. Reich, “Population structure and eigenanalysis,” *PLoS Genetics*, vol. 2, no. 12, p. e190, 2006.
- [73] N. Patterson, P. Moorjani, Y. Luo, S. Mallick, N. Rohland, Y. Zhan, T. Genschoreck, T. Webster, and D. Reich, “Ancient admixture in human history,” *Genetics*, vol. 192, pp. 1065–1093, 2012.
- [74] W. Haak, I. Lazaridis, N. Patterson, N. Rohland, S. Mallick, B. Llamas, G. Brandt, S. Nordenfelt, E. Harney, K. Stewardson, Q. Fu, A. Mittnik, E. Bánffy, C. Economou, M. Francken, S. Friederich, R. Garrido Pena, F. Hallgren, V. Khartanovich, A. Khokhlov, M. Kunst, P. Kuznetsov, H. Meller, O. Mochalov, V. Moiseyev, N. Nicklisch, S. L. Pichler, R. Risch, M. A. Rojo Guerra, C. Roth, A. Szécsényi-Nagy, J. Wahl, M. Meyer, J. Krause, D. Brown, D. Anthony, A. Cooper, K. W. Alt, and D. Reich, “Massive migration from the steppe was a source for Indo-European languages in Europe,” *Nature*, vol. 522, pp. 207–211, 2015.
- [75] Harney, N. Patterson, D. Reich, and J. Wakeley, “Assessing the performance of qpAdm: a statistical tool for studying population admixture,” *Genetics*, vol. 217, no. 4, p. iyaa045, 2021.
- [76] S. Bertman, *Handbook to Life in Ancient Mesopotamia*. Oxford University Press, 2003.
- [77] B. Lewis, *The Middle East: A Brief History of the Last 2,000 Years*. Simon and Schuster, 1995.
- [78] A. Palmisano, J. Woodbridge, C. N. Roberts, A. Bevan, R. Fyfe, S. Shennan, R. Cheddadi, R. Greenberg, D. Kaniewski, D. Langgut, S. A. Leroy, T. Litt, and A. Miebach, “Holocene landscape dynamics and long-term population trends in the Levant,” *The Holocene*, vol. 29, no. 5, pp. 708–727, 2019.
- [79] M. F. Abazari, *Investigation of mitochondrial hypervariable region I in an Iranian Neolithic livestock population: An exploration to understand the domestication origins*. PhD Thesis, 2018.
- [80] D. T. Potts, *A Companion to the Archaeology of the Ancient Near East*. Wiley-Blackwell, 1 ed., 2012.
- [81] F. C. Ceballos, K. Gürün, N. E. Altınışık, H. C. Gemicı, C. Karamurat, D. Koptekin, K. B. Vural, I. Mapelli, E. Sağlıcan, E. Sürer, Y. S. Erdal, A. Götherström, F. Özer, Atakuman, and M. Somel, “Human inbreeding has decreased in time through the Holocene,” *Current Biology*, vol. 31, pp. 3925–3934, 2021.
- [82] M. Feldman, G. A. Gnecci-Ruscione, T. C. Lamnidis, and C. Posth, “Where Asia meets Europe – recent insights from ancient human genomics,” *Annals of Human Biology*, vol. 48, no. 3, pp. 191–202, 2021.

- [83] Harney, H. May, D. Shalem, N. Rohland, S. Mallick, I. Lazaridis, R. Sarig, K. Stewardson, S. Nordenfelt, N. Patterson, I. Hershkovitz, and D. Reich, “Ancient DNA from Chalcolithic Israel reveals the role of population mixture in cultural transformation,” *Nature Communications*, vol. 9, p. 3336, 2018.
- [84] P. de Barros Damgaard, R. Martiniano, J. Kamm, J. V. Moreno-Mayar, G. Kroonen, M. Peyrot, G. Barjamovic, S. Rasmussen, C. Zacho, N. Baimukhanov, V. Zaibert, V. Merz, A. Biddanda, I. Merz, V. Loman, V. Evdokimov, E. Usmanova, B. Hemphill, A. Seguin-Orlando, F. E. Yediay, I. Ullah, K.-G. Sjögren, K. H. Iversen, J. Choin, C. de la Fuente, M. Ilardo, H. Schroeder, V. Moiseyev, A. Gromov, A. Polyakov, S. Omura, S. Y. Senyurt, H. Ahmad, C. McKenzie, A. Margaryan, A. Hameed, A. Samad, N. Gul, M. H. Khokhar, O. Goriunova, V. I. Bazaliiskii, J. Novembre, A. W. Weber, L. Orlando, M. E. Allentoft, R. Nielsen, K. Kristiansen, M. Sikora, A. K. Outram, R. Durbin, and E. Willerslev, “The first horse herders and the impact of early Bronze Age steppe expansions into Asia,” *Science*, vol. 360, p. eaar7711, 2018.
- [85] F. Clemente, M. Unterländer, O. Dolgova, C. E. G. Amorim, F. Coroado-Santos, S. Neuenschwander, E. Ganiatsou, D. I. Cruz Dávalos, L. Anchieri, F. Michaud, L. Winkelbach, J. Blöcher, Y. O. Arizmendi Cárdenas, B. Sousa da Mota, E. Kalliga, A. Souleles, I. Kontopoulos, G. Karamitrou-Mentessidi, O. Philaniotou, A. Sampson, D. Theodorou, M. Tsipopoulou, I. Akamatis, P. Halstead, K. Kotsakis, D. Urem-Kotsou, D. Panagiotopoulos, C. Ziota, S. Triantaphyllou, O. Delaneau, J. D. Jensen, J. V. Moreno-Mayar, J. Burger, V. C. Sousa, O. Lao, A.-S. Malaspinas, and C. Pappageorgopoulou, “The genomic history of the Aegean palatial civilizations,” *Cell*, vol. 184, pp. 2565–2586, 2021.
- [86] M. Haber, C. Doumet-Serhal, C. Scheib, Y. Xue, P. Danecek, M. Mezzavilla, S. Youhanna, R. Martiniano, J. Prado-Martinez, M. Szpak, E. Matisoo-Smith, H. Schutkowski, R. Mikulski, P. Zalloua, T. Kivisild, and C. Tyler-Smith, “Continuity and admixture in the last five millennia of Levantine history from ancient Canaanite and present-day Lebanese genome sequences,” *American Journal of Human Genetics*, vol. 101, pp. 274–282, 2017.
- [87] M. Haber, J. Nassar, M. A. Almarri, T. Saupe, L. Saag, S. J. Griffith, C. Doumet-Serhal, J. Chanteau, M. Saghieh-Beydoun, Y. Xue, C. L. Scheib, and C. Tyler-Smith, “A genetic history of the Near East from an aDNA time course sampling eight points in the past 4,000 years,” *American Journal of Human Genetics*, vol. 107, pp. 149–157, 2020.
- [88] I. Lazaridis, A. Mittnik, N. Patterson, S. Mallick, N. Rohland, S. Pfrengle, A. Furtwängler, A. Peltzer, C. Posth, A. Vasilakis, P. McGeorge, E. Konsolaki-Yannopoulou, G. Korres, H. Martlew, M. Michalodimitrakis, M. Özsait, N. Özsait, A. Papatheanasiou, M. Richards, S. Alpaslan Roodenberg, Y. Tzedakis, R. Arnott, D. M. Fernandes, J. R. Hughey, D. M. Lotakis, P. A. Navas, Y. Maniatis, J. A. Stamatoyannopoulos, K. Stewardson, P. Stockhammer, R. Pinhasi, D. Reich, J. Krause, and G. Stamatoyannopoulos, “Genetic origins of the Minoans and Mycenaeans,” *Nature*, vol. 548, pp. 214–218, 2017.
- [89] E. Skourtanioti, Y. S. Erdal, M. Frangipane, F. Balossi Restelli, K. A. Yener, F. Pinnock, P. Matthiae, R. Özbal, U. D. Schoop, F. Guliyev, T. Akhundov, B. Lyonnet, E. L.

- Hammer, S. E. Nugent, M. Burri, G. U. Neumann, S. Penske, T. Ingman, M. Akar, R. Shafiq, G. Palumbi, S. Eisenmann, M. D’Andrea, A. B. Rohrlach, C. Warinner, C. Jeong, P. W. Stockhammer, W. Haak, and J. Krause, “Genomic history of Neolithic to Bronze Age Anatolia, Northern Levant, and Southern Caucasus,” *Cell*, vol. 181, pp. 1158–1175, 2020.
- [90] C.-C. Wang, S. Reinhold, A. Kalmykov, A. Wissgott, G. Brandt, C. Jeong, O. Cheronet, M. Ferry, E. Harney, D. Keating, S. Mallick, N. Rohland, K. Stewardson, A. R. Kantorovich, V. E. Maslov, V. G. Petrenko, V. R. Erlikh, B. C. Atabiev, R. G. Magomedov, P. L. Kohl, K. W. Alt, S. L. Pichler, C. Gerling, H. Meller, B. Vardanyan, L. Yeganyan, A. D. Rezepkin, D. Mariaschk, N. Berezina, J. Gresky, K. Fuchs, C. Knipper, S. Schiffels, E. Balanovska, O. Balanovsky, I. Mathieson, T. Higham, Y. B. Berezin, A. Buzhilova, V. Trifonov, R. Pinhasi, A. B. Belinskij, D. Reich, S. Hansen, J. Krause, and W. Haak, “Ancient human genome-wide data from a 3000-year interval in the Caucasus corresponds with eco-geographic regions,” *Nature Communications*, vol. 10, p. 590, 2019.
- [91] Z. Mehrjoo, Z. Fattahi, M. Beheshtian, M. Mohseni, H. Poustchi, F. Ardalani, K. Jalalvand, S. Arzhangi, Z. Mohammadi, S. Khoshbakht, F. Najafi, P. Nikuei, M. Haddadi, E. Zohrehvand, M. Oladnabi, A. Mohammadzadeh, M. H. Jafari, T. Akhtarkhavari, E. S. Gooshki, A. Haghdoost, R. Najafipour, L. M. Niestroj, B. Helwing, Y. Gossmann, M. R. Toliat, R. Malekzadeh, P. Nürnberg, K. Kahrizi, H. Najmabadi, and M. Nothnagel, “Distinct genetic variation and heterogeneity of the Iranian population,” *PLoS Genetics*, vol. 15, no. 9, p. e1008385, 2019.
- [92] L. Agranat-Tamir, S. Waldman, M. A. Martin, D. Gokhman, N. Mishol, T. Eshel, O. Cheronet, N. Rohland, S. Mallick, N. Adamski, A. M. Lawson, M. Mah, M. Michel, J. Oppenheimer, K. Stewardson, F. Candilio, D. Keating, B. Gamarra, S. Tzur, M. Novak, R. Kalisher, S. Bechar, V. Eshed, D. J. Kennett, M. Faerman, N. Yahalom-Mack, J. M. Monge, Y. Govrin, Y. Erel, B. Yakir, R. Pinhasi, S. Carmi, I. Finkelstein, L. Carmel, and D. Reich, “The genomic history of the Bronze Age Southern Levant,” *Cell*, vol. 181, pp. 1146–1157, 2020.
- [93] M. Haber, M. Mezzavilla, Y. Xue, and C. Tyler-Smith, “Ancient DNA and the rewriting of human history: be sparing with Occam’s razor,” *Genome Biology*, vol. 17, p. 1, 2016.
- [94] M. Feldman, D. M. Master, R. A. Bianco, M. Burri, P. W. Stockhammer, A. Mittnik, A. J. Aja, C. Jeong, and J. Krause, “Ancient DNA sheds light on the genetic origins of early Iron Age Philistines,” *Science Advances*, vol. 5, p. eaax0061, July 2019.
- [95] J. R. Hughey, P. Paschou, P. Drineas, D. Mastropaolo, D. M. Lotakis, P. A. Navas, M. Michalodimitrakis, J. A. Stamatoyannopoulos, and G. Stamatoyannopoulos, “A European population in Minoan Bronze Age Crete,” *Nature Communications*, vol. 4, p. 1861, 2013.
- [96] A. Margaryan, M. Derenko, H. Hovhannisyanyan, B. Malyarchuk, R. Heller, Z. Khachatryan, P. Avetisyan, R. Badalyan, A. Bobokhyan, V. Melikyan, G. Sargsyan, A. Pili-posyan, H. Simonyan, R. Mkrtychyan, G. Denisova, L. Yepiskoposyan, E. Willerslev, and M. E. Allentoft, “Eight millennia of matrilineal genetic continuity in the South Caucasus,” *Current Biology*, vol. 27, pp. 2023–2028, 2017.

- [97] R. Yaka, A. Birand, Y. Yılmaz, C. Caner, S. C. Açıkan, S. Gündüzalp, P. Parvizi, A. Erim Özdoğan, Togan, and M. Somel, “Archaeogenetics of Late Iron Age Çemialo Sirtı, Batman: Investigating maternal genetic continuity in north Mesopotamia since the Neolithic,” *American Journal of Physical Anthropology*, vol. 166, pp. 196–207, 2018.
- [98] The 1000 Genomes Project Consortium, “A global reference for human genetic variation,” *Nature*, vol. 526, pp. 68–74, 2015.
- [99] G. Darbyshire, S. Mitchell, and L. Vardar, “The Galatian settlement in Asia Minor,” *Anatolian Studies*, vol. 50, pp. 75–98, 2000.
- [100] C. B. Rose, “The archaeology of Phrygian Gordion,” in *The Archaeology of Phrygian Gordion, Royal City of Midas: Gordion Special Studies 7* (C. B. Rose, ed.), pp. 1–20, University of Pennsylvania Press, 2013.
- [101] M. E. Kars, A. N. Başak, O. E. Onat, K. Bilguvar, J. Choi, Y. Itan, C. Çağlar, R. Palvadeau, J. L. Casanova, D. N. Cooper, P. D. Stenson, A. Yavuz, H. Buluş, M. Günel, J. M. Friedman, and T. Özçelik, “The genetic structure of the Turkish population reveals high levels of variation and admixture,” *PNAS*, vol. 118, no. 36, p. e2026076118, 2021.
- [102] F. Orsaria, “Shah Tepe: A new approach to an old excavation,” *Rivista degli studi orientali*, vol. 69, no. 3/4, pp. 481–495, 1995.
- [103] C. P. Thornton, “The Bronze Age in Northeastern Iran,” in *The Oxford Handbook of Ancient Iran* (D. T. Potts, ed.), Oxford University Press, 2013.
- [104] E. R. Jones, G. Gonzalez-Fortes, S. Connell, V. Siska, A. Eriksson, R. Martiniano, R. L. McLaughlin, M. Gallego Llorente, L. M. Cassidy, C. Gamba, T. Meshveliani, O. Bar-Yosef, W. Müller, A. Belfer-Cohen, Z. Matskevich, N. Jakeli, T. F. Higham, M. Currat, D. Lordkipanidze, M. Hofreiter, A. Manica, R. Pinhasi, and D. G. Bradley, “Upper Palaeolithic genomes reveal deep roots of modern Eurasians,” *Nature Communications*, vol. 6, p. 8912, 2015.
- [105] P. A. Rasia, L. Bitadze, E. Rova, and F. Bertoldi, “Bronze Age burials from Doghlauri (Georgia). Preliminary analysis of human remains reveals a change in burial customs,” *Journal of Archaeological Science: Reports*, vol. 38, p. 103048, 2021.
- [106] M. Haber, C. Doumet-Serhal, C. L. Scheib, Y. Xue, R. Mikulski, R. Martiniano, B. Fischer-Genz, H. Schutkowski, T. Kivisild, and C. Tyler-Smith, “A transient pulse of genetic admixture from the crusaders in the Near East identified from ancient genome sequences,” *American Journal of Human Genetics*, vol. 104, pp. 977–984, 2019.
- [107] A. M. Harris and M. DeGiorgio, “Admixture and ancestry inference from ancient and modern samples through measures of population genetic drift,” *Human Biology*, vol. 89, no. 1, pp. 21–46, 2017.
- [108] H. Ringbauer, J. Novembre, and M. Steinrücken, “Parental relatedness through time revealed by runs of homozygosity in ancient DNA,” *Nature Communications*, vol. 12, p. 5425, 2021.

- [109] F. C. Ceballos, S. Hazelhurst, and M. Ramsay, “Assessing runs of Homozygosity: a comparison of SNP Array and whole genome sequence low coverage data,” *BMC Genomics*, vol. 19, p. 106, 2018.
- [110] A. Goldberg, T. Günther, N. A. Rosenberg, and M. Jakobsson, “Ancient X chromosomes reveal contrasting sex bias in Neolithic and Bronze Age Eurasian migrations,” *PNAS*, vol. 114, no. 10, pp. 2657–2662, 2017.
- [111] I. Olalde, S. Mallick, N. Patterson, N. Rohland, V. Villalba-Mouco, M. Silva, K. Dulas, C. J. Edwards, F. Gandini, M. Pala, P. Soares, M. Ferrando-Bernal, N. Adamski, N. Broomandkoshbacht, O. Cheronet, B. J. Culleton, D. Fernandes, A. M. Lawson, M. Mah, J. Oppenheimer, K. Stewardson, Z. Zhang, J. M. Jiménez Arenas, I. J. Toro Moyano, D. C. Salazar-García, P. Castanyer, M. Santos, J. Tremoleda, M. Lozano, P. García Borja, J. Fernández-Eraso, J. A. Mujika-Alustiza, C. Barroso, F. J. Bermúdez, E. Viguera Mínguez, J. Burch, N. Coromina, D. Vivó, A. Cebrià, J. M. Fullola, O. García-Puchol, J. I. Morales, F. X. Oms, T. Majó, J. M. Vergès, A. Díaz-Carvajal, I. Ollich-Castanyer, F. J. López-Cachero, A. M. Silva, C. Alonso-Fernández, G. Delibes de Castro, J. Jiménez Echevarría, A. Moreno-Márquez, G. Pascual Berlanga, P. Ramos-García, J. Ramos-Muñoz, E. Vijande Vila, G. Aguilera Arzo, Esparza Arroyo, K. T. Lillios, J. Mack, J. Velasco-Vázquez, A. Waterman, L. Benítez de Lugo Enrich, M. Benito Sánchez, B. Agustí, F. Codina, G. de Prado, A. Estalrich, Fernández Flores, C. Finlayson, G. Finlayson, S. Finlayson, F. Giles-Guzmán, A. Rosas, V. Barciela González, G. García Atiénzar, M. S. Hernández Pérez, A. Llanos, Y. Carrión Marco, I. Collado Beneyto, D. López-Serrano, M. Sanz Tormo, A. C. Valera, C. Blasco, C. Liesau, P. Ríos, J. Daura, M. J. de Pedro Michó, A. A. Díez-Castillo, R. Flores Fernández, J. Francès Farré, R. Garrido-Pena, V. S. Gonçalves, E. Guerra-Doce, A. M. Herrero-Corral, J. Juan-Cabanilles, D. López-Reyes, S. B. McClure, M. Merino Pérez, A. Oliver Foix, M. Sanz Borràs, A. C. Sousa, J. M. Vidal Encinas, D. J. Kennett, M. B. Richards, K. W. Alt, W. Haak, R. Pinhasi, C. Lalueza-Fox, and D. Reich, “The genomic history of the Iberian Peninsula over the past 8000 years,” *Science*, vol. 363, pp. 1230–1234, 2019.
- [112] K.-H. Jun, “Demographics and migration: an overview,” in *The Encyclopedia of Global Human Migration* (I. Ness, ed.), Wiley-Blackwell, 2013.
- [113] A. Palmisano, D. Lawrence, M. W. de Gruchy, A. Bevan, and S. Shennan, “Holocene regional population dynamics and climatic trends in the Near East: A first comparison using archaeo-demographic proxies,” *Quaternary Science Reviews*, vol. 252, p. 106739, 2021.
- [114] J. Dabney, M. Knapp, I. Glocke, M.-T. Gansauge, A. Weihmann, B. Nickel, C. Valdiosera, N. García, S. Pääbo, J.-L. Arsuaga, and M. Meyer, “Complete mitochondrial genome sequence of a Middle Pleistocene cave bear reconstructed from ultrashort DNA fragments,” *PNAS*, vol. 110, no. 39, pp. 15758–15763, 2013.
- [115] M. Meyer and M. Kircher, “Illumina sequencing library preparation for highly multiplexed target capture and sequencing,” *Cold Spring Harbor Protocols*, vol. 2010, no. 6, p. pdb.prot5448, 2010.

- [116] M. Schubert, A. Ginolhac, S. Lindgreen, J. F. Thompson, K. A. AL-Rasheid, E. Willerslev, A. Krogh, and L. Orlando, “Improving ancient DNA read mapping against modern reference genomes,” *BMC Genomics*, vol. 13, p. 178, 2012.
- [117] M. Krzewińska, G. M. Kılınç, A. Juras, D. Koptekin, M. Chyleński, A. G. Nikitin, N. Shcherbakov, I. Shuteleva, T. Leonova, L. Kraeva, F. A. Sungatov, A. N. Sultanova, I. Potekhina, S. Łukasik, M. Krenz-Niedbała, L. Dalén, V. Sinika, M. Jakobsson, J. Storå, and A. Götherström, “Ancient genomes suggest the eastern Pontic-Caspian steppe as the source of western Iron Age nomads,” *Science Advances*, vol. 4, p. eaat4457, Oct. 2018. Publisher: American Association for the Advancement of Science.
- [118] T. L. Fulton and B. Shapiro, “Setting Up an Ancient DNA Laboratory,” *Methods in Molecular Biology (Clifton, N.J.)*, vol. 1963, pp. 1–13, 2019.
- [119] M. E. Allentoft, R. Heller, R. N. Holdaway, and M. Bunce, “Ancient DNA microsatellite analyses of the extinct New Zealand giant moa (*Dinornis robustus*) identify relatives within a single fossil site,” *Heredity*, vol. 115, pp. 481–487, 2015.
- [120] N. Psonis, D. Vassou, and D. Kafetzopoulos, “Testing a series of modifications on genomic library preparation methods for ancient or degraded DNA,” *Analytical Biochemistry*, vol. 623, p. 114193, June 2021.
- [121] P. J. Reimer, W. E. N. Austin, E. Bard, A. Bayliss, P. G. Blackwell, C. B. Ramsey, M. Butzin, H. Cheng, R. L. Edwards, M. Friedrich, P. M. Grootes, T. P. Guilderson, I. Hajdas, T. J. Heaton, A. G. Hogg, K. A. Hughen, B. Kromer, S. W. Manning, R. Muscheler, J. G. Palmer, C. Pearson, J. v. d. Plicht, R. W. Reimer, D. A. Richards, E. M. Scott, J. R. Southon, C. S. M. Turney, L. Wacker, F. Adolphi, U. Büntgen, M. Capano, S. M. Fahrni, A. Fogtmann-Schulz, R. Friedrich, P. Köhler, S. Kudsk, F. Miyake, J. Olsen, F. Reinig, M. Sakamoto, A. Sookdeo, and S. Talamo, “The IntCal20 Northern Hemisphere Radiocarbon Age Calibration Curve (0–55 cal kBP),” *Radiocarbon*, vol. 62, pp. 725–757, Aug. 2020.
- [122] M. Schubert, S. Lindgreen, and L. Orlando, “AdapterRemoval v2: rapid adapter trimming, identification, and read merging,” *BMC Research Notes*, vol. 9, p. 88, 2016.
- [123] H. Li and R. Durbin, “Fast and accurate short read alignment with Burrows-Wheeler transform,” *Bioinformatics*, vol. 25, no. 14, pp. 1754–1760, 2009.
- [124] M. Kircher, “Analysis of high-throughput ancient DNA sequencing data,” in *Ancient DNA: Methods and Protocols, Methods in Molecular Biology*, vol. 840 (B. Shapiro and M. Hofreiter, eds.), pp. 197–228, Humana Press, 2012.
- [125] H. Li, B. Handsaker, A. Wysoker, T. Fennell, J. Ruan, N. Homer, G. Marth, G. Abecasis, R. Durbin, and 1000 Genome Project Data Processing Subgroup, “The Sequence Alignment/Map format and SAMtools,” *Bioinformatics*, vol. 25, no. 16, pp. 2078–2079, 2009.
- [126] A. R. Quinlan and I. M. Hall, “BEDTools: a flexible suite of utilities for comparing genomic features,” *Bioinformatics*, vol. 26, pp. 841–842, Mar. 2010.

- [127] Q. Fu, A. Mittnik, P. L. Johnson, K. Bos, M. Lari, R. Bollongino, C. Sun, L. Giemsch, R. Schmitz, J. Burger, A. M. Ronchitelli, F. Martini, R. G. Cremonesi, J. Svoboda, P. Bauer, D. Caramelli, S. Castellano, D. Reich, S. Pääbo, and J. Krause, “A revised timescale for human evolution based on ancient mitochondrial genomes,” *Current Biology*, vol. 23, pp. 553–559, 2013.
- [128] T. S. Korneliussen, A. Albrechtsen, and R. Nielsen, “ANGSD: Analysis of next generation sequencing data,” *BMC Bioinformatics*, vol. 15, p. 356, 2014.
- [129] P. Skoglund, J. Storå, A. Götherström, and M. Jakobsson, “Accurate sex identification of ancient human remains using DNA shotgun sequencing,” *Journal of Archaeological Science*, vol. 40, pp. 4477–4482, 2013.
- [130] A. Mittnik, C. C. Wang, J. Svoboda, and J. Krause, “A molecular approach to the sexing of the triple burial at the upper paleolithic site of Dolní Věstonice,” *PLoS ONE*, vol. 11, no. 10, p. e0163019, 2016.
- [131] H. Li, “A statistical framework for SNP calling, mutation discovery, association mapping and population genetical parameter estimation from sequencing data,” *Bioinformatics*, vol. 27, no. 21, pp. 2987–93, 2011.
- [132] H. Weissensteiner, D. Pacher, A. Kloss-Brandstätter, L. Forer, G. Specht, H. J. Bandelt, F. Kronenberg, A. Salas, and S. Schönherr, “HaploGrep 2: mitochondrial haplogroup classification in the era of high-throughput sequencing,” *Nucleic Acids Research*, vol. 44, pp. W58–W63, 2016.
- [133] L. Excoffier and H. E. Lischer, “Arlequin suite ver 3.5: a new series of programs to perform population genetics analyses under Linux and Windows,” *Molecular Ecology Resources*, vol. 10, pp. 564–567, 2010.
- [134] Y. Benjamini and Y. Hochberg, “Controlling the false discovery rate: A practical and powerful approach to multiple testing,” *Journal of the Royal Statistical Society: Series B (Methodological)*, vol. 57, no. 1, pp. 289–300, 1995.
- [135] Q. Fu, C. Posth, M. Hajdinjak, M. Petr, S. Mallick, D. Fernandes, A. Furtwängler, W. Haak, M. Meyer, A. Mittnik, B. Nickel, A. Peltzer, N. Rohland, V. Slon, S. Talamo, I. Lazaridis, M. Lipson, I. Mathieson, S. Schiffels, P. Skoglund, A. P. Derevianko, N. Drozdov, V. Slavinsky, A. Tsybankov, R. G. Cremonesi, F. Mallegni, B. Gély, E. Vacca, M. R. G. Morales, L. G. Straus, C. Neugebauer-Maresch, M. Teschler-Nicola, S. Constantin, O. T. Moldovan, S. Benazzi, M. Peresani, D. Coppola, M. Lari, S. Ricci, A. Ronchitelli, F. Valentin, C. Thevenet, K. Wehrberger, D. Grigorescu, H. Rougier, I. Crevecoeur, D. Flas, P. Semal, M. A. Mannino, C. Cupillard, H. Bocherens, N. J. Conard, K. Harvati, V. Moiseyev, D. G. Drucker, J. Svoboda, M. P. Richards, D. Caramelli, R. Pinhasi, J. Kelso, N. Patterson, J. Krause, S. Pääbo, and D. Reich, “The genetic history of Ice Age Europe,” *Nature*, vol. 534, pp. 200–205, June 2016.
- [136] P. de Barros Damgaard, N. Marchi, S. Rasmussen, M. Peyrot, G. Renaud, T. Korneliussen, J. V. Moreno-Mayar, M. W. Pedersen, A. Goldberg, E. Usmanova, N. Baimukhanov, V. Loman, L. Hedeager, A. G. Pedersen, K. Nielsen, G. Afanasiev,

- K. Akmatov, A. Aldashev, A. Alpaslan, G. Baimbetov, V. I. Bazaliiskii, A. Beisenov, B. Boldbaatar, B. Boldgiv, C. Dorzhu, S. Ellingvag, D. Erdenebaatar, R. Dajani, E. Dmitriev, V. Evdokimov, K. M. Frei, A. Gromov, A. Goryachev, H. Hakonarson, T. Hegay, Z. Khachatryan, R. Khaskhanov, E. Kitov, A. Kolbina, T. Kubatbek, A. Kukushkin, I. Kukushkin, N. Lau, A. Margaryan, I. Merkyte, I. V. Mertz, V. K. Mertz, E. Mijiddorj, V. Moiyesev, G. Mukhtarova, B. Nurmukhanbetov, Z. Orozbekova, I. Panyushkina, K. Pieta, V. Smrčka, I. Shevnina, A. Logvin, K.-G. Sjögren, T. Štolcová, A. M. Taravella, K. Tashbaeva, A. Tkachev, T. Tulegenov, D. Voyakin, L. Yepiskoposyan, S. Undrakhbold, V. Varfolomeev, A. Weber, M. A. Wilson Sayres, N. Kradin, M. E. Allentoft, L. Orlando, R. Nielsen, M. Sikora, E. Heyer, K. Kristiansen, and E. Willerslev, “137 ancient human genomes from across the Eurasian steppes,” *Nature*, vol. 557, pp. 369–374, 2018.
- [137] A. Omrak, T. Günther, C. Valdiosera, E. M. Svensson, H. Malmström, H. Kiesewetter, W. Aylward, J. Storå, M. Jakobsson, and A. Götherström, “Genomic Evidence Establishes Anatolia as the Source of the European Neolithic Gene Pool,” *Current Biology*, vol. 26, pp. 270–275, Jan. 2016. Publisher: Elsevier.
- [138] T. Omori and T. Nakamura, “Radiocarbon Dating of Archaeological Materials Excavated at Kaman-Kalehöyük: Initial Report,” *Anatolian Archaeological Studies XV*, pp. 263–268, 2006.
- [139] A. G. Clark, M. J. Hubisz, C. D. Bustamante, S. H. Williamson, and R. Nielsen, “Ascertainment bias in studies of human genome-wide polymorphism,” *Genome Research*, vol. 15, pp. 1496–1502, Jan. 2005.
- [140] A. Bergström, S. A. McCarthy, R. Hui, M. A. Almarri, Q. Ayub, P. Danecek, Y. Chen, S. Felkel, P. Hallast, J. Kamm, H. Blanché, J.-F. Deleuze, H. Cann, S. Mallick, D. Reich, M. S. Sandhu, P. Skoglund, A. Scally, Y. Xue, R. Durbin, and C. Tyler-Smith, “Insights into human genetic variation and population history from 929 diverse genomes,” *Science*, vol. 367, p. eaay5012, 2020.
- [141] S. Tucci, S. H. Vohr, R. C. McCoy, B. Vernot, M. R. Robinson, C. Barbieri, B. J. Nelson, W. Fu, G. A. Purnomo, H. Sudoyo, E. E. Eichler, G. Barbujani, P. M. Visscher, J. M. Akey, and R. E. Green, “Evolutionary history and adaptation of a human pygmy population of Flores Island, Indonesia,” *Science*, vol. 361, pp. 511–516, Aug. 2018.
- [142] G. Jun, M. K. Wing, G. R. Abecasis, and H. M. Kang, “An efficient and scalable analysis framework for variant extraction and refinement from population-scale DNA sequence data,” *Genome Research*, vol. 25, pp. 918–925, 2015.
- [143] R. Kefi, M. Hechmi, C. Naouali, H. Jmel, S. Hsouna, E. Bouzaid, S. Abdelhak, E. Beraud-Colomb, and A. Stevanovitch, “On the origin of Iberomaurusians: new data based on ancient mitochondrial DNA and phylogenetic analysis of Afalou and Taforalt populations,” *Mitochondrial DNA. Part A, DNA mapping, sequencing, and analysis*, vol. 29, pp. 147–157, Jan. 2018.
- [144] J. Kelleher, A. M. Etheridge, and G. McVean, “Efficient coalescent simulation and genealogical analysis for large sample sizes,” *PLoS Computational Biology*, vol. 12, no. 5, p. e1004842, 2016.

- [145] V. M. Narasimhan, R. Rahbari, A. Scally, A. Wuster, D. Mason, Y. Xue, J. Wright, R. C. Trembath, E. R. Maher, D. A. van Heel, A. Auton, M. E. Hurles, C. Tyler-Smith, and R. Durbin, “Estimating the human mutation rate from autozygous segments reveals population differences in human mutational processes,” *Nature Communications*, vol. 8, p. 303, Aug. 2017.
- [146] H. Wickham, M. Averick, J. Bryan, W. Chang, L. D. McGowan, R. François, G. Grolemund, A. Hayes, L. Henry, J. Hester, M. Kuhn, T. L. Pedersen, E. Miller, S. M. Bache, K. Müller, J. Ooms, D. Robinson, D. P. Seidel, V. Spinu, K. Takahashi, D. Vaughan, C. Wilke, K. Woo, and H. Yutani, “Welcome to the Tidyverse,” *Journal of Open Source Software*, vol. 4, p. 1686, Nov. 2019.
- [147] H. Wickham, “The split-apply-combine strategy for data analysis,” *Journal of Statistical Software*, vol. 40, no. 1, pp. 1–29, 2011.
- [148] H. Wickham, “Reshaping Data with the reshape Package,” *Journal of Statistical Software*, vol. 21, pp. 1–20, Nov. 2007.
- [149] M. Conway, “gsheet: Download Google Sheets Using Just the URL. R package version 0.4.5. <https://CRAN.R-project.org/package=gsheet>,” 2020.
- [150] H. Wickham, *ggplot2: Elegant graphics for data analysis*. Springer, 2 ed., 2016.
- [151] C. Wilke, “ggtext: Improved Text Rendering Support for ‘ggplot2’. R package version 0.1.1. <https://CRAN.R-project.org/package=ggtext>,” 2020.
- [152] T. L. Pedersen, “ggforce: Accelerating ‘ggplot2’. <https://ggforce.data-imaginist.com>, <https://github.com/thomasp85/ggforce>,” 2022.
- [153] A. Kassambara, “ggpubr: ‘ggplot2’ Based Publication Ready Plots. R package version 0.4.0. <https://CRAN.R-project.org/package=ggpubr>,” 2020.
- [154] K. Slowikowski, “ggrepel: Automatically position non-overlapping text labels with ‘ggplot2’,” 2021. R package version 0.9.1.
- [155] R. A. Becker, A. R. Wilks, R. Brownrigg, T. P. Minka, and A. Deckmyn, “maps: Draw Geographical Maps. R package version 3.3.0. <https://CRAN.R-project.org/package=maps>,” 2018.
- [156] R. J. Hijmans, “raster: Geographic data analysis and modeling,” 2022. R package version 3.5-15.
- [157] R. Bivand, T. Keitt, and B. Rowlingson, “rgdal: Bindings for the ‘geospatial’ data abstraction library,” 2022. R package version 1.5-30.
- [158] T. L. Pedersen, “patchwork: The Composer of Plots. R package version 1.1.1. <https://CRAN.R-project.org/package=patchwork>,” 2020.
- [159] S. Rubinacci, D. M. Ribeiro, R. J. Hofmeister, and O. Delaneau, “Efficient phasing and imputation of low-coverage sequencing data using large reference panels,” *Nature Genetics*, vol. 53, pp. 120–126, Jan. 2021. Number: 1 Publisher: Nature Publishing Group.

APPENDIX A

Table 5: Information about all individuals used in the analyses.

SampleID	Population_Label	Country	Region	Publication	Date
Ash033	Anatolia_EN	Turkey	Anatolia	[47]	7883-7605 calBCE
Ash128	Anatolia_EN	Turkey	Anatolia	[47]	8240-7941 calBCE
Ash129	Anatolia_EN	Turkey	Anatolia	[47]	8004-7717 calBCE
Ash136	Anatolia_EN	Turkey	Anatolia	[47]	7997-7707 calBCE
Bar31	Anatolia_Barcin_N_SG	Turkey	Anatolia	[55]	6419-6238 calBCE
Bar8	Anatolia_Barcin_N_SG	Turkey	Anatolia	[55]	6212-6030 calBCE
BOG019	Anatolia_Bogazkoy_Roma	Turkey	Anatolia	This Study	100-350 CE
BOG020	Anatolia_Bogazkoy_Roma	Turkey	Anatolia	This Study	130-190 CE
BOG024	Anatolia_Bogazkoy_Roma	Turkey	Anatolia	This Study	130-190 CE
BOG028	Anatolia_Bogazkoy_Ottoman	Turkey	Anatolia	This Study	1000-1900 CE
Bon002	Anatolia_EN	Turkey	Anatolia	[45]	8279-7977 calBCE
Bon004	Anatolia_EN	Turkey	Anatolia	[45]	8300-7952 BCE
CBT001	Anatolia_CamlibelTarlasi_LC	Turkey	Anatolia	[89]	5581-5329 BP
CBT003	Anatolia_CamlibelTarlasi_LC	Turkey	Anatolia	[89]	5550-5350 BP
CBT004	Anatolia_CamlibelTarlasi_LC	Turkey	Anatolia	[89]	5585-5471 BP
CBT005	Anatolia_CamlibelTarlasi_LC	Turkey	Anatolia	[89]	5578-5327 BP
CBT010	Anatolia_CamlibelTarlasi_LC	Turkey	Anatolia	[89]	5540-5420 BP
CBT011	Anatolia_CamlibelTarlasi_LC	Turkey	Anatolia	[89]	5540-5420 BP
CBT014	Anatolia_CamlibelTarlasi_LC	Turkey	Anatolia	[89]	5589-5335 BP
CBT015	Anatolia_CamlibelTarlasi_LC	Turkey	Anatolia	[89]	5592-5472 BP
CBT016	Anatolia_CamlibelTarlasi_LC	Turkey	Anatolia	[89]	5641-5478 BP
CBT018	Anatolia_Buyukkaya_EC	Turkey	Anatolia	[89]	7576-7463 BP
CCH144	Anatolia_Catalhoyuk_N	Turkey	Anatolia	[47]	7035-6680 calBCE
CCH163	Anatolia_Catalhoyuk_N	Turkey	Anatolia	[47]	6775-6595 calBCE
CCH285	Anatolia_Catalhoyuk_N	Turkey	Anatolia	[47]	NA
CCH289	Anatolia_Catalhoyuk_N	Turkey	Anatolia	[47]	6825-6635 calBCE

Table 5 (continued)

SampleID	Population_Label	Country	Region	Publication	Date
CCH290	Anatolia_Catalhoyuk_N	Turkey	Anatolia	[47]	6690–6590 calBCE
CCH294	Anatolia_Catalhoyuk_N	Turkey	Anatolia	[47]	NA
CCH311	Anatolia_Catalhoyuk_N	Turkey	Anatolia	[47]	NA
CTG025	Anatolia_CineTepecik_BA	Turkey	Anatolia	This Study	1977-1862calBCE
cth006	Anatolia_Catalhoyuk_N	Turkey	Anatolia	[47]	6613-6467calBCE
cth217	Anatolia_Catalhoyuk_N	Turkey	Anatolia	[47]	6415-6244 calBCE
cth739	Anatolia_Catalhoyuk_N	Turkey	Anatolia	[47]	6234-6077 calBCE
cth747	Anatolia_Catalhoyuk_N	Turkey	Anatolia	[47]	6660-6497 calBCE
GOR001	Anatolia_Gordion_IA	Turkey	Anatolia	This Study	333 BC -0
GOR002	Anatolia_Gordion_IA	Turkey	Anatolia	This Study	333 BC -0
I0707	Anatolia_Barcin_N	Turkey	Anatolia	[59]	6500-6200 BCE
I0708	Anatolia_Barcin_N	Turkey	Anatolia	[59]	6221-6073 calBCE
I0709	Anatolia_Barcin_N	Turkey	Anatolia	[59]	6500-6200 BCE
I0723	Anatolia_Mentese_N	Turkey	Anatolia	[59]	5995-5845 calBCE
I0724	Anatolia_Mentese_N	Turkey	Anatolia	[59]	6400-5600 BCE
I0725	Anatolia_Mentese_N	Turkey	Anatolia	[59]	6400-5600 BCE
I0726	Anatolia_Mentese_N	Turkey	Anatolia	[59]	6400-5600 BCE
I0727	Anatolia_Mentese_N	Turkey	Anatolia	[59]	6400-5600 BCE
I0736	Anatolia_Barcin_N	Turkey	Anatolia	[59]	6500-6200 BCE
I0744	Anatolia_Barcin_N	Turkey	Anatolia	[59]	6402-6243 calBCE
I0745	Anatolia_Barcin_N	Turkey	Anatolia	[59]	6374-6227 calBCE
I0746	Anatolia_Barcin_N	Turkey	Anatolia	[59]	6067-5892 calBCE
I1096	Anatolia_Barcin_N	Turkey	Anatolia	[59]	6500-6200 BCE
I1097	Anatolia_Barcin_N	Turkey	Anatolia	[59]	6424-6251 calBCE
I1098	Anatolia_Barcin_N	Turkey	Anatolia	[59]	6500-6200 BCE

Table 5 (continued)

SampleID	Population_Label	Country	Region	Publication	Date
I1099	Anatolia_Barcin_N	Turkey	Anatolia	[59]	6500-6200 BCE
I1100	Anatolia_Barcin_N	Turkey	Anatolia	[59]	6500-6200 BCE
I1101	Anatolia_Barcin_N	Turkey	Anatolia	[59]	6500-6200 BCE
I1102	Anatolia_Barcin_N	Turkey	Anatolia	[59]	6500-6200 BCE
I1103	Anatolia_Barcin_N	Turkey	Anatolia	[59]	6500-6200 BCE
I1579	Anatolia_Barcin_N	Turkey	Anatolia	[59]	6500-6200 BCE
I1580	Anatolia_Barcin_N	Turkey	Anatolia	[59]	6387-6103 calBCE
I1581	Anatolia_Barcin_N	Turkey	Anatolia	[59]	6376-6231 calBCE
I1583	Anatolia_Barcin_N	Turkey	Anatolia	[59]	6426-6236 calBCE
I1584	Anatolia_Barcin_CA	Turkey	Anatolia	[51]	3943-3708 calBCE
I1585	Anatolia_Barcin_N	Turkey	Anatolia	[59]	6500-6200 BCE
I2495	Anatolia_Harmanoren_BA	Turkey	Anatolia	[88]	2558-2295 calBCE
I2499	Anatolia_Harmanoren_BA	Turkey	Anatolia	[88]	2836-2472 calBCE
I2683	Anatolia_Harmanoren_BA	Turkey	Anatolia	[88]	2618-2470 calBCE
IKI009	Anatolia_Ikiztepe_LC	Turkey	Anatolia	[89]	5316-5065 BP
IKI012	Anatolia_Ikiztepe_LC	Turkey	Anatolia	[89]	5318-5068 BP
IKI016	Anatolia_Ikiztepe_LC	Turkey	Anatolia	[89]	5468-5321 BP
IKI017	Anatolia_Ikiztepe_LC	Turkey	Anatolia	[89]	5444-5074 BP
IKI019	Anatolia_Ikiztepe_LC_lc	Turkey	Anatolia	[89]	5450-5050 BP
IKI020	Anatolia_Ikiztepe_LC_lc	Turkey	Anatolia	[89]	5450-5050 BP
IKI024	Anatolia_Ikiztepe_LC	Turkey	Anatolia	[89]	5908-5749 BP
IKI030	Anatolia_Ikiztepe_LC	Turkey	Anatolia	[89]	5462-5307 BP
IKI034	Anatolia_Ikiztepe_LC	Turkey	Anatolia	[89]	5450-5302 BP
IKI036	Anatolia_Ikiztepe_LC	Turkey	Anatolia	[89]	5577-5324 BP
IKI037	Anatolia_Ikiztepe_LC	Turkey	Anatolia	[89]	5585-5332 BP
IKI038	Anatolia_Ikiztepe_LC	Turkey	Anatolia	[89]	5583-5331 BP

Table 5 (continued)

SampleID	Population_Label	Country	Region	Publication	Date
Kumtepe006	Anatolia_Kumtepe_CA	Turkey	Anatolia	[137]	4846-4618 calBCE
MA2195	Anatolia_Kalehoyuk_OttomanI	Turkey	Anatolia	[84]	1200-1950 CE
MA2196	Anatolia_Kalehoyuk_OttomanII	Turkey	Anatolia	[84]	1200-1950 CE
MA2197	Anatolia_Kalehoyuk_IA	Turkey	Anatolia	[84]	278 BC - 0
MA2198	Anatolia_Kalehoyuk_OttomanIII	Turkey	Anatolia	[84]	1400-1800 CE
MA2200	Anatolia_Kalehoyuk_OldHittite_BA	Turkey	Anatolia	[84]	2500-1200 BCE
MA2203	Anatolia_Kalehoyuk_OldHittite_BA	Turkey	Anatolia	[84]	2500-1200 BCE
MA2205	Anatolia_Kalehoyuk_Assyrian_BA	Turkey	Anatolia	[84]	2500-1200 BCE
MA2206	Anatolia_Kalehoyuk_Assyrian_BA	Turkey	Anatolia	[84]	2500-1200 BCE
MA2208	Anatolia_Kalehoyuk_Assyrian_BA	Turkey	Anatolia	[84]	2500-1200 BCE
MA2210	Anatolia_Ovaoren_BA	Turkey	Anatolia	[84]	3000-2500 BCE
MA2212	Anatolia_Ovaoren_BA	Turkey	Anatolia	[84]	3000-2500 BCE
MA2213	Anatolia_Ovaoren_BA	Turkey	Anatolia	[84]	3000-2500 BCE
mus005	Anatolia_Musular_N	Turkey	Anatolia	This Study	7377-7167 BCE
mus006	Anatolia_Musular_N	Turkey	Anatolia	This Study	7180-7039 BCE
pch034	Anatolia_Catalhoyuk_N	Turkey	Anatolia	[47]	NA
Kayseri23827	Turkish	Turkey	Anatolia	[38]	0
Kayseri24424	Turkish	Turkey	Anatolia	[38]	0
Tep002	Anatolia_TepecikCiftlik_N	Turkey	Anatolia	[45]	6680-6590 calBCE
Tep003	Anatolia_TepecikCiftlik_N	Turkey	Anatolia	[45]	6635-6475 calBCE
ulu117	Anatolia_Ulucak_BA	Turkey	Anatolia	This Study	3000-2000 BCE
ZBC_IPB001	Anatolia_HG	Turkey	Anatolia	[49]	13642-13073 calBCE
ZHAG_BON004	Anatolia_EN	Turkey	Anatolia	[49]	8300-7800 BCE
ZHAJ_BON034	Anatolia_EN	Turkey	Anatolia	[49]	8269-8210 calBCE
ZHJ_BON024	Anatolia_EN	Turkey	Anatolia	[49]	8300-7800 BCE
ZKO_BON001	Anatolia_EN	Turkey	Anatolia	[49]	8300-7800 BCE

Table 5 (continued)

SampleID	Population_Label	Country	Region	Publication	Date
ZMOJ_BON014	Anatolia_EN	Turkey	Anatolia	[49]	8300–7800 BCE
AKT16	Anatolia_Aktopraklik_N	Turkey	Anatolia	[50]	8,635–8,460 BP
BAR25	Anatolia_Barcin_N_SG	Turkey	Anatolia	[50]	8,384–8,205 BP
AV-21	Crete	Greece	Aegean	[38]	0
TZ-11	Crete	Greece	Aegean	[38]	0
G23	Greece_Theopetra_BA	Greece,Theopetra	Aegean	This Study	2335-2140 calBCE
G37	Greece_Sarakinos_BA	Greece,Sarakinos	Aegean	This Study	2325-2300 calBCE
G76a	Greece_Perachora_BA	Greece,Perachora	Aegean	This Study	2565-2350 calBCE
I0070	Greece_MinoanLasithi_BA	Greece	Aegean	[88]	2400-1700 BCE
I0071	Greece_MinoanLasithi_BA	Greece	Aegean	[88]	2400-1700 BCE
I0073	Greece_MinoanLasithi_BA	Greece	Aegean	[88]	2400-1700 BCE
I0074	Greece_MinoanLasithi_BA	Greece	Aegean	[88]	2400-1700 BCE
I2318	Greece_Peloponnese_N_6th	Greece	Aegean	[63]	4043-3947 calBCE
I2937	Greece_Peloponnese_N_8th	Greece	Aegean	[88]	5479-5338 calBCE
I3708	Greece_Peloponnese_N_7th	Greece	Aegean	[63]	5500-3700 BCE
I3709	Greece_Peloponnese_N_6th	Greece	Aegean	[63]	3990-3804 calBCE
I3920	Greece_Peloponnese_N_6th	Greece	Aegean	[63]	3933-3706 calBCE
I5427	Greece_Peloponnese_N_8th	Greece	Aegean	[63]	6005-5879 calBCE
I9005	Greece_MinoanLasithi_BA	Greece	Aegean	[88]	2400-1700 BCE
I9006	Greece_Mycenaean_BA	Greece	Aegean	[88]	1411-1262 calBCE
I9010	Greece_Mycenaean_BA	Greece	Aegean	[88]	1400-1200 BCE
I9033	Greece_Mycenaean_BA	Greece	Aegean	[88]	1416-1280 calBCE
I9041	Greece_Mycenaean_BA	Greece	Aegean	[88]	1400-1200 BCE
I9123	Greece_CreteArmenoi_BA	Greece	Aegean	[88]	1390-1190 BCE
I9127	Greece_MinoanOdigitria_BA	Greece	Aegean	[88]	2210-1680 BCE
I9128	Greece_MinoanOdigitria_BA	Greece	Aegean	[88]	2210-1680 BCE

Table 5 (continued)

SampleID	Population_Label	Country	Region	Publication	Date
I9129	Greece_MinoanOdigitria_BA	Greece	Aegean	[88]	2210-1680 BCE
I9130	Greece_MinoanOdigitria_BA	Greece	Aegean	[88]	2210-1680 BCE
I9131	Greece_MinoanOdigitria_BA	Greece	Aegean	[88]	2210-1680 BCE
Klei10	Greece_Kleitros_N	Greece	Aegean	[55]	4230-3995 calBCE
Kou01_wgs	Greece_EBA	Greece	Aegean	[85]	2464–2349 BCE
Kou03_wgs	Greece_EBA	Greece	Aegean	[85]	2832–2578 BCE
Log02_wgs	Greece_MBA	Greece	Aegean	[85]	1924–1831 BCE
Log04_wgs	Greece_MBA	Greece	Aegean	[85]	2007–1915 BCE
Mik15_wgs	Greece_EBA	Greece	Aegean	[85]	2890–2764 BCE
Pal7	Greece_Paliambela_N	Greece	Aegean	[55]	4452-4350 calBCE
Pta08_wgs	Greece_EBA	Greece	Aegean	[85]	2849–2621 BCE
Rev5	Greece_Revenia_EN	Greece	Aegean	[55]	6438-6264 calBCE
NA17377	Greek	Greece	Aegean	[38]	0
NA17374	Greek	Greece	Aegean	[38]	0
Nea3	Greece_NeaNikomedeia_N	Greece	Aegean	[50]	8327–8040 BP
Nea2	Greece_NeaNikomedeia_N	Greece	Aegean	[50]	8173–8023 BP
g31	Greece_Perachora_BA	Greece	Aegean	This Study	2600-2300 BCE
g62	Greece_Perachora_BA	Greece	Aegean	This Study	2600-2300 BCE
g65	Greece_Perachora_BA	Greece	Aegean	This Study	2600-2300 BCE
g66	Greece_Perachora_BA	Greece	Aegean	This Study	2600-2300 BCE
Theo1***	Greece_Theopetra	Greece	Aegean	[55]	7288-6771 calBCE
Theo5***	Greece_Theopetra	Greece	Aegean	[55]	7605-7529 calBCE
bad017	Anatolia_BademAgaci_N	Turkey	Aegean	This Study	6400-6200 BCE
bad019	Anatolia_BademAgaci_N	Turkey	Aegean	This Study	6400-6200 BCE
bad022	Anatolia_BademAgaci_N	Turkey	Aegean	This Study	6400-6200 BCE
bad023	Anatolia_BademAgaci_N	Turkey	Aegean	This Study	6400-6200 BCE

Table 5 (continued)

SampleID	Population_Label	Country	Region	Publication	Date
bad024	Anatolia_BademAgaci_N	Turkey	Aegean	This Study	6400-6200 BCE
bad025	Anatolia_BademAgaci_N	Turkey	Aegean	This Study	6400-6200 BCE
bad026	Anatolia_BademAgaci_N	Turkey	Aegean	This Study	6400-6200 BCE
bad030	Anatolia_BademAgaci_N	Turkey	Aegean	This Study	6400-6200 BCE
bad033	Anatolia_BademAgaci_N	Turkey	Aegean	This Study	6400-6200 BCE
bad034	Anatolia_BademAgaci_N	Turkey	Aegean	This Study	6400-6200 BCE
gir001	Anatolia_Girmeler	Turkey	Aegean	This Study	7738 - 7597 cal BC
ulu007	Anatolia_Ulucak_N	Turkey	Aegean	This Study	6800-6600 BC
ulu008	Anatolia_Ulucak_N	Turkey	Aegean	This Study	6800-6600 BC
ulu009	Anatolia_Ulucak_N	Turkey	Aegean	This Study	6800-6600 BC
AH1	Iran_TepeAbdul_N	Iran	Iran	[52]	8200-7700 BCE
AH2	Iran_TepeAbdul_N	Iran	Iran	[52]	8205-7756 calBCE
AH4	Iran_TepeAbdul_N	Iran	Iran	[52]	8204-7755 calBCE
F38	Iran_TepeHasanlu_IA	Iran	Iran	[52]	971-832 calBCE
I11456	Iran_Shahr_I_Sokhta_BA2	Iran	Iran	[54]	2600-2500 BCE
I11458	Iran_Shahr_I_Sokhta_BA2	Iran	Iran	[54]	3200-2100 BCE
I11459	Iran_Shahr_I_Sokhta_BA2	Iran	Iran	[54]	2875-2631 calBCE
I11462	Iran_Shahr_I_Sokhta_BA1	Iran	Iran	[54]	2911-2880 calBCE
I11466	Iran_Shahr_I_Sokhta_BA2	Iran	Iran	[54]	2500-2000 BCE
I11472	Iran_Shahr_I_Sokhta_BA3	Iran	Iran	[54]	2900-2700 BCE
I11474	Iran_Shahr_I_Sokhta_BA1	Iran	Iran	[54]	2700-2600 BCE
I11476	Iran_Shahr_I_Sokhta_BA1	Iran	Iran	[54]	3200-2100 BCE
I11478	Iran_Shahr_I_Sokhta_BA1	Iran	Iran	[54]	3200-1900 BCE
I11479	Iran_Shahr_I_Sokhta_BA1	Iran	Iran	[54]	2911-2697 calBCE
I11483	Iran_Shahr_I_Sokhta_BA1	Iran	Iran	[54]	3090-2917 calBCE
I1290	Iran_GanjDareh_N	Iran	Iran	[51]	8179-7613 calBCE

Table 5 (continued)

SampleID	Population_Label	Country	Region	Publication	Date
I1293	Iran_HG	Iran	Iran	[51]	9100-8600 BCE
I1661	Iran_SehGabi_CA	Iran	Iran	[51]	4696-4491 calBCE
I1662	Iran_SehGabi_CA	Iran	Iran	[51]	4831-4612 calBCE
I1665	Iran_SehGabi_CA	Iran	Iran	[51]	3956-3796 calBCE
I1670	Iran_SehGabi_CA	Iran	Iran	[51]	4839-4617 calBCE
I1671	Iran_SehGabi_LN	Iran	Iran	[51]	5837-5659 calBCE
I1674	Iran_SehGabi_CA	Iran	Iran	[51]	3972-3800 calBCE
I1944	Iran_GanjDareh_N	Iran	Iran	[54]	8000-7700 BCE
I1945	Iran_GanjDareh_N	Iran	Iran	[54]	8000-7700 BCE
I1947	Iran_GanjDareh_N	Iran	Iran	[54]	8210-7836 calBCE
I1949	Iran_GanjDareh_N	Iran	Iran	[54]	8241-7962 calBCE
I1951	Iran_GanjDareh_N	Iran	Iran	[54]	8202-7681 calBCE
I1954	Iran_GanjDareh_N	Iran	Iran	[54]	8294-7992 calBCE
I1955	Iran_GanjDareh_MP	Iran	Iran	[51]	1430-1485 calCE
I2312_all	Iran_HG	Iran	Iran	[54]	12000-8000 BCE
I2323	Iran_HajjiFiruz_CA	Iran	Iran	[54]	6060-5851 calBCE
I2327	Iran_HajjiFiruz_IA	Iran	Iran	[54]	1193-1019 calBCE
I2337	Iran_TepeHissar_CA	Iran	Iran	[54]	3641-3519 calBCE
I2512	Iran_TepeHissar_CA	Iran	Iran	[54]	2916-2876 calBCE
I2513	Iran_TepeHissar_CA	Iran	Iran	[54]	2849-2492 calBCE
I2514	Iran_TepeHissar_CA	Iran	Iran	[54]	2474-2307 calBCE
I2918	Iran_TepeHissar_CA	Iran	Iran	[54]	3702-3536 calBCE
I2921	Iran_TepeHissar_CA	Iran	Iran	[54]	3656-3526 calBCE
I2922	Iran_TepeHissar_CA	Iran	Iran	[54]	2197-2027 calBCE
I2923	Iran_TepeHissar_CA	Iran	Iran	[54]	2878-2636 calBCE
I2924	Iran_TepeHissar_CA	Iran	Iran	[54]	2881-2666 calBCE

Table 5 (continued)

SampleID	Population_Label	Country	Region	Publication	Date
I2925	Iran_TepeHissar_CA	Iran	Iran	[54]	2881-2666 calBCE
I2927	Iran_TepeHissar_CA	Iran	Iran	[54]	2575-2350 calBCE
I2928	Iran_TepeHissar_CA	Iran	Iran	[54]	2858-2505 calBCE
I4241	Iran_HajjiFiruz_CA	Iran	Iran	[54]	6016-5899 calBCE
I4243	Iran_HajjiFiruz_BA	Iran	Iran	[54]	2465-2286 calBCE
I4349	Iran_HajjiFiruz_CA	Iran	Iran	[54]	5887-5724 calBCE
I4351	Iran_HajjiFiruz_CA	Iran	Iran	[54]	6056-5894 calBCE
I7527	Iran_GanjDareh_N	Iran	Iran	[54]	8200-7700 BCE
I8724	Iran_Shahr_I_Sokhta_BA1	Iran	Iran	[54]	3000-2800 BCE
I8725	Iran_Shahr_I_Sokhta_BA1	Iran	Iran	[54]	3010-2881 calBCE
I8726	Iran_Shahr_I_Sokhta_BA2	Iran	Iran	[54]	3100-3000 BCE
I8728	Iran_Shahr_I_Sokhta_BA2	Iran	Iran	[54]	2600-2500 BCE
iran17	Iranian	Iran	Iran	[38]	0
iran11	Iranian	Iran	Iran	[38]	0
sha003	Iran_ShahTepe_BA	Iran	Iran	This Study	3200 - 3100 BCE
sha004	Iran_ShahTepe_BA	Iran	Iran	This Study	3240 - 3102 calBCE
sha006	Iran_ShahTepe_BA	Iran	Iran	This Study	3200 - 3100 BCE
sha007	Iran_ShahTepe_BA	Iran	Iran	This Study	3242 - 3101 calBCE
sha008	Iran_ShahTepe_BA	Iran	Iran	This Study	3200 - 3100 BCE
sha009	Iran_ShahTepe_BA	Iran	Iran	This Study	3344 - 3086 calBCE
sha010	Iran_ShahTepe_BA	Iran	Iran	This Study	3200 - 3100 BCE
sha012	Iran_ShahTepe_BA	Iran	Iran	This Study	3200 - 3100 BCE
sha014	Iran_ShahTepe_BA	Iran	Iran	This Study	3200 - 3100 BCE
WC1	Iran_WezmehCave_N	Iran	Iran	[52]	7455-7082 calBCE
GD13a	Iran_Ganj_Dareh_N_SG	Iran	Iran	[53]	8000-7700 BCE
ALA001	Levant_Alalakh_MLBA	Turkey	Levant	[89]	3446-3275 BP

Table 5 (continued)

SampleID	Population_Label	Country	Region	Publication	Date
ALA002	Levant_Alalakh_MLBA	Turkey	Levant	[89]	3446-3351 BP
ALA004	Levant_Alalakh_MLBA	Turkey	Levant	[89]	3845-3702 BP
ALA008	Levant_Alalakh_MLBA	Turkey	Levant	[89]	3831-3650 BP
ALA011	Levant_Alalakh_MLBA	Turkey	Levant	[89]	3691-3574 BP
ALA013	Levant_Alalakh_MLBA	Turkey	Levant	[89]	3828-3643 BP
ALA014	Levant_Alalakh_MLBA	Turkey	Levant	[89]	3693-3580 BP
ALA015	Levant_Alalakh_MLBA	Turkey	Levant	[89]	3964-3731 BP
ALA016	Levant_Alalakh_MLBA	Turkey	Levant	[89]	3567-3456 BP
ALA017	Levant_Alalakh_MLBA	Turkey	Levant	[89]	3564-3416 BP
ALA018	Levant_Alalakh_MLBA	Turkey	Levant	[89]	3447-3276 BP
ALA020	Levant_Alalakh_MLBA	Turkey	Levant	[89]	3452-3345 BP
ALA023	Levant_Alalakh_MLBA	Turkey	Levant	[89]	3871-3713 BP
ALA024	Levant_Alalakh_MLBA	Turkey	Levant	[89]	4061-3729 BP
ALA025	Levant_Alalakh_MLBA	Turkey	Levant	[89]	3827-3636 BP
ALA026	Levant_Alalakh_MLBA	Turkey	Levant	[89]	3694-3578 BP
ALA028	Levant_Alalakh_MLBA	Turkey	Levant	[89]	3827-3616 BP
ALA029	Levant_Alalakh_MLBA	Turkey	Levant	[89]	3830-3645 BP
ALA030	Levant_Alalakh_MLBA	Turkey	Levant	[89]	3562-3407 BP
ALA034	Levant_Alalakh_MLBA	Turkey	Levant	[89]	3824-3616 BP
ALA035	Levant_Alalakh_MLBA	Turkey	Levant	[89]	3898-3724 BP
ALA037	Levant_Alalakh_MLBA	Turkey	Levant	[89]	3832-3651 BP
ALA039	Levant_Alalakh_MLBA	Turkey	Levant	[89]	3398-3253 BP
ALA084	Levant_Alalakh_MLBA	Turkey	Levant	[89]	3956-3727 BP
ALA095	Levant_Alalakh_MLBA	Turkey	Levant	[89]	3863-3706 BP
BAJ001_BAJ001	Levant_Baja_N	Jordan	Levant	[49]	7027–6685 calBCE
ERS1790729	Levant_Sidon_BA	Lebanon	Levant	[86]	1900-1700 BCE

Table 5 (continued)

SampleID	Population_Label	Country	Region	Publication	Date
ERS1790730	Levant_Sidon_BA	Lebanon	Levant	[86]	1800-1600 BCE
ERS1790731	Levant_Sidon_BA	Lebanon	Levant	[86]	1900-1700 BCE
ERS1790732	Levant_Sidon_BA	Lebanon	Levant	[86]	1800-1600 BCE
ERS1790733	Levant_Sidon_BA	Lebanon	Levant	[86]	1950-1690 calBCE
ETM001	Levant_Ebla_EMBA	Syria	Levant	[89]	3750-3850 BP
ETM004	Levant_Ebla_EMBA	Syria	Levant	[89]	3950-3750 BP
ETM005	Levant_Ebla_EMBA	Syria	Levant	[89]	3950-3750 BP
ETM006	Levant_Ebla_EMBA	Syria	Levant	[89]	3950-3750 BP
ETM010	Levant_Ebla_EMBA	Syria	Levant	[89]	4650-4450 BP
ETM012	Levant_Ebla_EMBA	Syria	Levant	[89]	4420-4471 BP
ETM014	Levant_Ebla_EMBA	Syria	Levant	[89]	3950-3750 BP
ETM016	Levant_Ebla_EMBA	Syria	Levant	[89]	3976-3846 BP
ETM018	Levant_Ebla_EMBA	Syria	Levant	[89]	4085-3914 BP
I0644	Levant_Peqi_In_CA	Israel	Levant	[83]	4500-3900 BCE
I0861	Levant_HG	Israel	Levant	[51]	11840-9760 BCE
I0867	Levant_Motza_PPNB	Israel	Levant	[51]	7300-6200 BCE
I10092	Levant_Megiddo_MLBA	Israel	Levant	[92]	1900-1700 BCE
I10093	Levant_Megiddo_MLBA	Israel	Levant	[92]	1900-1700 BCE
I10097	Levant_Megiddo_MLBA	Israel	Levant	[92]	1600-1500 BCE
I10099	Levant_Megiddo_MLBA	Israel	Levant	[92]	1600-1500 BCE
I10104	Levant_Megiddo_MLBA	Israel	Levant	[92]	1950-1800 BCE
I10106	Levant_Megiddo_MLBA	Israel	Levant	[92]	1700-1500 BCE
I10263	Levant_Megiddo_MLBA	Israel	Levant	[92]	1600-1500 BCE
I10264	Levant_Megiddo_MLBA	Israel	Levant	[92]	1880-1700 calBCE
I10265	Levant_Megiddo_MLBA	Israel	Levant	[92]	1950-1800 BCE
I10266	Levant_Megiddo_MLBA	Israel	Levant	[92]	1638-1413 calBCE

Table 5 (continued)

SampleID	Population_Label	Country	Region	Publication	Date
I10268	Levant_Megiddo_MLBA	Israel	Levant	[92]	1971-1782 calBCE
I10359	Levant_Megiddo_MLBA	Israel	Levant	[92]	1623-1518 calBCE
I1072	Levant_HG	Israel	Levant	[51]	11840-9760 BCE
I10768	Levant_Megiddo_MLBA	Israel	Levant	[92]	1600-1500 BCE
I10769	Levant_Megiddo_MLBA	Israel	Levant	[92]	1550-1450 BCE
I10770	Levant_Megiddo_MLBA	Israel	Levant	[92]	1550-1450 BCE
I10771	Levant_Megiddo_MLBA	Israel	Levant	[92]	1650-1550 BCE
I1152	Levant_Peqi_In_CA	Israel	Levant	[83]	4500–3900 BCE
I1154	Levant_Peqi_In_CA	Israel	Levant	[83]	4500–3900 BCE
I1155	Levant_Peqi_In_CA	Israel	Levant	[83]	4500–3900 BCE
I1160	Levant_Peqi_In_CA	Israel	Levant	[83]	4500–3900 BCE
I1164	Levant_Peqi_In_CA	Israel	Levant	[83]	4500–3900 BCE
I1165	Levant_Peqi_In_CA	Israel	Levant	[83]	4500–3900 BCE
I1166	Levant_Peqi_In_CA	Israel	Levant	[83]	4500–3900 BCE
I1168	Levant_Peqi_In_CA	Israel	Levant	[83]	4500–3900 BCE
I1170	Levant_Peqi_In_CA	Israel	Levant	[83]	4500–3900 BCE
I1171	Levant_Peqi_In_CA	Israel	Levant	[83]	4500–3900 BCE
I1172	Levant_Peqi_In_CA	Israel	Levant	[83]	4500–3900 BCE
I1177	Levant_Peqi_In_CA	Israel	Levant	[83]	4500–3900 BCE
I1178	Levant_Peqi_In_CA	Israel	Levant	[83]	4500–3900 BCE
I1179	Levant_Peqi_In_CA	Israel	Levant	[83]	4500–3900 BCE
I1181	Levant_Peqi_In_CA	Israel	Levant	[83]	4500–3900 BCE
I1182	Levant_Peqi_In_CA	Israel	Levant	[83]	4500–3900 BCE
I1183_d	Levant_Peqi_In_CA	Israel	Levant	[83]	4500–3900 BCE
I1184	Levant_Peqi_In_CA	Israel	Levant	[83]	4500–3900 BCE
I1187	Levant_Peqi_In_CA	Israel	Levant	[83]	4500–3900 BCE

Table 5 (continued)

SampleID	Population_Label	Country	Region	Publication	Date
I1414	Levant_AinGhazal_N	Jordan	Levant	[51]	8300-7900 BCE
I1679	Levant_AinGhazal_N	Jordan	Levant	[51]	6900-6800 BCE
I1685	Levant_HG	Israel	Levant	[51]	11840-9760 BCE
I1699	Levant_AinGhazal_N	Jordan	Levant	[51]	6800-6700 BCE
I1700	Levant_AinGhazal_N	Jordan	Levant	[51]	8300-7900 BCE
I1704	Levant_AinGhazal_N	Jordan	Levant	[51]	7446-7058 calBCE
I1705	Levant_AinGhazal_BA	Jordan	Levant	[51]	2198-1966 calBCE
I1706	Levant_AinGhazal_BA	Jordan	Levant	[51]	2490-2300 BCE
I1707	Levant_AinGhazal_N	Jordan	Levant	[51]	7722-7541 calBCE
I1710	Levant_AinGhazal_N	Jordan	Levant	[51]	7733-7526 calBCE
I1727	Levant_AinGhazal_N	Jordan	Levant	[51]	8300-7900 BCE
I1730	Levant_AinGhazal_BA	Jordan	Levant	[51]	2489-2299 calBCE
I2190	Levant_Megiddo_MLBA	Israel	Levant	[92]	1496-1302 calBCE
I2195	Levant_Megiddo_MLBA	Israel	Levant	[92]	1600-1278 calBCE
I2198	Levant_Megiddo_MLBA	Israel	Levant	[92]	1509-1432 calBCE
I2201	Levant_Abel_IA	Israel	Levant	[92]	1011-846 calBCE
I3703	Levant_Baqah_MLBA	Jordan	Levant	[92]	1550-1150 BCE
I3705	Levant_Baqah_MLBA	Jordan	Levant	[92]	1492-1303 calBCE
I3706	Levant_Baqah_MLBA	Jordan	Levant	[92]	1424-1288 calBCE
I3707	Levant_Baqah_MLBA	Jordan	Levant	[92]	1409-1265 calBCE
I3832	Levant_Hazor_MLBA	Israel	Levant	[92]	1450-1250 BCE
I3965	Levant_Hazor_MLBA	Israel	Levant	[92]	1800-1700 BCE
I3966	Levant_Hazor_MLBA	Israel	Levant	[92]	1800-1700 BCE
I3985	Levant_Baqah_MLBA	Jordan	Levant	[92]	1412-1234 calBCE
I3986	Levant_Baqah_MLBA	Jordan	Levant	[92]	1550-1150 BCE
I3987	Levant_Baqah_MLBA	Jordan	Levant	[92]	1428-1293 calBCE

Table 5 (continued)

SampleID	Population_Label	Country	Region	Publication	Date
I4517	Levant_Megiddo_IA	Israel	Levant	[92]	1107-923 calBCE
I4518	Levant_Megiddo_MLBA	Israel	Levant	[92]	1550-1300 BCE
I4521	Levant_Megiddo_IBA	Israel	Levant	[92]	2334-2149 calBCE
I4525	Levant_Megiddo_MLBA	Israel	Levant	[92]	1600-1500 BCE
I6459	Levant_Baqah_MLBA	Jordan	Levant	[92]	1384-1213 calBCE
I6460	Levant_Baqah_MLBA	Jordan	Levant	[92]	1550-1150 BCE
I6462	Levant_Baqah_MLBA	Jordan	Levant	[92]	1550-1150 BCE
I6464	Levant_Baqah_MLBA	Jordan	Levant	[92]	1550-1150 BCE
I6564	Levant_Baqah_MLBA	Jordan	Levant	[92]	1550-1150 BCE
I6565	Levant_Baqah_MLBA	Jordan	Levant	[92]	1550-1150 BCE
I6566	Levant_Baqah_MLBA	Jordan	Levant	[92]	1550-1150 BCE
I6567	Levant_Baqah_MLBA	Jordan	Levant	[92]	1550-1150 BCE
I6569	Levant_Baqah_MLBA	Jordan	Levant	[92]	1550-1150 BCE
I6570	Levant_Baqah_MLBA	Jordan	Levant	[92]	1550-1150 BCE
I6571	Levant_Baqah_MLBA	Jordan	Levant	[92]	1496-1396 calBCE
I6572	Levant_Baqah_MLBA	Jordan	Levant	[92]	1550-1150 BCE
I6923	Levant_Yehud_IBA	Israel	Levant	[92]	2500-2000 BCE
I7003	Levant_Yehud_IBA	Israel	Levant	[92]	2500-2000 BCE
KFH2_KFH002	Levant_KfarH_N	Kfar Hahoresht	Levant	[49]	7700-7600 calBCE
KRD001	Levant_TellKurdu_EC	Turkey	Levant	[89]	7670-7590 BP
KRD002	Levant_TellKurdu EMC	Turkey	Levant	[89]	6955-6799 BP
KRD003	Levant_TellKurdu_EC	Turkey	Levant	[89]	7656-7572 BP
KRD004	Levant_TellKurdu_EC	Turkey	Levant	[89]	7664-7582 BP
KRD005	Levant_TellKurdu_EC	Turkey	Levant	[89]	7706-7614 BP
KRD006	Levant_TellKurdu_EC	Turkey	Levant	[89]	7750-7350 BP
QED-12	Levant_QornetedDeir_Roma	Lebanon	Levant	[106]	NA

Table 5 (continued)

SampleID	Population_Label	Country	Region	Publication	Date
QED-2	Levant_QornetedDeir_Roma	Lebanon	Levant	[106]	244- 400 calCE
QED-4	Levant_QornetedDeir_Roma	Lebanon	Levant	[106]	426- 632 calCE
QED-7	Levant_QornetedDeir_Roma	Lebanon	Levant	[106]	237- 389 calCE
HGDP00616	BedouinB	Israel(Negev)	Levant	[38]	0
HGDP00650	BedouinB	Israel(Negev)	Levant	[38]	0
HGDP00569	Druze	Israel(Carmel)	Levant	[38]	0
HGDP00597	Druze	Israel(Carmel)	Levant	[38]	0
Jordan445	Jordanian	Jordan	Levant	[38]	0
Jordan603	Jordanian	Jordan	Levant	[38]	0
Jordan214	Jordanian	Jordan	Levant	[38]	0
HGDP00722	Palestinian	Israel(Central)	Levant	[38]	0
HGDP00725	Palestinian	Israel(Central)	Levant	[38]	0
HGDP00737	Palestinian	Israel(Central)	Levant	[38]	0
Sam02	Samaritan	Israel	Levant	[38]	0
SFI-11	Levant_Beirut_MP	Lebanon	Levant	[87]	119 BCE–27 CE
SFI-12	Levant_Beirut_Hellenistic	Lebanon	Levant	[87]	209 BCE–89 BCE
SFI-15	Levant_Beirut_MP	Lebanon	Levant	[87]	176 BCE–3 CE
SFI-20	Levant_Beirut_Hellenistic	Lebanon	Levant	[87]	199 BCE–37 BCE
SFI-24	Levant_Beirut_MP	Lebanon	Levant	[87]	55 BCE–58 CE
SFI-33	Levant_Beirut_MP	Lebanon	Levant	[87]	48 CE–222 CE
SFI-34	Levant_Beirut_IAIII	Lebanon	Levant	[87]	NA
SFI-35	Levant_Beirut_IAIII	Lebanon	Levant	[87]	NA
SFI-36	Levant_Beirut_IAIII	Lebanon	Levant	[87]	NA
SFI-39	Levant_Beirut_IAIII	Lebanon	Levant	[87]	NA
SFI-42	Levant_Beirut_IAIII	Lebanon	Levant	[87]	540 BCE–396 BCE
SFI-43	Levant_Beirut_IAIII	Lebanon	Levant	[87]	567 BCE–404 BCE

Table 5 (continued)

SampleID	Population_Label	Country	Region	Publication	Date
SFI-44	Levant_Beirut_IAIII	Lebanon	Levant	[87]	NA
SFI-45	Levant_Beirut_IAIII	Lebanon	Levant	[87]	NA
SFI-47	Levant_Beirut_IAIII	Lebanon	Levant	[87]	NA
SFI-5	Levant_Beirut_Hellenistic	Lebanon	Levant	[87]	234 BCE–92 BCE
SFI-50	Levant_Beirut_IAIII	Lebanon	Levant	[87]	NA
SFI-55	Levant_Beirut_IAII	Lebanon	Levant	[87]	NA
SFI-56	Levant_Beirut_IAII	Lebanon	Levant	[87]	NA
SI-38	Levant_Sidon_MP	Lebanon	Levant	[106]	NA
SI-39	Levant_Sidon_MP_EU	Lebanon	Levant	[106]	1191- 1283 calCE
SI-40	Levant_Sidon_MP_EU	Lebanon	Levant	[106]	NA
SI-41	Levant_Sidon_MP_Adm	Lebanon	Levant	[106]	1187- 1266 calCE
SI-42	Levant_Sidon_MP	Lebanon	Levant	[106]	1058-1075 calCE
SI-44	Levant_Sidon_MP	Lebanon	Levant	[106]	NA
SI-45	Levant_Sidon_MP	Lebanon	Levant	[106]	1219- 1278 calCE
SI-47	Levant_Sidon_MP_EU	Lebanon	Levant	[106]	NA
SI-53	Levant_Sidon_MP_Adm	Lebanon	Levant	[106]	1025- 1154 calCE
ALX002	Caucasus_lowlands_LC	Azerbaijan	S Caucasus	[89]	5726-5611 BP
ARM001	Caucasus_KuraAraxes_BA	Armenia	S Caucasus	[90]	3349-3033 calBCE
ARM002_ARM003	Caucasus_KuraAraxes_BA	Armenia	S Caucasus	[90]	3341-3030 calBCE
DA31	Armenia_LchashenMetsamor_BA	Armenia	S Caucasus	[136]	1400-1100 BCE
DA35	Armenia_LchashenMetsamor_BA	Armenia	S Caucasus	[136]	1419-1135 calBCE
geo005	Georgia_Didnauri_BA	Georgia, Didnauri	S Caucasus	This Study	1257-1051 calBCE
geo006	Georgia_Didnauri_BA	Georgia, Didnauri	S Caucasus	This Study	1017-846 calBCE
geo015	Georgia_Doghlauri_KuraAraxes_BA	Georgia, Toglaura	S Caucasus	This Study	3015-2890 calBCE
geo017	Georgia_Doghlauri_BA	Georgia, Toglaura	S Caucasus	This Study	1291-1119 calBCE
geo029	Georgia_Didnauri_BA	Georgia, Didnauri	S Caucasus	This Study	1219-1036 calBCE

Table 5 (continued)

SampleID	Population_Label	Country	Region	Publication	Date
I1407	Armenia_CA	Armenia	S Caucasus	[51]	4350-3500 BCE
I1409	Armenia_CA	Armenia	S Caucasus	[51]	4229-3985 calBCE
I1631	Armenia_CA	Armenia	S Caucasus	[51]	4250-4050 calBCE
I1632	Armenia_CA	Armenia	S Caucasus	[51]	4230-4000 calBCE
I1633	Armenia_EBA	Armenia	S Caucasus	[51]	2619-2410 calBCE
I1634	Armenia_CA	Armenia	S Caucasus	[51]	4330-4060 calBCE
I1635	Armenia_EBA	Armenia	S Caucasus	[51]	2619-2465 calBCE
I1656	Armenia_MBA	Armenia	S Caucasus	[51]	1501-1402 calBCE
I1658	Armenia_EBA	Armenia	S Caucasus	[51]	3347-3092 calBCE
I1720	Caucasus_Maykop_BA	Russia	S Caucasus	[90]	NA
I2051	Caucasus_Dolmen_BA	Russia	S Caucasus	[90]	NA
I2056	Caucasus_Eneolithic	Russia	S Caucasus	[90]	4546-4466
I6266	Caucasus_MaykopNovosvobodnaya_BA	Russia	S Caucasus	[90]	NA
I6267	Caucasus_MaykopNovosvobodnaya_BA	Russia	S Caucasus	[90]	3614-3362 calBCE
I6268	Caucasus_MaykopNovosvobodnaya_BA	Russia	S Caucasus	[90]	3696-3532 calBCE
I6272	Caucasus_MaykopNovosvobodnaya_BA	Russia	S Caucasus	[90]	NA
KDC001	Caucasus_North_BA	Russia	S Caucasus	[90]	1953-1776 calBCE
KDC002	Caucasus_North_BA	Russia	S Caucasus	[90]	NA
Kotias	CHG	Georgia	S Caucasus	[104]	7940-7600 calBCE
MK5004	Caucasus_LateMaykop_BA	Russia	S Caucasus	[90]	3347-3095
MK5008	Caucasus_LateMaykop_BA	Russia	S Caucasus	[90]	3364-3107
MTT001	Caucasus_lowlands_LN	Azerbaijan	S Caucasus	[89]	7679-7594 BP
OSS001	Caucasus_Maykop_BA	Russia	S Caucasus	[90]	3695-3545 BCE
POT002	Caucasus_lowlands_LN	Azerbaijan	S Caucasus	[89]	7458-7323 BP
RISE396	Armenia_LBA	Armenia	S Caucasus	[119]	1192-937 calBCE
RISE397	Armenia_LBA	Armenia	S Caucasus	[119]	1048-855 calBCE

Table 5 (continued)

SampleID	Population_Label	Country	Region	Publication	Date
RISE407	Armenia_LBA	Armenia	S Caucasus	[119]	1115-895 calBCE
RISE408	Armenia_LBA	Armenia	S Caucasus	[119]	1209-1009 calBCE
RISE412	Armenia_LBA	Armenia	S Caucasus	[119]	1193-945 calBCE
RISE413	Armenia_MBA	Armenia	S Caucasus	[119]	1906-1698 calBCE
RISE416	Armenia_MBA	Armenia	S Caucasus	[119]	1643-1445 calBCE
RISE423	Armenia_MBA	Armenia	S Caucasus	[119]	1402-1211 calBCE
armenia293	Armenian	Armenia	S Caucasus	[38]	0
Armenian222	Armenian	Armenia	S Caucasus	[38]	0
mg27	Georgian	Georgia	S Caucasus	[38]	0
mg31	Georgian	Georgia	S Caucasus	[38]	0
Satsurblia	CHG	Georgia	S Caucasus	[104]	11430-11180 calBCE
SIJ002	Caucasus_LateMaykop_BA	Russia	S Caucasus	[90]	3349-3033 calBCE
zrj003	Azerbaijan_Shamakhi_IA	Azerbaijan	S Caucasus	This Study	133 - 324 CE
gur016	Georgia_Nazarlebi_BA	Georgia	S Caucasus	This Study	1500-1000 BCE
gur017	Georgia_Nazarlebi_BA	Georgia	S Caucasus	This Study	1500-1000 BCE
gur019	Georgia_Nazarlebi_BA	Georgia	S Caucasus	This Study	1500-1000 BCE
AY2001	Steppe_Maykop	Russia	N Caucasus	[90]	3514-3360 calBCE
AY2003	Steppe_Maykop	Russia	N Caucasus	[90]	3630-3376 calBCE
BU2001	North_Caucasus	Russia	N Caucasus	[90]	2866-2582 calBCE
GW1001	North_Caucasus	Russia	N Caucasus	[90]	2883-2638 calBCE
I1723	North_Caucasus	Russia	N Caucasus	[90]	2877-2626 calBCE
KBD002	Late_North_Caucasus	Russia	N Caucasus	[90]	2192-1985 calBCE
LYG001	North_Caucasus	Russia	N Caucasus	[90]	2866-2580 calBCE
MK3003	Russia_Catacomb	Russia	N Caucasus	[90]	2580-2470 calBCE
MK5009	North_Caucasus	Russia	N Caucasus	[90]	2879-2631 calBCE
NV3001	Russia_Lola	Russia	N Caucasus	[90]	2127-1924 calBCE

Table 5 (continued)

SampleID	Population_Label	Country	Region	Publication	Date
PG2001	Russia_Eneolithic_steppe	Russia	N Caucasus	[90]	4994-4802 calBCE
PG2002	North_Caucasus	Russia	N Caucasus	[90]	2476-2303 calBCE
PG2004	Russia_Eneolithic_steppe	Russia	N Caucasus	[90]	4240-4047 calBCE
RK1003	North_Caucasus	Russia	N Caucasus	[90]	2899-2701 calBCE
RK4001	Russia_Catacomb	Russia	N Caucasus	[90]	2451-2201 calBCE
RK4002	Russia_Catacomb	Russia	N Caucasus	[90]	2662-2474 calBCE
SA6001	Steppe_Maykop	Russia	N Caucasus	[90]	3520-3371 calBCE
SA6003	Russia_Catacomb	Russia	N Caucasus	[90]	2470-2209 calBCE
SA6004	Steppe_Maykop	Russia	N Caucasus	[90]	3359-3034 calBCE
VJ1001	Russia_Eneolithic_steppe	Russia	N Caucasus	[90]	4337-4177 calBCE
DA245	Russia_ShamankaII_EN	Russia	Baikal	[136]	6069-5914 calBCE
DA246	Russia_ShamankaII_EN	Russia	Baikal	[136]	5884-5669 calBCE
DA247	Russia_ShamankaII_EN	Russia	Baikal	[136]	5837-5660 calBCE
DA248	Russia_ShamankaII_EN	Russia	Baikal	[136]	5762-5629 calBCE
DA249	Russia_ShamankaII_EN	Russia	Baikal	[136]	5987-5782 calBCE
DA250	Russia_ShamankaII_EN	Russia	Baikal	[136]	5524-5365 calBCE
DA251	Russia_ShamankaII_EN	Russia	Baikal	[136]	5471-5222 calBCE
DA252	Russia_ShamankaII_EN	Russia	Baikal	[136]	5473-5229 calBCE
DA253	Russia_ShamankaII_EN	Russia	Baikal	[136]	5371-5216 calBCE
DA334	Russia_ShamankaII_EN	Russia	Baikal	[136]	2284-2055 calBCE
DA335	Russia_ShamankaII_EN	Russia	Baikal	[136]	2500-2000 BCE
DA336	Russia_ShamankaII_EN	Russia	Baikal	[136]	2500-2000 BCE
DA337	Russia_ShamankaII_EN	Russia	Baikal	[136]	2461-2295 calBCE
DA339	Russia_ShamankaII_EN	Russia	Baikal	[136]	2200-1977 calBCE
DA340	Russia_Lokomotiv_EN	Russia	Baikal	[136]	5217-4852 calBCE
DA341	Russia_Lokomotiv_EN	Russia	Baikal	[136]	5714-5561 calBCE

Table 5 (continued)

SampleID	Population_Label	Country	Region	Publication	Date
DA342	Russia_Ust-Ida_LN	Russia	Baikal	[136]	3793-3526 calBCE
DA343	Russia_Ust-Ida_EBA	Russia	Baikal	[136]	3083-2638 calBCE
DA344	Russia_Ust-Ida_LN	Russia	Baikal	[136]	3945-3373 calBCE
DA345	Russia_Ust-Ida_LN	Russia	Baikal	[136]	3637-3371 calBCE
DA353	Russia_Ust-Ida_EBA	Russia	Baikal	[136]	2565-2140 calBCE
DA354	Russia_Kurma_EBA	Russia	Baikal	[136]	2856-2492 calBCE
DA355	Russia_Ust-Ida_LN	Russia	Baikal	[136]	3644-3372 calBCE
DA356	Russia_Ust-Ida_EBA	Russia	Baikal	[136]	2456-2206 calBCE
DA357	Russia_Lokomotiv_EN	Russia	Baikal	[136]	5981-5723 calBCE
DA358	Russia_Kurma_EBA	Russia	Baikal	[136]	2883-2633 calBCE
DA359	Russia_Lokomotiv_EN	Russia	Baikal	[136]	5713-5482 calBCE
DA360	Russia_Kurma_EBA	Russia	Baikal	[136]	2878-2631 calBCE
DA361	Russia_Ust-Ida_EBA	Russia	Baikal	[136]	2445-1978 calBCE
DA362	Russia_ShamankaII_EN	Russia	Baikal	[136]	5362-5216 calBCE
I0061	EHG	Russia	EHG/Steppe	[59]	7050-5950 BCE
I0211	EHG	Russia	EHG/Steppe	[59]	7050-5950 BCE
I0231	Yamnaya	Russia	EHG/Steppe	[54]	2911-2881 calBCE
I0357	Yamnaya	Russia	EHG/Steppe	[59]	3093-2911 calBCE
I0370	Yamnaya	Russia	EHG/Steppe	[59]	3300-2500 BCE
I0429	Yamnaya	Russia	EHG/Steppe	[59]	3339-2916 calBCE
I0438	Yamnaya	Russia	EHG/Steppe	[59]	3020-2631 calBCE
I0439	Yamnaya	Russia	EHG/Steppe	[59]	3322-2921 calBCE
I0441	Yamnaya	Russia	EHG/Steppe	[59]	3010-2623 calBCE
I0443	Yamnaya	Russia	EHG/Steppe	[59]	3300-2500 BCE
I0444	Yamnaya	Russia	EHG/Steppe	[59]	3335-2883 calBCE
I2105	Yamnaya	Ukraine	EHG/Steppe	[59]	3300-2500 BCE

Table 5 (continued)

SampleID	Population_Label	Country	Region	Publication	Date
I3141	Yamnaya	Ukraine	EHG/Steppe	[63]	3300-2500 BCE
I7489	Yamnaya	Russia	EHG/Steppe	[54]	3326-2926 calBCE
RISE240	Yamnaya	Russia	EHG/Steppe	[119]	2879-2631 calBCE
RISE546	Yamnaya	Russia	EHG/Steppe	[119]	3300-2500 BCE
RISE547	Yamnaya	Russia	EHG/Steppe	[119]	2886-2631 calBCE
RISE548	Yamnaya	Russia	EHG/Steppe	[119]	3300-2500 BCE
RISE550	Yamnaya	Russia	EHG/Steppe	[119]	3335-2634 calBCE
RISE552	Yamnaya	Russia	EHG/Steppe	[119]	2846-2144 calBCE
Sidelkino	EHG	Russia	EHG/Steppe	[136]	9649-9284 calBCE
BerryAuBac	Villabruna	France	WHG	[63]	5368-5216 calBCE
Brillenhohle	ElMiron	Germany	WHG	[135]	13170-12490 calBCE
Burkhardtshohle	ElMiron	Germany	WHG	[135]	13127-12211 calBCE
Chaudardes1	Villabruna	France	WHG	[135]	6400-6086 calBCE
ElMiron	ElMiron	Spain	WHG	[135]	16880-16660 calBCE
Falkenstein	Villabruna	Germany	WHG	[63]	7460-7040 calBCE
GoyetQ-2	ElMiron	Belgium	WHG	[135]	13280-12830 calBCE
GoyetQ376-19	Vestonice	Belgium	WHG	[135]	25770-25360 calBCE
GoyetQ53-1	Vestonice	Belgium	WHG	[135]	26280-25770 calBCE
GoyetQ56-16	Vestonice	Belgium	WHG	[135]	24650-24090 calBCE
HohleFels49	ElMiron	Germany	WHG	[135]	14050-12310 BCE
HohleFels79	ElMiron	Germany	WHG	[135]	13120-12320 calBCE
I1875	Villabruna	Croatia	WHG	[63]	7308-7027 calBCE
I2158	Villabruna	Italy	WHG	[63]	14776-9873 BCE
Iboussieres25-1	Villabruna	France	WHG	[63]	10090-9460 BCE
Iboussieres31-2	Villabruna	France	WHG	[63]	10090-9460 BCE
KremsWA3	Vestonice	Austria	WHG	[135]	29500-28500 BCE

Table 5 (continued)

SampleID	Population_Label	Country	Region	Publication	Date
LesCloseaux13	Villabruna	France	WHG	[135]	8290-7610 calBCE
Loschbour	Villabruna	Luxembourg	WHG	[58]	6210-5990 calBCE
Ofnet	Villabruna	Germany	WHG	[135]	6480-6110 calBCE
Ostuni1	Vestonice	Italy	WHG	[135]	25860-25480 calBCE
Ostuni2	Vestonice	Italy	WHG	[135]	27360-26690 calBCE
Paglicci108	Vestonice	Italy	WHG	[135]	26480-25120 BCE
Paglicci133	Vestonice	Italy	WHG	[135]	32630-29260 BCE
Pavlov1	Vestonice	Czech Republic	WHG	[135]	29160-27460 BCE
Ranchot88	Villabruna	France	WHG	[135]	8290-7980 calBCE
Rigney1	ElMiron	France	WHG	[135]	13740-13290 calBCE
Rochedane	Villabruna	France	WHG	[63]	11140-10880 calBCE
Vestonice13	Vestonice	Czech Republic	WHG	[135]	29120-28720 BCE
Vestonice14	Vestonice	Czech Republic	WHG	[135]	29120-28720 BCE
Vestonice15	Vestonice	Czech Republic	WHG	[135]	29120-28720 BCE
Vestonice16	Vestonice	Czech Republic	WHG	[135]	28760-27360 BCE
Vestonice43	Vestonice	Czech Republic	WHG	[135]	28760-27360 BCE
Villabruna	Villabruna	Italy	WHG	[135]	12230-11830 calBCE
I1958	West_Siberian_HG	Russia	WSHG	[54]	4723-4550 calBCE
I1960	West_Siberian_HG	Russia	WSHG	[54]	6329-6079 calBCE
I5766	West_Siberian_HG	Russia	WSHG	[54]	4230-3984 calBCE

CURRICULUM VITAE

PERSONAL INFORMATION

Surname, Name: Koptekin, Dilek

EDUCATION

Degree	Institution	Year of Graduation
M.S.	Ege University, İzmir, Turkey	2015
B.Ed. & M.Ed.	Hacettepe University, Ankara, Turkey	2011

GRANTS AND FELLOWSHIPS

2020 European Molecular Biology Organization (EMBO), Scientific Exchange Grant, Where did the expansion start? Inferring the demographic history of the first farmers in the Aegean using Approximate Bayesian Computation (PI: Flora Jay), Université Paris-Saclay, Centre National de la Recherche Scientifique, Inria, Laboratoire de Recherche en Informatique, Orsay, France

2018 The Wenner-Gren Foundation, Dissertation Fieldwork Grant, Ancient genomic analysis of Neolithization in Anatolia and the Aegean

2015 The European Society for Evolutionary Biology, ESEB Outreach Initiative Fund with T Çetin, M Somel, M Tuğrul

2014 Erasmus+ Traineeship, Computational Biology of small RNAs (PI: Tamas Dalmay). University of East Anglia, School of Biological Sciences, Norwich, UK

PUBLICATIONS

Koptekin D, Yüncü E, Rodriguez-Varela R*, Altınışık NE*, Psonis N*, Kashuba N, Yorulmaz S, George R, Kazancı DD, Kaptan D, Gürün K, Vural KB, Gemici HC, Vassou D, Daskalaki E, Karamurat C, Lagerholm VK, Erdal ÖD, Kırdök E, Marangoni A, Schachner A, Üstündağ H, Shengelia R, Bitadze L, Elashvili M, Stravopodi E, Özbaşaran M, Duru G, Nafplioti A, Rose CB, Gencer T, Darbyshire G, Gavashelishvili A, Pitskhelauri K, Çevik Ö, Vu-

ruşkan O, Kyparissi-Apostolika N, Büyükkarakaya AM, Oğuzhanoğlu U, Günel S, Tabakaki E, Aliev A, Ibrahimov A, Shadlinski V, Sampson A, Kılınç GM, Atakuman Ç, Stamatakis A, Poulakakis N, Erdal YS, Pavlidis P, Stora J, Özer F, Götherström A, Somel M. (2022). Spatial and temporal heterogeneity in human mobility patterns in Holocene Southwest Asia and the East Mediterranean. (Under review).

Altınışik NE, Kazancı DD, Aydoğan A, Gemici HC, Erdal ÖD, Sarıaltun S, Vural KB, **Koptekin D**, Gürün K, Sağlıcan E, Çakan G, Koruyucu MM, Lagerholm VK, Karamurat C, Özkan M, Kılınç GM, Sevkar A, Süre E, Götherström A, Atakuman Ç, Erdal YS, Özer F, Özdoğan AE, Somel M (2022). A genomic snapshot of demographic and cultural dynamism in Upper Mesopotamia during the Neolithic Transition. bioRxiv 2022.01.31.478487

Yurtman E*, Özer O*, Yüncü E*, Dağtaş ND, **Koptekin D**, Çakan YG, Özkan M, Akbaba A, Kaptan D, Atağ G, Vural KB, Gündem CY, Martin L, Kılınç GM, Ghalichi A, Açıan SC, Yaka R, Sağlıcan E, Lagerholm VK, Krzewińska M, Günther T, Morell MP, Pişkin E, Şevke-toğlu M, Bilgin CC, Atakuman Ç, Erdal YS, Süre E, Altınışik NE, Lenstra JA, Yorulmaz S, Abazari MF, Hoseinzadeh J, Baird D, Bıçakçı E, Çevik Ö, Gerritsen F, Özbal R, Götherström A, Somel M, Togan İ, Özer F (2021). Archaeogenetic analysis of Neolithic sheep from Anatolia suggests a complex demographic history since domestication. *Communications Biology*, 1279:4, 2399-3642

Ceballos FC*, Gürün K*, Altınışik NE, Gemici HC, Karamurat C, **Koptekin D**, Vural KB, Mapelli I, Sağlıcan E, Süre E, Erdal YS, Götherström A, Özer F, Atakuman Ç, Somel M. (2021). Human inbreeding has decreased in time through the Holocene. *Current Biology*, 31:17

Yaka R, Mapelli I*, Kaptan D*, Doğu A*, Chyleński M*, Erdal ÖD, **Koptekin D**, Vural KB, Bayliss A, Mazzucato C, Fer E, Çokoğlu SS, Lagerholm VK, Krzewińska M, Karamurat C, Gemici HC, Sevkar A, Dağtaş ND, Kılınç GM, Adams D, Munters AR, Sağlıcan E, Milella M, Schotsmans EMJ, Yurtman E, Çetin M, Yorulmaz S, Altınışik NE, Ghalichi A, Juras A, Bilgin CC, Günther T, Storå J, Jakobsson M, de Kleijn M, Mustafaoğlu G, Fairbairn A, Pearson J, Togan İ, Kayacan N, Marciniak A, Larsen CS, Hodder I, Atakuman Ç, Pilloud M, Süre E, Gerritsen F, Özbal R, Baird D, Erdal YS, Duru G, Özbaşaran M, Haddow SD, Knüsel CJ, Götherström A, Özer F, Somel M (2021) Variable kinship patterns in Neolithic Anatolia revealed by ancient genomes, *Current Biology*,31:11

Kılınç GM*, Kashuba N*, **Koptekin D**, Bergfeldt N, Dönertaş HM, Rodríguez-Varela R, Shergin D, Ivanov G, Kichigin D, Pestereva K, Volkov D, Mandryka P, Kharinskii A, Tishkin A, Ineshin E, Kovychev E, Stepanov A, Dalén L, Günther T, Kirdök E, Jakobsson M, Somel M, Krzewińska M, Storå J, Götherström A. (2021). Human population dynamics and *Yersinia pestis* in ancient northeast Asia. *Science Advances*, Vol 7, No 2, eabc4587

Yaka R, Doğu A, Kaptan D, Dağtaş ND, Chyleński M, Vural KB, Altınışik NE, Mapelli I, **Koptekin D**, Karamurat C, Gemici HC, Yorulmaz S, Lagerholm VK, Fer E, Işıldak U, Ghalichi A, Kılınç GM, Mazzucato C, Juras A, Marciniak A, Larsen CS, Pilloud M, Haddow SD, Knüsel CJ, Togan İ, Götherström A, Erdal YS, Süre E, Özer F, Atakuman Ç, Somel M. (2021). Ancient genomics in Neolithic Central Anatolia and Catalhöyük. In I. Hodder (ed.),

Peopling the Landscape of Catalhöyük: Reports from the 2009-2017 Seasons (Çatalhöyük Research Project Series Volume 13). London: British Institute at Ankara, pp. 395-405

Krzewińska M*, Kılınç GM*, Juras A, **Koptekin D**, Chyleński M, Nikitin AG, Shcherbakov N, Shutteleva I, Leonova T, Kraeva L, Sungatov FA, Sultanova AN, Potekhina I, Łukasik S, Krenz-Niedbała M, Dalén L, Sinika V, Jakobsson M, Storå J, Götherström A. (2018). Ancient genomes suggest the eastern Pontic-Caspian steppe as the source of western Iron Age nomads. *Science Advances*, Vol. 4, no. 10, eaat4457.

Kılınç GM, **Koptekin D***, Atakuman Ç*, Sümer AP, Dönertaş HM, Yaka R, Bilgin CC, Büyükkarakaya AM, Baird D, Altınışik E, Flegontov P, Götherström A, Togan İ, Somel M. (2017). Archaeogenomic analysis of the first steps of Neolithization in Anatolia and the Aegean. *Proc. R. Soc. B.*, 284:20172064

Kılınç GM*, Omrak A*, Özer F*, Günther T, Büyükkarakaya AM, Bıçakçı E, Baird D, Dönertaş HM, Ghalichi A, Yaka R, **Koptekin D**, Açıan SC, Parvizi P, Krzewińska M, Daskalaki EA, Yüncü E, Dağtaş ND, Fairbairn A, Pearson J, Mustafaoğlu G, Erdal YS, Çakan YG, Toğan İ, Somel M, Storå J, Jakobsson M, Götherström A. (2016). The Demographic Development of the First Farmers in Anatolia. *Current Biology*, 26:19, 2659–2666.

Koptekin D and Aktaş LY. (2016). Identification of conserved miRNAs and their target genes in faba bean by EST based homology analysis. *EJOSAT*, 5(9).

Koptekin D and Aktaş LY. (2013). Plant microRNAs: Biogenesis, Origin and Evolution. *Turkish Journal of Scientific Reviews*, 6(2):140-148

*Equal contribution

PRESENTATIONS

Koptekin D, Yüncü E, Gürün K, Rodriguez-Varela R, Götherström A, Pavlidis P, Özer F, Somel M (2021) Tracking population structure of Southwest Asia human populations during Holocene. Oral Presentation at 7th Ecology and Evolutionary Biology Symposium Turkey, İstanbul, Turkey (virtual).

Koptekin D, Yapar E, Sağlıcan E, Alkan C, Somel M. (2020). New solutions to old problems: Mitigating data loss and bias in ancient genome data processing. Oral Presentation at 13th The International Symposium on Health Informatics and Bioinformatics, Sabancı University, İstanbul, Turkey (virtual).

Koptekin D, Özer F, Somel M. (2019). Investigating genetic continuity of human populations in Anatolia over the past 15,000 years. Oral Presentation at RSG Turkey Student Symposium, İzmir Biomedicine and Genome Center, İzmir, Turkey

Koptekin D, Kılınç GM, Atakuman Ç, Sümer AP, Yaka R, Bilgin CC, Büyükkarakaya A, Baird D, Götherström A, Togan İ, Somel M. (2017). Investigation of the Neolithisation in Anatolia and the Aegean by using ancient DNA. Oral Presentation at 4th Ecology and Evolutionary Biology Symposium Turkey, İstanbul, Turkey.

Koptekin D. (2017). Ancient genome analysis of the Anatolian and Aegean Neolithic populations. Oral Presentation at 39th International Excavation, Research and Archeometry Symposium, Bursa, Turkey

Koptekin D, Kılınç GM, Sümer AP, Dönertaş HM, Somel M. (2017) Genome-wide cytosine methylation differences between ancient hunter-gatherers and farmers. Oral Presentation at 86th Annual Meeting of the American Association of Physical Anthropologists, New Orleans, LA, US

Koptekin D, Dağtaş ND, Özer F, Kılınç GM, Yüncü E, Omrak A, Gündem CY, Özer O, Dönertaş HM, Götherström A, Somel M, Bıçakçı E, Togan İ. (2016). First ancient genomic data from Anatolian sheep. Presented as poster at 3rd Ecology and Evolutionary Biology Symposium Turkey, Ankara, Turkey.

Koptekin D, Kılınç GM, Dönertaş HM, Somel M. (2015). Genome-wide DNA methylation analysis of 8,000 year old hunter gatherers. Presented as poster at 4th International Congress of the Molecular Biology Association of Turkey, Ankara, Turkey.

Koptekin D and Aktaş LY. (2015). Computational identification of conserved miRNAs and their target genes in faba bean (*Vicia faba*). Presented as poster at 2nd Ecology and Evolutionary Biology Symposium Turkey, Ankara, Turkey.

Koptekin D. (2013). Origin and Evolution Plant microRNAs. Presented as poster at The Workshop on Theoretical Evolutionary Biology, İzmir, Turkey

COMPUTER SKILLS

R, Python, SQL, Unix environment (bash, awk etc.)

LANGUAGE SKILLS

Turkish (Native), English (Advanced), German (Beginner)